WNT16 in Chondrocyte Biology and Lineage Determination

By Bethan Thomas

Thesis submitted for the degree of Doctor of Philosophy at the University of London

Queen Mary University of London

William Harvey Research Institute

2014

Abstract

Background. During development WNT16 is a specific marker of the superficial zone of the developing articular cartilage. In adult joints WNT16 is no longer expressed, but it becomes rapidly upregulated in the articular cartilage following injury and in osteoarthritis. Unpublished data from our laboratory show that WNT16 deficient mice are more susceptible to instability-induced osteoarthritis. The superficial zone of the articular cartilage contains chondrogenic progenitor cells which are essential for the long-term maintenance of cartilage homeostasis. These cells express WNT16 and also specifically express Lubricin. Lubricin, in adulthood, is essential for joint lubrication and in its absence, mice develop spontaneous osteoarthritis.

Results. Exogenous WNT16 dose-dependently increased Lubricin expression in *wnt16*$^{-/-}$ superficial zone cells and primary bovine chondrocytes. WNT16 treatment also dose-dependently modulated Axin2, a transcriptional target of the canonical Wnt pathway. At low concentration Wnt16 downregulated axin2 expression, while higher concentrations caused upregulation compared to control. WNT16 also caused a dose-dependent phosphorylation of c-Jun transcription factor. In keeping with my data in chondrocytes, in xenopus laevis experiments, WNT16 had a limited capacity to induce features of axis duplication, but could efficiently inhibit axis duplication induced by WNT8. Importantly, both DKK1 and TCS (inhibitors of the canonical Wnt pathway and of the JNK pathways, respectively) prevented the WNT16-induced Lubricin upregulation, thereby demonstrating that modulation of the gene by WNT16 requires both the canonical Wnt pathway and the JNK pathways.

WNT16 supported the phenotype of superficial zone cells by enhancing Lubricin expression and by preventing their full chondrocytic maturation: extracellular matrix production was increased in *wnt16*$^{-/-}$ superficial zone cells and chondrocyte specific marker were lost upon WNT16 stimulation in these cells as well as in bovine primary chondrocytes.

Conclusion. WNT16 is a weak activator of the canonical Wnt pathway which supports lubricin expression and the phenotype of the cartilage superficial zone cells.

Acknowledgements

I am tremendously grateful to my supervisor, Francesco Dell'Accio, who has guided me through my PhD and taught me how to be a scientist. His passion and enthusiasm for science is always inspiring.
I am also thankful to my group and in particular Giovanna Nalesso, who has supported me from beginning to end.

I would like to thank my friends at EMR and WHRI, who I have learnt so much from, and who have made my PhD experience an unforgettable one. My 'non science' friends deserve a massive thankyou for putting up with me and for the constant support you provided.

A huge thankyou to my mum, my dad and my sister, who have always been there for me and have encouraged me through all my years of study. Without them I would not be where I am today.

I also wish to thank Prof. Teh for providing WNT16 plasmids, Prof. McMahon for the *wnt16*$^{-/-}$ mice, Prof. Moon for the Super8TOP and FOP reporter plasmids, and Dr. Bertrand for her help and guidance with plasmid cloning. In addition, I would like to thank the orthopaedic surgeons, Mr Achan and Mr Ramachandran for providing human cartilage samples.

Finally, I would like to thank Prof. Costantino Pitzalis and the Nuffield foundation, for giving me the opportunity to do a PhD. The Oliver Bird programme, and all those involved, has provided fantastic opportunities and endless support.

Declaration

The work presented in this thesis is less than 100,000 words and was performed and analysed by the candidate except for the Xenopus axis duplication assay which was performed by Dr. Leslie Dale, UCL.

The immunofluorescence staining in **Figure 47** was done in collaboration with Dr. Giovanna Nalesso. Sub-cloning of mammalian WNT16 expression plasmids was done in collaboration with Dr. Jessica Bertrand.

Prof. Francesco Dell'Accio and Dr Giovanna Nalesso closely supervised the project and provided scientific advice and guidance regarding experimental design and interpretation of results.

Candidate:

Bethan Thomas

Supervisors:

First supervisor:

Prof. Francesco Dell'Accio

Second supervisor:

Prof. Costantino Pitzalis

Third supervisor

Dr Giovanna Nalesso

Table of Contents

List of Figures

List of Tables

Abbreviations

ECM	Extracellular Matrix
AA	Antibiotic and Antimycotic
BCA	Bicinchoninic Acid
BMP	Bone Morphogenetic Protein
CACP	camptodactyly Athropathy Coxa vara Pericarditis
CaMKII	Calcium Calmodulin Kinase II
CDMP1	Cartilage Derived Morphogenic Protein
CHO	Chinese Hamster Ovary
CREB	cAMP response element-binding protein
CS	Chondroitin Sulphate
DKK	Dickkopf-related Protein 1
DMEM/F12	Dulbecco's Modified Eagle Medium with nutrient mixture F-12
DMM	Destabilisation of the Medial Meniscus
DNA	Deoxyribonucleic acid
dNTP	Deoxyribonucleotide
DS	Dermatan Sulphate
Dsh	Dishevelled
DZC	Deep Zone Chondrocytes
ECL	Enhanced Chemiluminescence
eGFP	Enhanced Green Fluorescence Protein
FBS	Foetal Bovine Serum
FnF	Fibronectin Factor
frzb	Frizzled-related Protein B
FZD	Frizzled
GAGs	Glycosaminoglycans
GDF5	Growth Differentiation Factor 5
HA	Hyaluronan
HAC	Human Articular Chondrocytes
HAPO	Hemangiopoietin
HMG	High Mobility Group

HS	Heparan Sulphate
IHH	Indian Hedgehog
JNK	c-Jun N-terminal kinase
KO	Knockout
KS	Keratan sulphate
LB	Luria Broth
LiCl	Lithium Chloride
MAC	Mouse Articular Chondrocytes
MAPK	Mitogen-Activated Protein Kinase
MCC	Mouse Costal Chondrocytes
MMP	Matrix Metalloproteinase
MSF	Megakaryocyte stimulating Factor
NaCl	Sodium Chloride
NFAT	Nuclear Factor of Activated T-cells
OA	Osteoarthritis
PCP	Planar Cell Polarity
PCR	Polymerase Chain Reaction
PKA	Protein Kinase A
PTHrP	Parathyroid Hormone-related Protein
RNA	Ribonucleic Acid
SDS-PAGE	Sodium dodecyl Sulphate Polyacrylamide Gel Electrophoresis
sFRP3	Secreted Frizzled Related Protein 3
SMO	Smoothened
SNP	Single Nucleotide Polymorphism
SZC	Superficial Zone Chondrocytes
TCA	Trichloroacetic Acid
TCF	Transcription Factor 4
TIMP	Tissue Inhibitor Of Metalloproteinase
TNF	Tumour Necrosis Factor
WT	Wild Type

CHAPTER 1:

Introduction

Development of the appendicular skeleton

This section includes an overview of the main processes taking place during appendicular skeletal development and joint formation (a schematic in **Figure 3** gives an overview of the process). The individual aspects of this process will be detailed separately with particular emphasis on the molecular mechanism relevant to WNT signalling in cartilage biology. As it will be clear from my results, many aspects of WNT16 function in adult cartilage biology and osteoarthritis recapitulate events that are very well studied in joint morphogenesis.

The appendicular skeleton forms within the limb buds from the condensation of mesenchymal cells in uninterrupted rods called anlagen (Karsenty and Wagner 2002). Subsequently, the cells within the anlagen undergo chondrogenesis, marked by the expression of the cartilage transcription factor SOX9 (Bi, Deng et al. 1999) and consequently, its target genes COL2A1, which encodes for the alpha-1 chain of type II collagen (Lefebvre, Huang et al. 1997), and aggrecan (Han and Lefebvre 2008). These molecules contribute to the accumulation of an abundant extracellular matrix (ECM) rich in highly sulphated glycosaminoglycans (GAGs) and collagen type II (Karsenty and Wagner 2002). The fibroblast-like cells surrounding the cartilage anlagen are called perichondrium.

Early during skeletal development, the uninterrupted anlagen undergo segmentation into the individual skeletal elements. This is dependent on the formation of specialised structures called joint interzones which will subsequently cavitate and differentiate into the mature joint structures.

Finally, the epiphyseal cartilage of the skeletal elements undergoes a maturation process which involves the hypertrophic differentiation of the chondrocytes (marked by the expression of collagen type X and other markers). The hypertrophic cartilage is eventually replaced by trabecular bone through a process called endochondral bone formation. Cortical bone develops from within the perichondrium through intramembranous bone formation.

The joint interzones undergo chondrogenic differentiation very late during development and never, in physiological conditions, undergo hypertrophic differentiation or endochondral bone formation. The articular cartilage, originating from these structures will persist, avascular, throughout life (Karsenty and Wagner 2002; Mariani and Martin 2003).

Endochondral Ossification

Endochondral bone formation is the process through which most of the cartilage forming the anlage, with the exception of the prospective articular cartilage, is replaced by bone (Olsen, Reginato et al. 2000; Colnot, Lu et al. 2004). Ossification initiates at the central part of each skeletal element, called the diaphysis, and extends proximally and distally towards the epiphyses, where we find the prospective articular surface and the developing joint, described later. A scheme of the developing long bones (the region between the interzone and the ossified area), can be found in **Figure 1**.

As the limbs continue to grow the interzone and the mineralised bone are separated by the epiphyseal cartilage, which is composed of 4 layers. Epiphyseal chondrocytes adjacent to the cells of the interzone are small and rounded and are called resting chondrocytes. They express collagen type II and matrilin-1 (Hyde, Dover et al. 2007). Proceeding towards the diaphysis, we encounter an area of “proliferating chondrocytes”, which contribute to longitudinal growth of the anlage. The next area of the epiphysis is composed of flat chondrocytes organised in columns called pre-hypertrophic chondrocytes and expressing Indian Hedgehog (IHH). Finally, large, terminally differentiated chondrocytes expressing collagen type X are called hypertrophic chondrocytes (Karsenty and Wagner 2002)

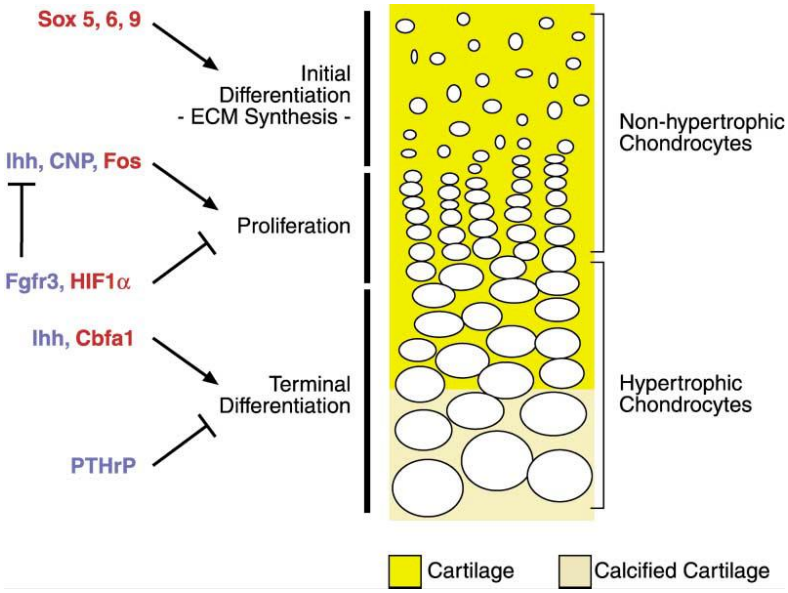

Figure 1: Representation of growth plate chondrocytes, including from top to bottom, resting, proliferating, pre-hypertrophic and hypertrophic chondrocytes (Karsenty and Wagner 2002).Permission granted by Elsevier, licence number: 3471390689539.

Hypertrophic cartilage undergoes vascular invasion which progresses from the diaphysis towards the epiphyses. Osterix-expressing osteogenic progenitors from the perichondrium enter the cartilage anlagen together with the vessels as pericyte-like cells (Maes, Kobayashi et al. 2010). The hypertrophic chondrocytes eventually undergo apoptosis (Hatori, Klatte et al. 1995), and their extracellular matrix is resorbed by chondroclasts (Vu, Shipley et al. 1998). Eventually, the incoming osterix-positive progenitor cells become osteoblasts, which give rise to the trabecular bone.

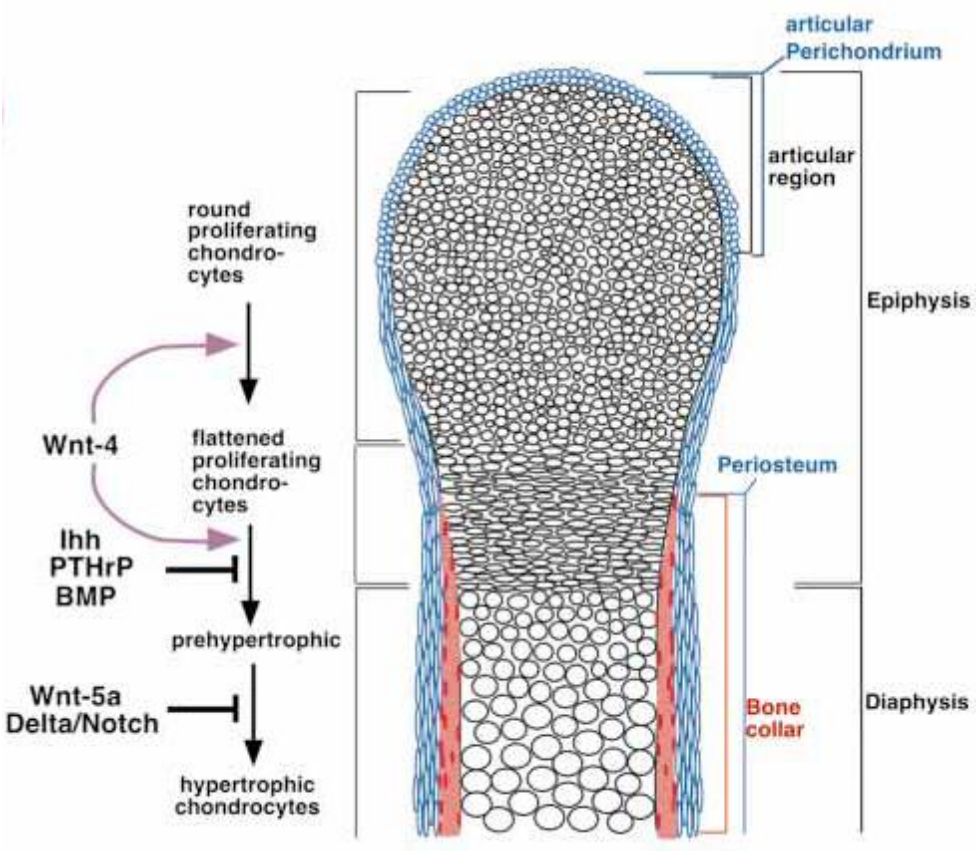

Figure 2: Molecular regulation of chondrocytes in the developing limb (Hartmann and Tabin 2000).Permission granted by company of biologists, licence number 3478121387476.

As seen in **Figure 1** and **Error! Not a valid bookmark self-reference.**, this process is tightly regulated. Parythroid hormone related protein (PTHrP), secreted in the periarticular perichondrium, prevents late proliferating chondrocytes, expressing PTHrP receptor, from entering hypertrophy and thereby confers positional information (Chung, Schipani et al. 2001). As chondrocytes eventually exit the PTHrP gradient and become prehypertrophic they start expressing IHH. IHH signals to perchondrial cells expressing the IHH receptors patched and smoothened and induces the formation of bone collars around the area of chondrocyte pre-hypertrophy (Chung, Schipani et al. 2001) through direct, intramembranous ossification. Ihh also induces the expression of PTHrP in the periarticular perichondrium (Vortkamp, Lee et al. 1996). Several other well-known signalling pathways, such as Bone morphogenic protein (BMP), Fibroblast growth factor (FGF), and WNT signalling, are also heavily involved in this system. BMPs modulate IHH expression, and negatively regulates later stages of hypertrophic differentiation but has no role in regulating the onset of hypertrophy which is controlled by IHH

(Minina, Wenzel et al. 2001). FGF signalling on the other hand, reduced the expression of IHH and accelerated the onset of hypertrophy (Minina, Kreschel et al. 2002). Components of WNT signalling also drive chondrocyte differentiation, as Calcium Calmodulin Kinase II (CaMKII) a downstream component of Ca^{2+} dependant WNT signalling, was required for the initiation of chondrocyte hypertrophy (Li, Ahrens et al. 2011). This system of molecular controls, first identified by Andrea Vortkamp et al. in 1996, provides a mechanism for both longitudinal growth and positional information (Chung, Schipani et al. 2001; Wuelling and Vortkamp 2010).

Joint Development

Joint development takes place in 3 stages: joint specification, cavitation, and maturation. Joint specification is the process through which the position of the prospective joints is defined within the uninterrupted cartilage anlagen; cavitation is the process by which the different skeletal elements are physically separated; maturation is the process through which cells in the prospective joint region, the joint interzone, differentiate and pattern the joint tissues including the articular cartilage, the tendons and ligaments, the synovial membrane, and the joint capsule.

Joint specification.

The location of the joints within the anlage is determined in the early mesenchymal condensation, and is marked by the expression of specific interzone markers including WNT9A, WNT4 and WNT16 (Hartmann and Tabin 2000; Guo, Day et al. 2004), Growth differentiation factor 5, (GDF5), or cartilage derived morphogenetic protein 1 (CDMP1) in humans (Storm, Huynh et al. 1994), autotaxin (Bachner, Ahrens et al. 1999), tenascin C (Pacifici, Iwamoto et al. 1993) and a splice variant of collagen type II skipping the second exon (COL2A1-A) (Upholt, Strom et al. 1985). Markers of the epiphyseal cartilage COL2A1-B (Upholt, Strom et al. 1985; Koyama, Shibukawa et al. 2008) and Matrilin (Hyde, Dover et al. 2007)) are excluded. This layer of cells also expresses markers of stem cells including SOX2, CD34 and CD105 (Yasuhara, Ohta et al. 2011). The cells in this area acquire a specific fibroblast-like morphology, with the longer axis perpendicular to the axis of the anlage.

The molecular control of joint determination is still not completely understood. WNT9a was identified as one of the first initiators of joint formation: Hartmann and Tabin showed that it is one of the earliest markers of the joint interzone, and that its miss-expression in the chick limb bud leads to the formation of joint-like structures expressing other joint interzone markers including GDF5 (Hartmann and Tabin 2001). This function of WNT9A is β-catenin dependent

and not exclusive of WNT9A. In fact WNT9A deficient mice have essentially normal joints except for a mild phenotype characterised by synovial chondromatosis (Spater, Hill et al. 2006). Other WNT molecules including WNT4 and WNT16 are co-expressed with WNT9a in the joint interzone and may play a redundant role at this site in activating β-catenin signalling, which is both required and sufficient for development of joint interzones as its disruption leads to joint fusion in mice. Furthermore its forced activation leads to joint-like structures expressing interzone markers (Guo, Day et al. 2004).

More recently, the activation of the transcription factor c-Jun was described to be a further upstream event in the determination of joint location (Kan and Tabin 2013). C-Jun is expressed in the prospective joint interzones and directly activates WNT9a transcription by binding and activating its promoter (Kan and Tabin 2013). Compared to the genetic deletion of WNT9A however, mice lacking c-jun in the mesenchyme of the early limb bud (Prx1-cre; c-jun$^{FL/FL}$), have a more severe phenotype and form abnormal joint interzones, which fail to cavitate. This discrepancy may be attributed to the ability of c-Jun to also bind the WNT16 promoter, leading to transcription of another canonical WNT (Kan and Tabin 2013).

Although c-Jun is essential in joint formation and cavitation, it is not required for joint determination as joint interzones were clearly evident in the c-Jun conditional deficient mice (Kan and Tabin 2013). Therefore, the primary signal of the molecular mechanism initiating joint specification is still unknown.

GDF5, (a transcriptional target of the canonical WNT pathway within the joint interzone) is a member of the Bone morphogenetic protein (BMP) family (Karsenty and Wagner 2002) and was one of the first markers of the joint interzone to be identified (Chang, Hoang et al. 1994; Storm, Huynh et al. 1994). Despite being a marker of the joint interzone, it is prochondrogenic and is thought to initially stimulate condensation of pre-chondrogenic mesenchymal cells and later to promote cell proliferation in the surrounding skeletal elements, (Francis-West, Abdelfattah et al. 1999). Its role in the formation of the joint interzone is unclear, since its absence causes a phenotype characterised by short distal bone elements and absence of some phalanges (Storm, Huynh et al. 1994; Thomas, Lin et al. 1996). Loss of function mutation of the same gene in humans result in a variety of phenotypes ranging from the very mild brachydactyly C (Polinkovsky, Robin et al. 1997) to very severe chondrodysplasia including the Hunter-Thompson thanatophoric dysplasia (Thomas, Lin et al. 1996) and the Grebe-type chondrodysplasia, which is due to the formation of a protein that is not secreted, and produces

a dominant negative effect by preventing the secretion of other, related BMP family members (Thomas, Kilpatrick et al. 1997). Although these phenotypes are severe, they do not result specifically in joint fusion, but rather in epiphyseal phenotypes. Therefore, it is currently unclear whether the function of GDF5/CDMP1 is inherent to bone formation or whether it is a regulatory function that the interzone cells exert on the underlying epiphyseal chondrocytes. Interestingly, ALK6, its cognate type II BMP receptor, is not specifically expressed within the joint interzone, but rather in the underlying epiphyseal chondrocytes, just underneath the joint interzone cells (Baur, Mai et al. 2000).

Noggin is a secreted BMP antagonist which binds to BMPs and inhibits their interaction with the receptors. Noggin is expressed in the late joint interzones and is essential to normal joint development. Noggin knockout mice exhibit shorter limbs and joint fusions. Noggin knockout mice also fail to upregulate GDF-5 in the presumptive joint regions suggesting that Noggin determines GDF5 transcription in some way, as well as interacting with the protein (Brunet et al., 1998).

Other BMPs are also heavily involved. At early stages, BMP2 is expressed in the joint interzones as well as the region between the digits (Macias, Ganan et al. 1997). BMP2-soaked beads implanted by the diaphysis induced the formation of ectopic joint interzones in the chick embryo, and enlargement of pre-existing joint interzones when implanted in their vicinity. In contrast, OP-1/BMP-7 is expressed in the perichondrium except in the region of the joint interzone, and implantation of BMP-7-soaked beads in correspondence of joint interzones caused joint fusion (Macias, Ganan et al. 1997).

Subsequently, following specification, the joint interzones develop into a three-layered structure consisting of a central region of densely packed undifferentiated cells flanked by two chondrogenic layers on the ends of the developing bones.

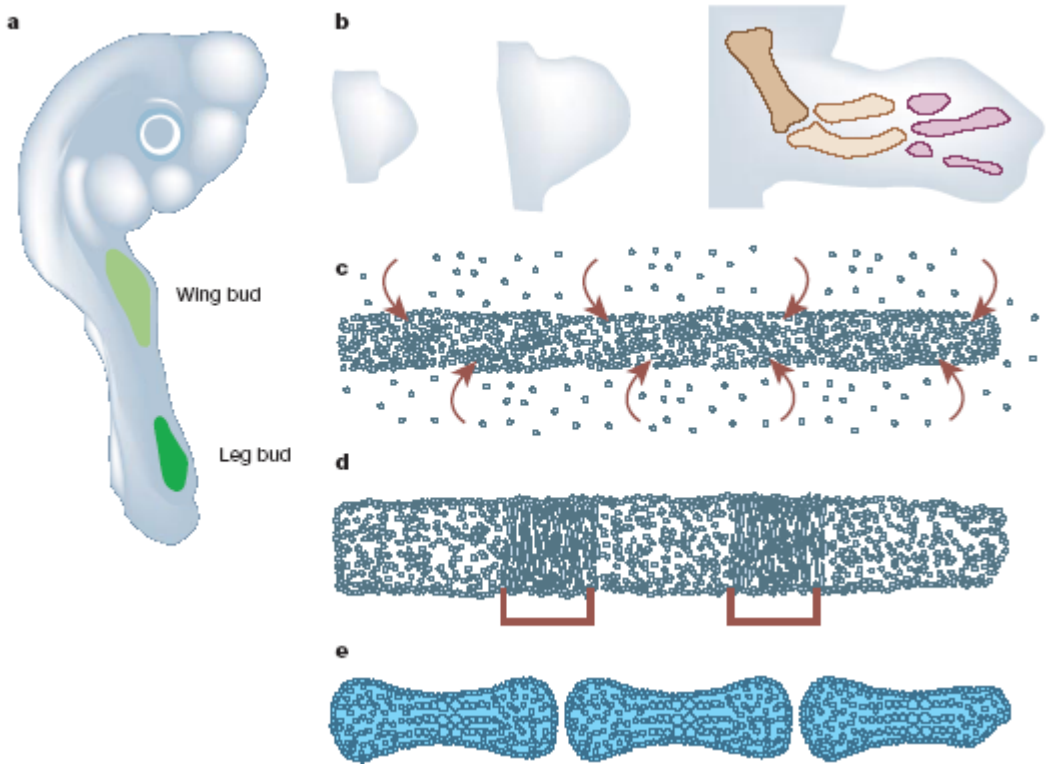

Figure 3: Initial stages of limb development. (a) Initiation, (b) outgrowth and patterning, (c) Aggregation and condensation, (d) joint determination, (e) Joint cavitation (Mariani and Martin 2003). Permission granted by Macmillan Publishers Ltd, licence number 3477730899141.

Joint cavitation.

After formation of the joint interzones, the two chondrogenic layers cavitate, separating the two skeletal elements (**Figure 3**). The precise mechanism leading to cavitation is not yet well understood, however, at least 3 mechanisms may contribute: i) apoptosis of the central layer, ii) deposition of large amounts of hyaluronic acid (HA), and iii) embryonic movements.

Cell death. Cell death and apoptosis have been traditionally assumed to play a role in joint cavitation (Pacifici, Koyama et al. 2005). Indeed, evidence of DNA fragmentation has been reported prior, but not at the time of cavitation within interzones (Nalin, Greenlee et al. 1995). Other reports fail to show such evidence (Ito and Kida 2000; Kavanagh, Abiri et al. 2002) and the functional role of cell death still remains a controversial issue.

Deposition of HA. Pitsillides et al., reported that, before cavitation, the cells in the joint interzone start expressing uridine diphosphoglucose dehydrogenase (UDPGD), a key enzyme in the synthesis of HA, resulting in the production of large amounts of the molecule. UDPG activity

and HA synthesis culminated with the first signs of cavity formation, suggesting that HA accumulation contributes to mechanically separate the developing skeletal elements (Edwards, Wilkinson et al. 1994; Pitsillides, Archer et al. 1995; Hartmann and Tabin 2001).

Foetal movements. It has been postulated that the mechanical strains induced by the first foetal movement may contribute to cavitation. Indeed, in immobilised chick embryos, synovial joints fail to develop (Mitrovic 1982; Persson 1983) leading to hypotheses that foetal muscle activity may contribute to ECM disruption in the joint regions. However mice deficient in myogenin, (a muscle transcription factor), which do not develop contracting skeletal muscles, undergo normal joint cavitation.

Although foetal movements play a part in the process the combination of the proposed central apoptosis and of HA production ultimately results in the physical separation of the two skeletal elements, and the formation of the joint cavity rich in HA, (Pitsillides, Archer et al. 1995).

Joint maturation.

The destiny and lineage determination of the cells of the joint interzone have been determined only recently, (Settle, Rountree et al. 2003; Rountree, Schoor et al. 2004; Koyama, Shibukawa et al. 2008; Yasuhara, Ohta et al. 2011). A transgenic mouse in which cre recombinase was expressed under the transcriptional control of the gdf5 promoter was developed and crossed with ROSA26R line (carrying a LacZ cassette preceded by a floxed stop codon within the ROSA26 locus, which drives ubiquitous expression). In interzone cells, therefore, cre recombinase is expressed, deletes the stop codon preceding the LacZ cassette and activates LacZ expression within these cells and their progeny, regardless of subsequent gdf5 expression (Rountree, Schoor et al. 2004). This and subsequent experiments (Koyama, Shibukawa et al. 2008), convincingly demonstrated that the cells of the joint interzone give rise to the articular cartilage, ligaments and synovium but not to the chondrocytes of the epiphysis (Koyama, Shibukawa et al. 2008). The importance of these data is that they identify unequivocally the cells of the joint interzone as a separate lineage from those of the epiphyseal cartilage, and therefore, in this respect, it is not surprising that the progeny of these cells does not undergo, in physiological condition, hypertrophic differentiation and endochondral bone formation.

In spite of the morphological similarity between articular and epiphyseal cartilage, these two tissues arise from separate progenitors and are profoundly different from the molecular and functional point of view as disruption of specific molecular controls from specific regions result in very different phenotypes. PTHrP and PTHrP receptor are highly involved in endochondral

ossification. Mice lacking PTHrP receptor (expressed in prehypertrophic and hypertrophic chondrocytes of epiphyseal cartilage) exhibit severe epiphyseal chondrodysplasia but have no reports of abnormal articular surfaces (Lanske, Karaplis et al. 1996; Lanske, Amling et al. 1999; Chung, Schipani et al. 2001). In contrast, mice lacking transcription factor c-Jun (expressed solely in the region of developing joints) from the mesenchyme of the limb bud, (Prx1-cre; c-jun$^{FL/FL}$), had long bones that developed normally, however joint development was disrupted from the early stages of interzone formation to adulthood: at 4 weeks of age mice had irregularities in their articular surface, defects of cavitation with cartilage bridging and underdeveloped ligaments and tendons (Kan and Tabin 2013).

In later development through to adult life, the cells of the superficial layer of the articular cartilage retain a phenotype similar to that of the cells of the joint interzone and are considered a specific pool of cartilage progenitor cells, retaining chondrogenic capacity and expressing stem cell markers including SOX2, CD34 and CD105 (Dowthwaite, Bishop et al. 2004; Koyama, Shibukawa et al. 2008; Yasuhara, Ohta et al. 2011) (**Figure 4**, shown in yellow). They also synthesise the protein lubricin, a proteoglycan essential for joint lubrication. Lubricin is encoded by the prg4 gene, which also encodes for 3 other proteins; Superficial zone protein, Megakaryocyte-stimulating factor (MSF) and hemangiopoietin (HAPO), which are generated by alternative splicing, (Rhee, Marcelino et al. 2005) and post-translational modifications such as the addition of glycosaminoglycan side chains. Both superficial zone protein and lubricin are expressed within joints (Dercksen, Weimar et al. 1995). They have similar protein sequences but differ in their side chain composition which distinguishes them (Jay, Tantravahi et al. 2001). MSF was shown to stimulate the growth of platelet forming cells, while HAPO induced growth of hematopoietic and endothelial stem cells *in vitro* but their function *in vivo* is still unknown (Rhee, Marcelino et al. 2005).

In the deeper layers of the articular cartilage (**Figure 4**, shown in blue), however, under the effects of pro-chondrogenic stimuli including BMPs and TGFβ, the cells acquire a chondrogenic phenotype, with upregulation of SOX9, Aggrecan and COL2A1, which in part resembles that of the resting layer of epiphyseal chondrocytes, but never express, in normal conditions, epiphyseal marker Matrilin-1, (Hyde, Dover et al. 2007) or hypertrophy marker (COL10A1) (Saito, Fukai et al. 2010; Yang, Kim et al. 2010).

Perinatally, a secondary ossification centre appears in the epiphysis and expands towards the joint. The junction between the primary and the secondary ossification centre will form the

growth plate or metaphysis, and the junction between the secondary ossification centre and the articular cartilage will form the subchondral plate.

The molecular control of the morphogenesis and maturation of non-cartilaginous soft tissues including tendons, menisci and ligaments remains poorly understood (**Figure 4**).

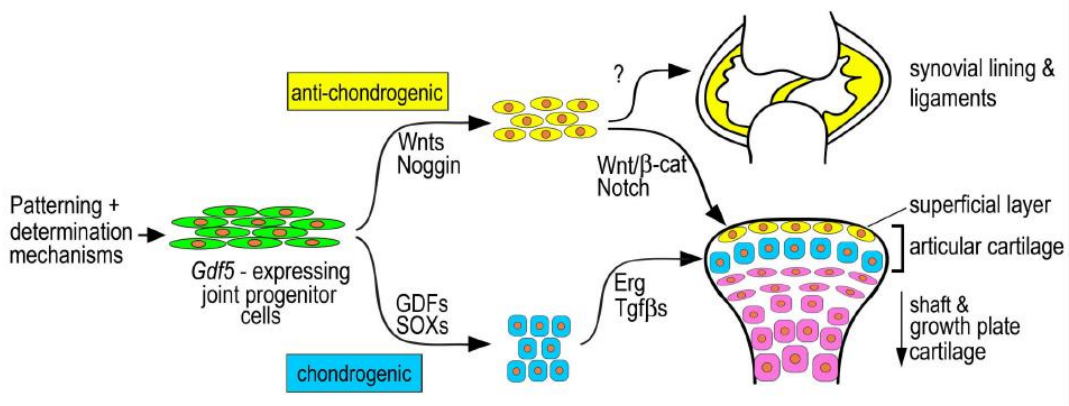

Figure 4: Lineage determination of the interzone cells. Progenitor cells expressing GDF5, depending on molecular cues, differentiate to form both the articular cartilage, and the soft tissues of the joint (Koyama, Shibukawa et al. 2008). Permission granted by Elsevier, licence number 3477731317413.

Articular Cartilage

The adult articular cartilage is as an avascular, aneural tissue separating the articulating skeletal elements in the joint. Its structure and composition allows it to provide for the smooth motion of the joint and for the capacity to withstand mechanical forces including sheer stresses and load. The only cell type present in the articular cartilage is the articular chondrocyte which is responsible for maintaining the ECM.

The cartilage ECM is very abundant, and is specifically characterised by the high content of heavily sulphated GAGs, which stain metachromatic with cationic dyes such as Safranin O or Toluidine blue (Rosenberg 1971). Sulphated GAGs are also bound by alcian blue even at very low pH (at pH 0.2 the staining is extremely specific and can be used to quantitate GAGs in 3D culture systems (De Bari, Dell'Accio et al. 2001)).

GAGs are attached to proteoglycans such as aggrecan, which is the largest and most abundant proteoglycan in cartilage. Several other small proteoglycans such as the dermatan sulphate proteoglycans (decorin and biglycan) and the keratan sulphate proteoglycans (fibromodulin and lumican) represent the minority of cartilage proteoglycans, but still have important functions, since their genetic deletions results in different types of chondrodyspasia. In the ECM several aggrecan molecules are bound to a single molecule of hyaluronan (Figure 6) (Roughley 2006) forming very large molecular complexes.

Being highly hygroscopic, GAGs confer cartilage its remarkable capacity to withstand impact load. Cartilage ECM is also rich in fibrillar collagens, with type II collagen representing approximately 90%. Collagen fibres are arranged parallel to the surface of the cartilage in the superficial layer, and curve to acquire a perpendicular course in the deeper layers, where they anchor themselves to the subchondral bone (Figure 5). Fibrillar collagens confer cartilage its tensile strength.

In adulthood, cartilage is separated into four layers consisting of a superficial zone; a middle zone; a deep zone; and a calcified zone, as seen in **Figure 5**. Chondrocytes in the different layers of the articular cartilage vary in morphology and biological properties. Although it was previously thought that chondrocytes in the deeper layers of adult articular cartilage originated from epiphyseal cartilage, recent data from Professor M. Warman's group, (Harvard medical school), presented at the OsteoArthritis Research Society International 2014 conference showed that chondrocytes in all layers of the adult articular cartilage originate from the cells of the interzone and the very superficial layer of the developing cartilage during joint formation

(Warman 2014). Lineage tracking using a lubricin reporter mouse, which labels all lubricin expressing cells and their progeny, showed that all articular chondrocytes were labelled indicating that they originally derive from the SZC, the cartilage progenitors described in late development shortly after birth that express lubricin and later differentiate into mature chondrocytes (Warman 2014).

Superficial zone. The superficial zone is populated by so-called superficial zone chondrocytes (SZC), which are essential for cartilage homeostasis. They are flat cells oriented parallel to the surface of the cartilage and express specific molecular markers including lubricin and superficial zone protein, and CDMP1/gdf5 (Erlacher, Ng et al. 1998; Schumacher, Hughes et al. 1999).

The SZC, as mentioned above, derive from the interzone cells during development, but retain, throughout adult life, features of stem/progenitor cells: they are highly clonogenic (Williams, Khan et al. 2010; Yasuhara, Ohta et al. 2011) and retain chondrogenic potential after multiple passages (Yasuhara, Ohta et al. 2011). Recent data also show that these cells display markers of stem cells including SOX2, CD105 and CD34, and in vivo, have a slow cycling rate (Yasuhara, Ohta et al. 2011; Candela, Cantley et al. 2014).

The SZC also respond to injury, an in vitro study demonstrated that following mechanical injury in osteochondral explants resulting in chondrocyte apoptosis, the SZC from the surrounding area of the cartilage acquire a fibroblastic phenotype, migrate to the injury site and repopulate the damaged cartilage area (Seol, McCabe et al. 2012). This phenomenon was activated by and dependent on the release of HMGB1 from the chondrocytes undergoing apoptosis. HMGB1 is a transcription factor that was previously shown, when released by apoptotic cells, to function as a chemo-attractant for mesenchymal stem cells within the damaged muscle (Palumbo, Sampaolesi et al. 2004). It is therefore possible, that these cells represent the 'progenitor pool' of cells for the articular cartilage, but this has not been demonstrated *in vivo* yet.

As well as their progenitor features, SZC express molecules that are essential for the maintenance of cartilage homeostasis. Genetic deletion of lubricin results in spontaneous OA in mice (Coles, Zhang et al. 2010), and patients with loss of function mutations in the *Prg4* gene develop a clinical syndrome called camptodactyly–arthropathy–coxavara–pericarditis syndrome (CACP) which also results in articular cartilage breakdown. Waller et al. demonstrated that absence of lubricin, or mutations in lubricin resulted in an increased coefficient of friction in ex vivo and in vitro models, followed by apoptosis of the SZC. Such apoptosis was also confirmed in vivo. Importantly, recombinant wild type lubricin, but not

lubricin from patients with CACP syndrome decreased both the coefficient of friction and chondrocyte apoptosis in such models (Waller, Zhang et al. 2013). Finally, *Prg4* overexpression protected mice from instability-induced OA (Flannery, Zollner et al. 2009).

The SZCs themselves are dependent on canonical WNT signalling for proper function, since local ablation of β catenin resulted in the loss of their capacity to persist in G0 (Candela, Cantley et al. 2014), in ectopic hypertrophic differentiation (Yasuhara, Ohta et al. 2011), disruption of the articular cartilage architecture (Koyama, Shibukawa et al. 2008) and loss of lubricin expression (Yasuhara, Ohta et al. 2011). Conversely, overexpression of constitutively active β catenin in the cartilage (Col11-CA-βcatER), resulted in proliferation of the SZC and thickening of the articular cartilage in adult mice (Yuasa, Kondo et al. 2009).

Taken together, although formal proof using genetic labelling techniques and *in vivo* experiments are still lacking, it is conceivable that the SZCs represent the cartilage stem cells in adulthood, which are normally in G0 in quiescent cartilage, but supply progenitor cells for cartilage homeostasis and replacement of mature chondrocytes when necessary.

Middle and deep zone. The middle zone is characterised by chondrocytes that are more rounded. Cell density decreases as we move towards the deep zone and ECM content becomes progressively richer in aggrecan, with collagen fibrils arching away from the cartilage surface. In the deep zone, chondrocytes are arranged in columns with the collagen fibrils ordered perpendicular to the surface, which gives mature cartilage the typical “glassy” (hyaline) appearance under in light microscopy (Poole, Kojima et al. 2001). Chondrocytes in the intermediate layer are often found in small groups of 2-3 cells, called chondrons surrounded by a specific “territorial matrix” rich in perlecan and collagen type VI. Markers of the intermediate deep cartilage layer include chondrocyte transcription factor sox9 and its target genes collagen type II and aggrecan.

C**alcified layer.** This layer separates the cartilage and the subchondral bone and is rich in hydroxyapatite crystals (Arsenault and Grynpas 1988). This area is sometimes thought to represent a remnant of the growth plate and contains hypertrophic chondrocytes which express collagen type X, a marker of hypertrophy. The limit between the deep and calcified layer is called “tide-mark” because of its appearance in haematoxylin-eosin staining. The presence of this feature is a token of well-organised cartilage (e.g. after regeneration) and is lost early in OA (Mankin, Dorfman et al. 1971).

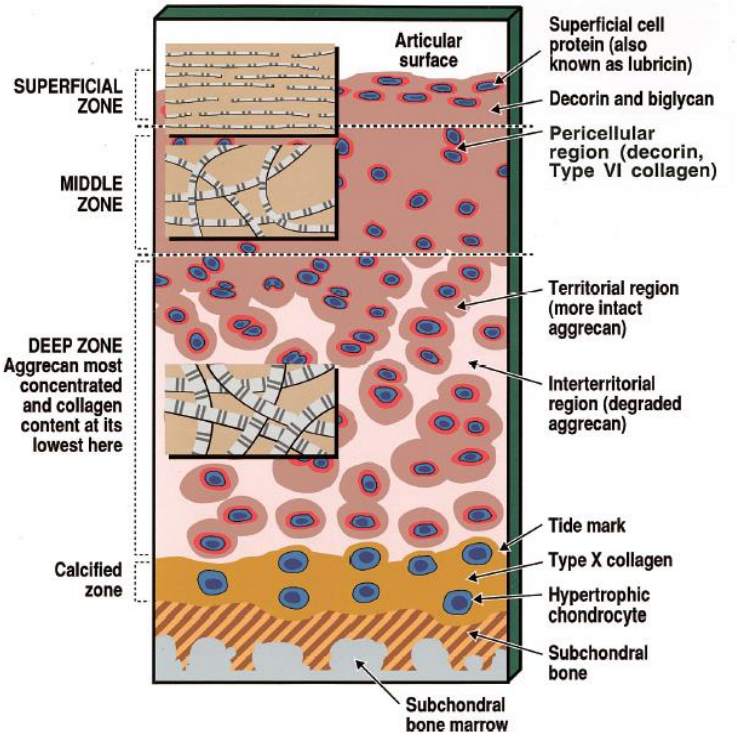

Figure 5: Schematic representation of articular cartilage layers. (Poole, Kojima et al. 2001). Permission granted by Wolters Kluwer Health, licence number 3477740335544.

Proteoglycans

Approximately 10% of ECM consists of highly sulphated proteoglycans. Proteoglycans consist of a protein core with long polysaccharide chains consisting of repeating disaccharide units called glycosaminoglycans (GAGs). A number of GAGs are found in cartilage. These include; chondroitin sulphate (CS), which is the most abundant; keratan sulphate (KS); heparan sulphate (HS); and dermatan sulphate (DS).

Cartilage proteoglycans have a characteristic high negative charge due to an extremely high level of sulphation. This causes the movement of water into the cartilage, resulting in cartilage swelling which provides osmotic resistance, required to bear compressive loads (Kiani, Chen et al. 2002). The sulphation pattern is also important for binding of growth factors including TGFβ, FGFs, BMPs and WNTs. Deletion of sulphatases sulf-1 and sulf-2 resulted in an imbalance of FGF and BMP signalling, spontaneous cartilage breakdown, and more severe experimental OA in mice (Otsuki, Hanson et al. 2010).

In the inter-territorial ECM (between different chondrons), the most abundant proteoglycan is aggrecan. Aggrecan, represented in **Figure 6**, is a large molecule of 220KDa consisting of 3 globular domains, (G1, G2 and G3, which contain cysteines that form disulphide bonds), separated by an interglobular domain, (between G1 and G2) and a large region containing chondroitin sulphate and keratan sulphate side chains, (between G2 and G3) (Kiani, Chen et al. 2002). Aggrecan also contains side chains of O- and N- linked oligosaccharides. Domain G1 is situated at the N-terminus of the protein and is responsible for indirect binding to hyaluronic acid (HA) through interaction of a separate protein called link protein. HA is a long chain of disaccharide repeats (D-glucuronic acid and D-N-acetylglucosamine). One molecule of HA binds several molecules of aggrecan, thereby forming very large aggregates, represented in **Figure 7**. Aggrecan interacts with chondrocytes, via the CD44 receptor, and collagen type II, (Watanabe, Yamada et al. 1998; Poole, Kojima et al. 2001) (see figure 7).

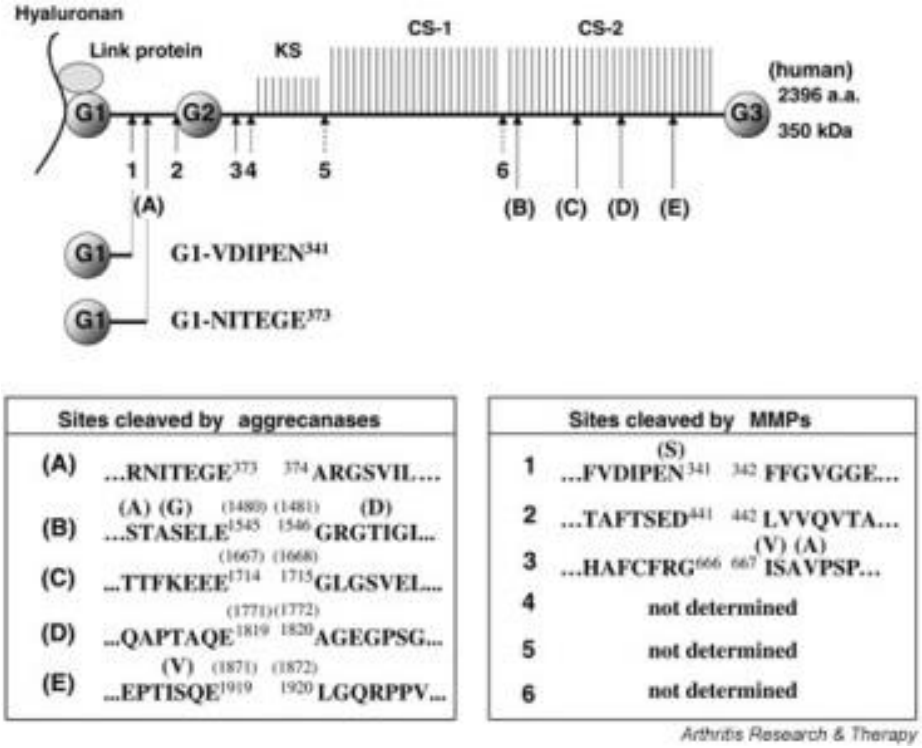

Figure 6: Representation of aggrecan domains, including core domains, (G1, G2 and G3), as well as aggrecanse (A-E), and MMP (1-6), cleavage sites (Nagase and Kashiwagi 2003). Under permission of BioMed Central.

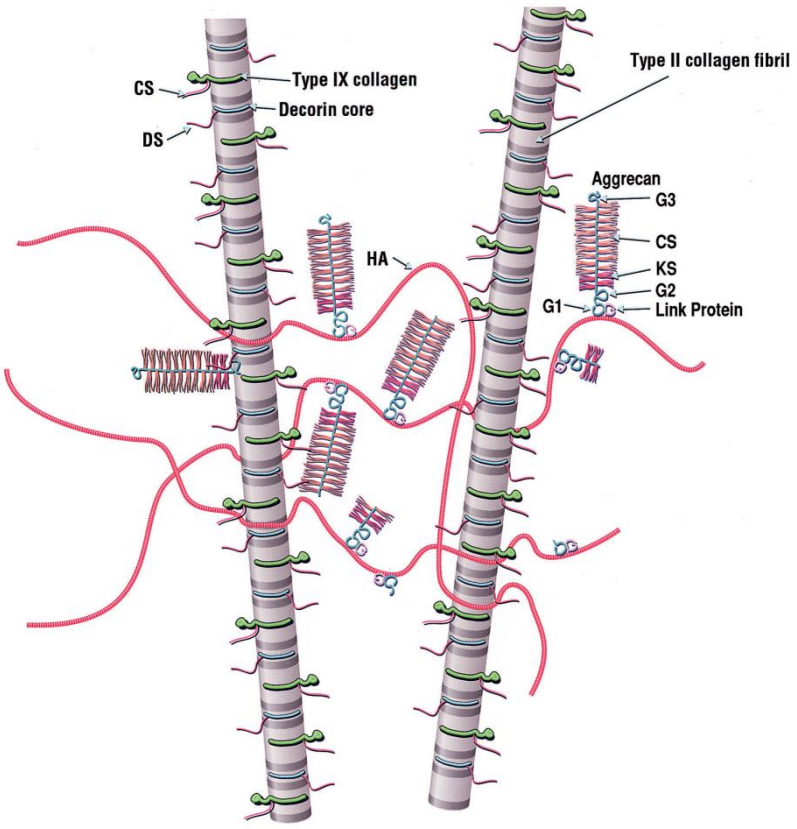

Figure 7: Interactions between cartilage molecules type II collagen, HA and aggrecan which make up the ECM (Poole, Kojima et al. 2001).Permission granted from Wolters Kluwer Health, licence number 3477871478444

In addition to the large proteoglycans aggrecan and versican, cartilage also contains small, leucine rich proteoglycans including decorin and biglycan (DS- proteoglycans) which are most concentrated in the superficial zone (Poole, Rosenberg et al. 1996); fibromodulin and lumican (KS-proteoglycans); and perlecan (HS-proteoglycan), located in the pericellular matrix (Poole, Kojima et al. 2001; Roughley 2006). These molecules can bind collagen during fibril formation and stabilise the ECM. They are also known to bind small molecules such as growth factors TGFβ and FGFs, thereby aiding in the formation of gradients and modulation of signalling activity (Hildebrand, Romaris et al. 1994; Vincent, McLean et al. 2007).

Collagens

Collagens account for 15-20% of the ECM and confer to the tissue its tensile strength (Eyre 2004; Dudhia 2005). The articular cartilage contains both fibrillar collagens (mostly collagen type II, with small amounts of collagen type I particularly in the superficial layer) and non-fibrillar collagens including collagen type IV. By far the most abundant collagen in cartilage is collagen type II, which is mostly specific to cartilage (it is also expressed in minimal part in the developing brain).

In the articular cartilage, collagen is arranged in vast fibrils which range from 20nm in diameter in the superficial zone to up to 120nm in the deep zone (Poole, Kojima et al. 2001). Procollagen chains are secreted in the extracellular matrix where C- and N terminal telopeptides are cleaved. Following cleavage of the telopeptides, a triple helix of α, β or γ chains is assembled extracellularly to form tropocollagen molecules. Type II collagen, which forms over 90% of cartilage collagen, consists of 3 α chains. Post-translationally hydroxylated proline and lysine residues allow crosslinking of different fibrils to form compact and stable collagen fibres. Different α chains vary in their amino acid sequence but all contain repeating units: (Gly-X-Y)n (Stenzel, Miyata et al. 1974), (Poole, Kojima et al. 2001). Collagen type IX and XII are associated with collagen type II fibres and contribute to their crosslinking and stabilization. Collagen VI is found in the pericellular region of the ECM (Poole, Kojima et al. 2001). Collagen X is expressed by hypertrophic chondrocytes and is thus found in the calcified layer or in the epiphyseal cartilage and in the growth plate.

The Chondrocyte

Between 5% and 10% of the total cartilage volume consists of chondrocytes, the only cell type present in the tissue. They are approximately 13-19 µm in diameter and occupy ECM lacunae. Given that the articular cartilage is avascular, chondrocytes are well adapted to thrive in a hypoxic environment by using glycolysis for energy production. It is believed that chondrocytes receive the nutrients from the synovial membrane by diffusion, however this has not been fully studied. In particular it is not known what contribution the subchondral bone makes and whether active mechanisms of transport are also involved.

As already discussed above, in spite of their apparent morphological homogeneity, at least 2 sub-populations of chondrocytes are present in the articular cartilage: the first are superficial zone chondrocytes, which display characteristics of stem cells and possibly contribute to cartilage self-renewal; and secondly the intermediate and deeper layer cells that display a more

chondrocytic phenotype and have as high expression of sox9, collagen type II and aggrecan. Epiphyseal chondrocytes from the growth plate share many of the features of deep chondrocytes but also naturally undergo hypertrophy whereas articular cartilage chondrocytes do not.

Chondrocytes share some characteristics of tumour cells: Chondrocytes are capable of anchorage independent growth (Benya and Shaffer 1982), and have a remarkable phenotypic stability that allows them to form stable cartilage if implanted ectopically , even as a single cell suspension, in the muscle of immune deficient mice. This capacity is lost however, with serial passaging, and it is correlated with the potency of expanded chondrocyte preparations for ACI (Dell'Accio, Vanlauwe et al. 2003; Saris, Vanlauwe et al. 2009). Therefore, the preservation of this capacity is essential in tissue engineering applications.

Cartilage homeostasis and osteoarthritis.

Cartilage homeostasis occurs through a balanced modulation of catabolism and anabolism which maintains the ECM in a stable condition. In physiological conditions the chondrocyte supports a very low turnover of matrix molecules. For instance, the half-life of collagen type II has been estimated around 117 years (Verzijl, DeGroot et al. 2000). Upon injury however, vigorous anabolic responses are initiated to counteract cartilage damage. These include chondrocyte proliferation and increased synthesis of ECM molecules including collagen type II and proteoglycans (Eltawil, De Bari et al. 2009; Dell'accio and Vincent 2010). When these responses are adequate, homeostasis is re-established and cartilage integrity can be preserved or restored. When they are insufficient, however, further degradation of the cartilage occurs leading eventually to osteoarthritis (OA).

For years it has been believed that damaged cartilage has a very poor capacity to repair, or does not repair at all after injury. “If we consult the standard Chirurgical writers form Hippocrates down to the present age, we shall find that an ulcerated Cartilage is universally allowed to be a very troublesome disease and when destroyed, it is never recovered.” (W. Hunter 1743).

This statement is still true for more severe abrasions, however, studies have highlighted that joint defects do have the capacity to heal. In 1996, an investigation reported that, from a cohort of 28 young adult athletes with cartilage injury, almost 80% had good to excellent knee function 14 years following trauma and returned to pre-injury sports activity level. With the exception of 3 patients, no treatment was administered (Messner and Maletius 1996). A similar study investigating the effect of young adult athletes undergoing ACL reconstruction and correlating their outcome to the presence or absence of a chondral lesion saw almost 80% returning to previous sports activity levels after 8.7 years and no difference was seen between those with and without cartilage injury (Shelbourne, Jari et al. 2003). This capacity to repair was later strengthened by clinical and imaging studies by MRI. A study which screened a group of "healthy" individuals with a mean age of 45 years, showed that of the 44% that had chondral defects, about 30% improved spontaneously, while another 30% remained stable over a period of approximately 2 years. However, the group also reported that 30% worsened over this timeframe (Ding, Cicuttini et al. 2005; Ding, Garnero et al. 2005; Ding, Cicuttini et al. 2006). A similar study performed on a group of older healthy individuals (with a mean age of 57),

showed that over 60% of defects worsened, while approximately 30% remained the same and only 5% improved (Wang, Ding et al. 2006).

This data shows that isolated chondral defects have a remarkable capacity for repair when they occur in young individuals with otherwise healthy joints. However the chance of repair decreases progressively with age, body weight, mal-alignment and other co-morbidity. In such case, not only does repair not happen, but the presence of such isolated lesions predisposes the patient to accelerated cartilage loss and OA (Ding, Cicuttini et al. 2007). In addition, a study that used arthroscopy to follow the natural progression of chondral defects following ACL reconstruction, showed that femoral condyle defects had a far superior capacity to heal compared to those on the tibial plateau or patella-femoral joint, highlighting that the location of the defect is also important (Nakamura, Horibe et al. 2008).

The response of the articular cartilage to injury involves the simultaneous activation of both catabolic and anabolic pathways. The former is possibly needed for the breakdown of damaged tissue, and the latter for the repair. While in normal conditions these two aspects of repair are balanced and coordinated, following injury they can become pathogenic and drive further cartilage breakdown. However, even if a particular mechanism (such as MMP activity (see below)), is considered pathogenic, an element of their function is still essential for the repair process, as mice carrying a mutation in the MMP cleavage site of aggrecan are more susceptible than wild type controls to instability induced OA (Little, Meeker et al. 2007), thus proving the importance of a balanced response.

Catabolic factors

The main enzymes that contribute to cartilage breakdown are aggrecanases and collagenases that belong to the metalloproteinase family. Metalloproteinases are proteolytic enzymes that require a metal, such as zinc, for their activity. The most abundant in the joint are Matrix Metalloproteinases (MMPs) and A Disintegrin And Metalloproteinase with Thombospondin Motifs (ADAMTs).

***MMPs*.** Matrix metalloproteinases are divided into 4 sub categories; collagenases (MMP-1 -8 and -13), which can degrade collagens I-IV and VII; gelatinases (MMP-2 and -9), which further break down the fragments produced by the collagenases; stromelysins (MMP-3 -10 and -11), have a wider range of substrates including collagen IX and proteoglycans; Membrane type MMPs (MMP-14 -15 -16 -17 -24 and -25), which have several substrates but can also activate other MMPs. All MMPs consist of 3 structural domains: a catalytic domain, responsible for the

enzymes activity; a pro domain, which interacts with the catalytic site and must be cleaved before the enzyme can exert its activity, and the pre domain, required for maturation and secretion from the cell (Rannou, Francois et al. 2006).

MMPs are heavily involved upon injury and OA, for example MMP-13 and -9 are both upregulated in human OA (Mitchell, Magna et al. 1996; Bau, Gebhard et al. 2002; Kevorkian, Young et al. 2004). MMP13 knockout mice are resistant to instability induced OA (Little, Barai et al. 2009), while mice overexpressing MMP13 have an increase in cartilage lesions (Neuhold, Killar et al. 2001). Interestingly MMP-3 is downregulated in OA (Swingler, Waters et al. 2009), and compared to wild type, MMP3 knockout mice had a worse outcome of OA, 3-4 weeks following surgical induction by transection of the medial collateral ligament and partial menisectomy (Clements, Price et al. 2003).

ADAMTS. The aggrecanases (ADAMTS-1 -4 and -5) contribute to cartilage breakdown by cleaving the Glu^{373}-Ala^{374} of aggrecan. They consist of a signal domain, a prodomain, a metalloproteinase domain, a disintegrin domain, and two thrombospondin-like domains. As well as aggrecan and a number of other substrates, ADAMTS are able to process procollagen (e.g. type I and II), into its active form, (Colige, Vandenberghe et al. 2002; Nagase and Kashiwagi 2003).

The most highly expressed aggrecanase in human OA is ADAMTS5 (although ADAMTS4 is also slightly upregulated) and mice lacking the functional protein, were protected from cartilage degradation in murine models of both osteoarthritis and inflammatory arthritis (Bau, Gebhard et al. 2002; Glasson, Askew et al. 2005; Stanton, Rogerson et al. 2005). It was later shown that specific cleavage of aggrecan in the inter-globular domain is the main contributor to this phenomenon as blocking cleavage of this site alone diminished cartilage loss (Little, Meeker et al. 2007). Specific inhibitors of ADAMTSs have been developed and are being tested in clinical trials (Chockalingam, Sun et al. 2011).

TIMPs. Tissue inhibitors of metalloproteinases (TIMPs) are a class of secreted molecules that inhibit MMPs. They are relatively small molecules of around 21KDa and all four inhibit the active forms of MMPs, which occurs primarily through their N terminal (Brew, Dinakarpandian et al. 2000; Baker, Edwards et al. 2002); (Amour, Slocombe et al. 1998; Amour, Knight et al. 2000) The spectrum of MMP inhibition varies between different TIMPs. TIMP-3 has the broadest range of activity, inhibiting all MMPs, as does TIMP-2. TIMP-1 has a much narrower spectrum of inhibition but exhibits stronger activity on a number of MMPs than TIMP-2/-3

(MMP-3/-7). TIMP-3 inhibits other metalloproteinases as well, for example, ADAMTS-4 and -5 (Brew, Dinakarpandian et al. 2000).

The importance of these molecules in homeostasis is demonstrated by the fact that the TIMP-3 knockout mice undergo spontaneous cartilage breakdown, (Sahebjam, Khokha et al. 2007) and like MMPs, TIMPs are also regulated in OA (Kevorkian, Young et al. 2004). TIMPs and synthetic inhibitors of metalloproteinases have therefore been considered potential tools to limit cartilage breakdown. Nevertheless, clinical trials with MMP inhibitors have been so far unsuccessful, largely due to the occurrence of severe side effects.

Anabolic factors

Considering the evidence above (section 1.3), it is now clear that cartilage lesions have the capacity to repair. This, along with catabolic factors involved in remodelling of the tissue (above), is largely dependent on the anabolic response of the cartilage.

Many of the pathways involved in this response of cartilage to injury include those that feature heavily during limb development, particularly WNT signalling (Dell'Accio, De Bari et al. 2006), BMPs (Lories and Luyten 2005) and FGFs, (Vincent, Hermansson et al. 2002; Lories and Luyten 2005; Dell'Accio, De Bari et al. 2006). Growth factors such as insulin-like growth factors I and II, as well as the TGFβ superfamily members, such as TGFβ-2 are also involved in proteoglycan synthesis, (Luyten, Hascall et al. 1988; van Osch, van den Berg et al. 1998).

Loss of these molecules can result in an imbalance during the response to injury. For instance, mice deficient in FGF2 developed accelerated OA after Destabilisation of the Medial Meniscus, DMM, (a murine model of OA), and delivery of exogenous FGF2 was sufficient to rescue the phenotype (Chia, Sawaji et al. 2009).

The BMPs, which are known to promote cartilage and bone formation, are involved in matrix synthesis and remodelling in normal cartilage and after injury, (Urist 1965; Wozney 1995; Dell'Accio, De Bari et al. 2006). BMP2 has been shown to enhance matrix turnover and proteoglycan synthesis following IL1-induced injury, (Blaney Davidson, Vitters et al. 2007) and mice lacking BMP receptor 1 undergo spontaneous cartilage degradation (Rountree, Schoor et al. 2004). However, intrarticular delivery of BMP2 to mice resulted in osteophytosis and ectopic tissue formation (van Beuningen, Glansbeek et al. 1998). In fact the complications associated with BMP2 and its differential responses depending on the target tissue has led to halting of clinical trials.

Single nucleotide polymorphisms (SNPs) in GDF5 have been associated with OA in humans (Miyamoto, Mabuchi et al. 2007) and loss of TGFβ receptor also causes loss of healthy articular cartilage which is replaced by hypertophic cartilage or bone (Serra, Johnson et al. 1997). However, loss of TGFβ signalling from the underlying subchondral bone improved the outcome of OA (Zhen, Wen et al. 2013).

It is clear that disruption of the above pathways or loss of function of individual molecules can have damaging effects on the cartilage. As well as consequences directly caused by mutations, many of these molecules interact with each other and changes in activity of one may affect many others. For example, WNT-3a was shown to regulate a number of FGFs in limb development (Kawakami, Capdevila et al. 2001). This must be taken into consideration when searching for disease targets.

Mechanical loading can also stimulate an anabolic response. For example, compression of explanted bovine articular cartilage caused an upregulation of aggrecan expression after 1 hour (Valhmu, Stazzone et al. 1998). Isolated cells also exhibit a response to compression when suspended in a 3 dimensional scaffold (Buschmann, Gluzband et al. 1995)

Osteoarthritis.

When injury persists or is too severe, the cartilage cannot repair and continues to degenerate until eventually the tissue develops osteoarthritis (OA). Differences between the healthy (a) and OA (b) joint are highlighted in **Figure 8**.

OA is a chronic disease, characterised by degradation of the articular cartilage. Other features include sclerosis of the subchondral bone, osteophytosis, a relatively modest and usually transient inflammation of the synovial membrane, and damage to several other joint structures such as ligaments, joint capsule and menisci, which contribute to aggravate the joint altered biomechanics. The symptoms include chronic pain, stiffness and loss of mobility.

OA affects over a third of the population worldwide (Lawrence, Helmick et al. 1998; Lawrence, Felson et al. 2008). Due to the high disability that it causes, it has a huge impact on social costs and at present, available treatments only provide symptomatic relief without halting the progression of the disease (Alcaraz, Megías et al. 2010). In many cases joint replacement is therefore required and although it is an efficacious solution, it has several shortcomings, particularly in advancing age. These include the limited life-span of the replacement joint, which is a problem with the ageing population and the ever increasing patient population with early OA who will require complex revisions. In addition, in nearly one third of cases, joint

replacement does not meet patient expectations (Dieppe, Lim et al. 2011). Finally, prosthetic joint replacements are not an adequate solution in young individuals who expect an active lifestyle. Therefore, a better understanding of the molecular mechanisms driving the pathogenesis of OA and possibly joint repair are required to develop more efficacious treatments.

Throughout life, cartilage is constantly subjected to small repetitive trauma. From data previously discussed in section 1.3 Cartilage Homeostasis and Osteoarthritis, we know that in young healthy individuals, cartilage has a remarkable capacity to repair. However this ability is decreased with increasing age, and the failure to restore tissue homeostasis following injury often leads to OA. As well as age and other common risk factors such as weight, another risk factor that plays a key role is genetic background. For example, a number of SNPs have been associated with OA. Secreted frizzled-related protein 3 (sFRP3), is a WNT protein antagonist, and is encoded by the gene frizzled motif associated with bone development (frzb), which was associated with hip OA in females. Another SNP in the 5' untranslated region of gdf5 has also shown strong associations with OA (Settle, Rountree et al. 2003; Loughlin, Dowling et al. 2004; Dodd, Rodriguez-Fontenla et al. 2011). The same genetic variability observed in humans at individual level are also observed between inbred mouse strains (Glasson 2007). Such variability correlates with the capacity to heal acute cartilage defects: for example, following acute mechanical injury DBA/1 mice showed superior healing when compared to C57BL/6 (Eltawil, De Bari et al. 2009).

The importance of the acute phase following injury has recently been highlighted; Following destabilisation of the medial meniscus (DMM) in mice, (a model for OA), genes involved in the pathogenesis of the disease were upregulated 6 hours following surgery but were not upregulated in those mice whose joints were immobilised. This resulted in the prevention of OA for up to 12 weeks (Fitzgerald, Jin et al. 2004; Kurz, Lemke et al. 2005; Burleigh, Chanalaris et al. 2012).

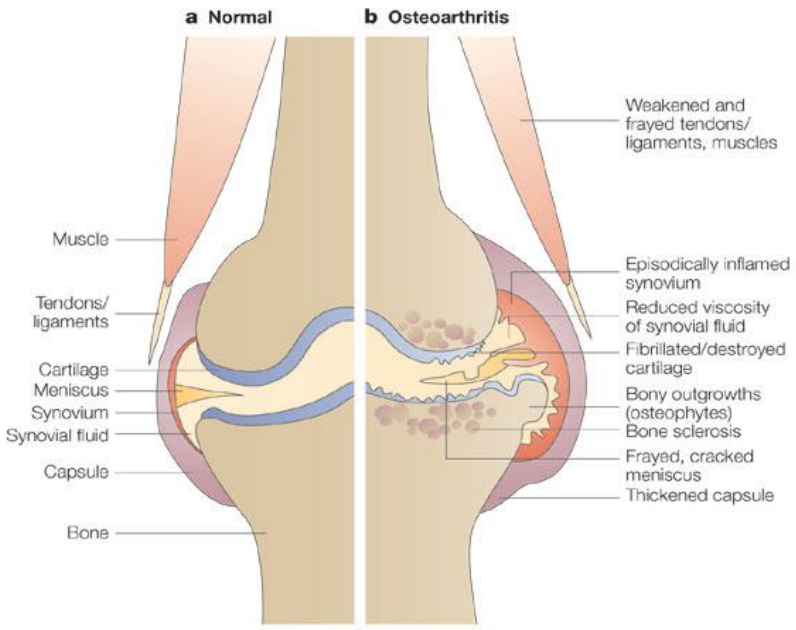

Figure 8: Diagrammatical representation of pathological processes associated with OA, (right side) in comparison to a normal healthy joint, (left) (Wieland, Michaelis et al. 2005). Permission Granted from Nature publishing group, Licence number 3477880269565.

Inflammation and OA

Although synovial inflammation can occur in the early phases of OA and in subsets of patients later on, its role in disease pathogenesis is debatable. There is abundant evidence of synovitis in subsets of patients with OA, including features such as thickening of the synovium lining layer, thickening of the stroma and infiltrates of inflammatory cells, and at times, samples are histologically indistinguishable from those of rheumatoid arthritis (Krenn et al., 2006). Production of inflammatory molecules is a feature of the OA synovium and even cartilage. In fact, Gruber et al. reported that even explantation of cartilage and cutting of explants in vitro results in IL-1 release and local downstream signalling in chondrocytes (Gruber, Vincent et al. 2004).

OA synovitis was shown to contribute macrophage-derived cytokines such as ILβ and TNFα. As well as driving inflammation these molecules upregulated the expression of MMPs and aggrecanases resulting in degradation of the ECM, (Tetlow, Adlam et al. 2001; Bondeson,

Wainwright et al. 2006). In particular treatment of meniscus with IL1β, IL6 or fibronectin fragments (FnF) which is found in the synovial fluid and extracellular matrix of arthritic joints, increased expression of matrix degrading enzymes such as MMP-1. However, the response was specific depending on the stimuli, with IL1β inducing MMP-2 and MMP-10, IL6 inducing MMP-3 and ADAMTS1, and FnF inducing MMPs -2, -3, -8, -10, and -13 as a result their effect on ECM proteins was slightly different (Stone, Loeser et al. 2014). As well as ECM breakdown, TNFα was also shown to induce apoptosis in chondrocytes from chick embryo (Aizawa, Kon et al. 2001). Chondrocytes themselves also express these cytokines as well as others including IL6 and IGF1, (Guerne, Carson et al. 1990; Moos, Fickert et al. 1999), further contributing to catabolism.

In spite of this abundant descriptive literature and of in vitro evidence, the attempts of blocking OA progression by targeting inflammation have been consistently frustrating with few exceptions. Caron et al was able to show that IL-1 blockade protected from cartilage lesions in a dog model of OA (Caron, Fernandes et al. 1996). However, similar studies have failed to confirm these results. In fact, IL1 knockout mice develop more severe OA than wild type controls (Clements, Price et al. 2003).

WNT Proteins

WNTs are a family of extracellular, secreted signalling molecules, of which there are nineteen expressed in humans and mice. Their sequence is highly conserved across species, and share up to 60% sequence homology, (Nusse and Varmus 1992; Miller 2002).

WNTs are heavily glycosylated and lipid-modified proteins: the addition of a palmitic acid and a pamiytoleic acid are essential for their secretion and biological activity, but also the cause of their hydrophobicity (Willert et al., 2003). This makes their preparation as highly purified recombinant molecules complicated and our understanding regarding their conformation, receptor specificity, and other structural features, is limited. WNTs share 22 cysteine residues, distributed throughout the protein, which are likely involved in their folding through the formation of disulphide bonds, (Mason, Kitajewski et al. 1992).

WNT receptors

WNTs bind a family of at least 10 receptors called Frizzled receptors (FZD). FZDs are 7 transmembrane domain receptors which bind WNT ligands through their extracellular N-terminus that contains a cysteine rich domain, (Xu and Nusse 1998). After WNT binds, FZD mediate their signalling through the association of different co-receptors and intracellular kinases which lead to downstream effects on gene expression.

In humans, FZD receptors can be clustered into 4 groups; FZD1,FZD2 and FZD7 share 75% sequence identity; FZD5 and FZD8 share 70% homology; FZD4, FZD9 and FZD10 approximately 65%; and FZD3 and FZD6 are 50% similar. Between clusters the receptors share among 20% and 40% identity. Another receptor, often considered as the 11th FZD is Smoothened (SMO), a receptor for the hedgehog pathway which shares 24% homology with FZD2 (Fredriksson, Lagerstrom et al. 2003). Expression patterns vary throughout development and between different FZDs. For example FZD1 expression is found in foetal lung and kidney and in adulthood expands to include heart, pancreas, prostate, ovary and placenta, whereas FZD2 is expressed in foetal brain, lung and kidney, but only in the heart during adulthood (Sagara, Toda et al. 1998). A certain amount of redundancy however, is seen between FZDs of the same groups. *Fzd2*$^{-/-}$ embryos have partial defects in palate closure while double mutants (*fzd2*$^{-/-}$*:fzd7*$^{-/-}$*)* have fully penetrant palate closure defects (Yu, Ye et al. 2012). Some FZDs have also been shown to exhibit specificity towards certain WNT pathways. For example rat FZD-1 induced β-catenin signalling but not rat FZD-2, which instead was shown to induce Ca2+ release (Yang-Snyder, Miller et al. 1996; Slusarski, Corces et al. 1997).

Engagement of WNT ligands with FZD receptors can induce association with specific co-receptors which are responsible for the activation of different pathways. For example, WNT1 a canonical WNT ligand, (see below) induces LRP-6 association (Tamai, Semenov et al. 2000). LRP-5 is another co-receptor associated with canonical WNT signalling and shares 71% sequence homology with LRP-6 (Tamai, Semenov et al. 2000). These receptors are essential for the proper function of WNT pathway activation and activity, as *lrp5*$^{-/-}$ mice had increased cartilage breakdown after destabilisation of the medial meniscus (Lodewyckx, Luyten et al. 2012).

Although FZD are considered the main class of WNT receptors there are others that are able to bind and mediate the activity of WNT proteins, for example the ROR transmembrane tyrosine kinases. ROR2, a receptor which triggers the activation of a non-canonical WNT pathway, the planar cell polarity pathway through binding of WNT5a (Gao et al., 2011; Grumolato et al., 2010) (see below).

WNT signalling pathways

WNTs can activate several signalling cascades. The best described is the canonical WNT pathway, which is dependent on β-catenin. Some WNTs, (e.g. Wnt5a) can also signal through alternative pathways, generally called “non-canonical”, many of which are activated by calcium mobilization (Kühl, Sheldahl et al. 2000). For a long time it has been thought that some WNTs can activate the canonical pathway (canonical WNTs; i.e. WNT1, WNT8, WNT3A), and some others, the non canonical pathways (i.e. WNT5A and WNT11). This was based on a number of assays including the capacity of canonical WNTs to induce primary axis duplication in Xenopus Laevis embryos, and the capacity to activate the Super8TOPFlash reporter assay, (a plasmid containing TCF/Lef response elements upstream of a luciferase gene and therefore reporting β-catenin activity). Equally, it was shown that some FZD receptors mediated one or the other pathway (Kuhl, Sheldahl, Malbon, & Moon, 2000) and therefore it was assumed that the affinity of different ligands for different receptors and the receptor repertoire in different cells determined their capacity to activate one or another pathway. Although this view still stands, it has been challenged by a recent paper from our laboratory, showing that, in chondrocytes, WNT-3A can activate either CaMKII or the canonical WNT pathway in a dose dependent manner, and that the activation of one or the other pathway determines the final functional outcome (Nalesso et al., 2011). This information resolved a number of paradoxes associated with the “one WNT-one pathway” theory. For instance in early Xenopus Laevis development

where dorsal accumulation of WNT11 was necessary for dorso-ventral patterning, but both WNT11-dependent canonical signalling in the dorsal embryo and WNT11-dependent CaMKII signalling in the ventral region, were equally necessary for dorsoventral patterning (Kestler, Kuhl, & Kühl, 2011).

The Canonical/β-catenin pathway

In the absence of a WNT ligand, β-catenin is constitutively phosphorylated by GSK-3β and targeted for degradation through the ubiquitin proteasome pathway. When a WNT ligand binds to FZD, FZD associates with LRP5/6, which is subsequently phosphorylated in the PPPSP motif of the intracellular domain. This results in the recruitment and sequestration of GSK3β and Axin into multivescicular bodies. Consequently, GSK3β is no longer available to phosphorylate its several substrates including β catenin (Taelman, Dobrowolski et al. 2010). As a result, β-catenin accumulates in the cytoplasm before translocating into the nucleus where it interacts with TCF/LEF transcription factors, and activates the expression of cell specific target genes, such as axin2 (Kikuchi 2000; Logan and Nusse 2004; Macdonald, Semenov et al. 2007). This is represented in the scheme in **Figure 9**.

The canonical WNT pathway is important in both embryogenesis and in adult life: for example, the determination of the anteroposterior and dorsoventral axis, gastrulation, organ development during embryogenesis and cell proliferation, differentiation, tissue repair, and stem cell maintenance in adulthood (Logan and Nusse 2004).

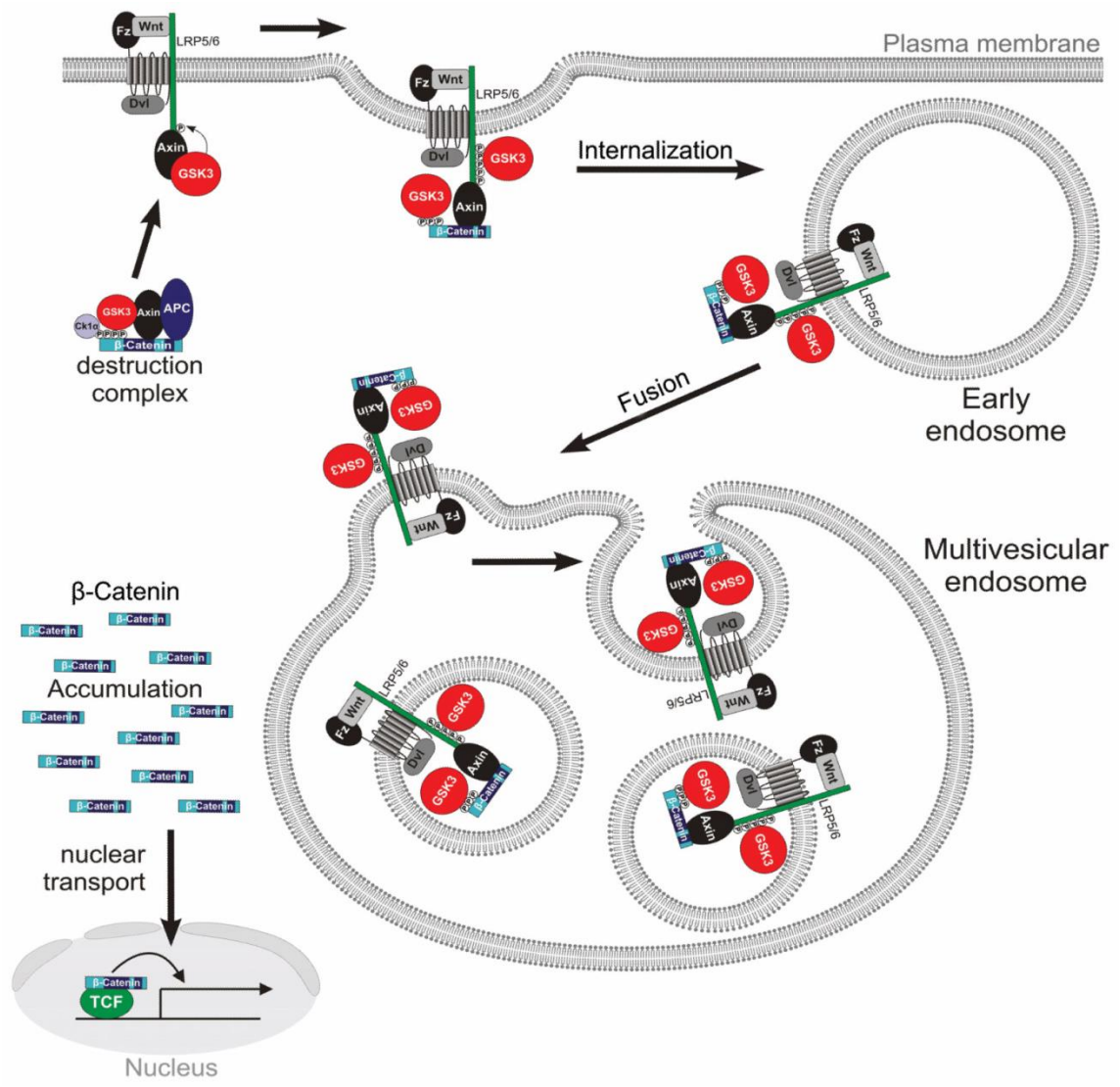

Figure 9: The β-catenin dependent pathway. In the presence of a ligand, GSK3β is sequestered into multivesicular bodies, which allows β-catenin to translocate to the nucleus and activate transcription (Taelman, Dobrowolski et al. 2010).Permission granted from Elsevier, Licence number 3477880448530.

The canonical WNT pathway is both necessary and sufficient for joint formation. Conditional deletion of β catenin resulted in some degree of joint fusion and its misexpression resulted in the ectopic formation of joint-like structures (Hartmann and Tabin 2000; Guo, Day et al. 2004) More recently, WNT/β-catenin signalling was shown to maintain the phenotype of superficial zone cells within the developing and adult articular cartilage and inhibits chondrocytes from progressing towards hypertrophy, (Yasuhara, Ohta et al. 2011).

In adulthood β-catenin was still expressed in the superficial zone cells but not in chondrocytes of the deeper zones of the articular cartilage, (Ryu, Kim et al. 2002), suggesting a similar role for the pathway as during development.

The non canonical/Ca^{2+} dependent and independent pathways

The non-canonical pathways are far less understood than the β catenin pathway. One branch of these pathways involve the engagement of WNT ligands (e.g. WNT5A) with FZDs, which promotes G-protein dependent intracellular calcium accumulation (Kühl, Sheldahl et al. 2000) (see **Figure 10**). This results in the initiation of several downstream cascades leading to the activation of CaMKII, PKC and calcineurin (Semenov, Habas et al. 2007). There are also a number of Ca^{2+} independent non canonical pathways including the planar cell polarity pathway (PCP) and the c-Jun N-terminal kinase (JNK) pathway which involve WNTs binding to ROR2 rather than FZD receptors.

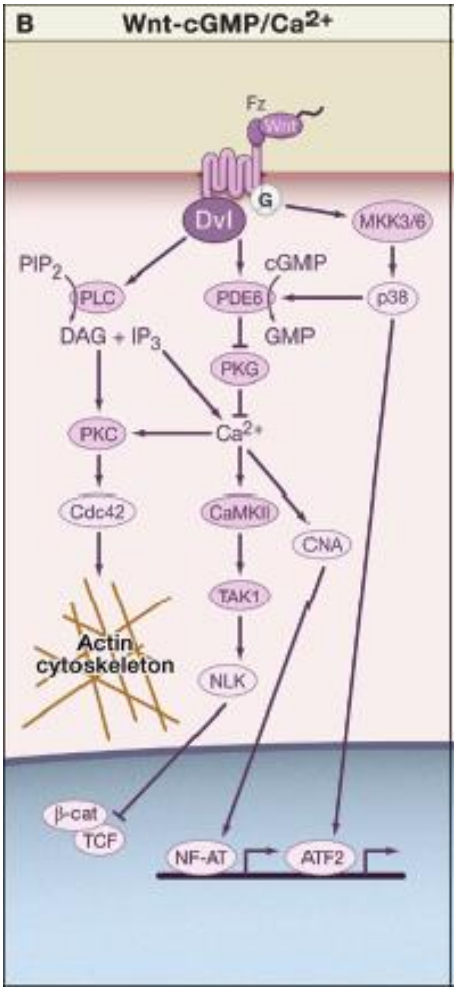

Figure 10: Scheme for activation of calcium dependent WNT pathways. (Semenov, Habas et al. 2007). Permission granted by Elsevier, licence number 3478120069059.

CaMKII Pathway.

A well-studied non-canonical pathway is the Ca^{2+}/calmodulin kinase II (CaMKII) pathway. CamKII is a serine/threonine kinase of which there are four isoforms (α, β, γ and δ) (Shimazaki, Wright et al. 2006), with primarily γ and δ found in adult articular cartilage (Unpublished data by Kristina Wagner within our laboratory). CaMKII exists in the cells in the form of a multimeric complex composed of estimated 8-14 monomers. Each monomer is composed of a catalytic domain, a regulatory domain, and an association domain. The catalytic domain is responsible for the phosphorylation of substrates including CaMKII itself; the regulatory domain, under resting conditions, auto inhibits the enzymes activity by binding and blocking the catalytic domain; The association domain is necessary for the CaMKII monomers to associate in the large

multimer, (Griffith, Lu et al. 2003)(represented in **Figure 11**. Following ligand-receptor interaction (i.e. WNT-5A with FZD-2, -3, -4 and -6 receptors in Xenopus Laevis (Kühl, Sheldahl et al. 2000)or isoproterenol with adrenergic receptors), Ca^{2+} is released and induces a conformational change that frees the catalytic domain from the inhibitory domain. Subsequently, CaMKII phosphorylates itself in Thr286. This phosphorylation, very near the catalytic site, prevents the binding of the inhibitory domain to the catalytic domain, and from then on CaMKII is active even in the absence of Ca^{2+} (Ca^{2+}-independent activity) (Hudmon and Schulman 2002). At least in the heart, CaMKII activation can also take place through oxidation: following cardiomyocyte stimulation with angiotensin I, after an initial activation of the enzyme by Ca^{2+} stimulation, the re-association of the regulatory domain to the catalytic domain is blocked by oxidation of methionines 281/282 (Erickson, Joiner et al. 2008).

In embryogenic skeletogenesis, the CaMKII pathway plays a role in endochondral bone formation, by driving cells to undergo the transition from proliferative to hypertrophic chondrocytes, (Li, Ahrens et al. 2011). In adult cartilage, CaMKII is activated in osteoarthritis (Nalesso G, Thomas B. et al. Manuscript in preparation), and mediates loss of phenotypic markers in chondrocytes driven by WNT-3A (Nalesso, Sherwood et al. 2011) and WNT-5A (Nalesso G, Thomas B et al. Manuscript in preparation).

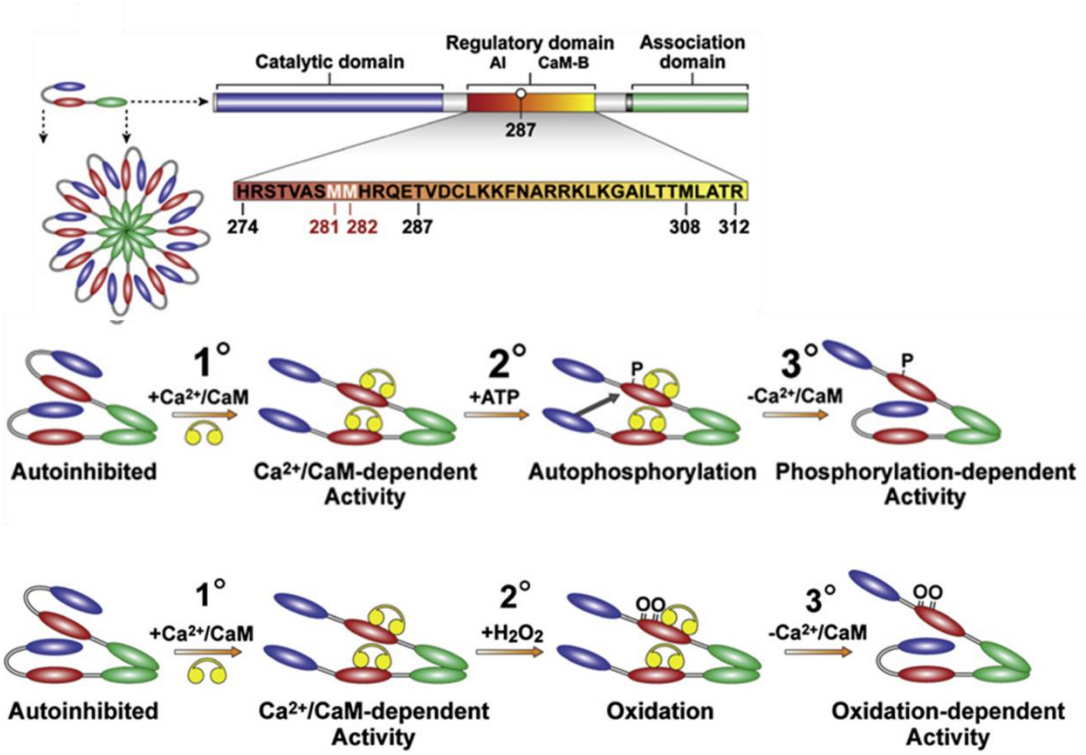

Figure 11: Representation of CaMKII domains and mechanisms of activation involving both phosphorylation and oxidation. Yellow symbols represent calmodulin. Following initial activation, phosphorylation or oxidation of the regulatory domain maintains activity (Erickson, Joiner et al. 2008).Permission granted by Elsevier, licence number 3478130998354.

Other calcium dependent pathways include: calcineurin, a protein phosphatase that has been linked with anabolic and catabolic activities in chondrocytes (Yoo, Park et al. 2007); and PKC, which plays an important role in many cellular functions (proliferation, survival), and in the chondrocyte is involved in phenotypic maintenance and regulation of apoptosis (Lee and Yang 2010).

Planar cell polarity pathway (PCP).

The PCP is a well characterised Ca^{2+} independent pathway (Bradley and Drissi 2010). It has been shown to drive cell migration and polarity during developmental processes, (Borovina, Superina et al. 2010). The PCP pathway is involved in regulating limb elongation in the limb bud, where WNT5a caused formation of a complex between ROR2 and Vangl2 and resulted in the differential phosphorylation of Vangl2 by CK1δ, as shown in **Figure 12** (Gao, Song et al. 2011).

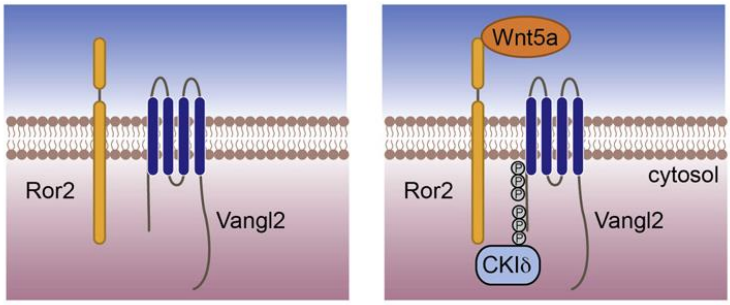

Figure 12: Phosphorylation of Vangl2 following WNT5a stimulation. WNT5A led to activation of Vangl2 through phosphorylation of serine and threonine residues. This was mediated through complex formation with ROR2 (Gao, Song et al. 2011).Permission granted by Elsevier, licence number 3478131117334.

JNK pathway.

c-Jun N-terminal kinase (JNK) is a mitogen-activated protein kinase (MAPK), best known for its involvement in apoptosis but it is also involved in many other processes such as autophagy, inflammation (Han, Jung et al. 2013), and joint morphogenesis (Kan and Tabin 2013). The JNK pathway can be activated via two mechanisms. One is through WNT binding ROR2 and mediating JNK activity by activating PI3K which signals to small GTPase, cdc42, leading to activation of downstream kinases (shown in **Figure 13**A) (Schambony and Wedlich 2007). The other is through WNT binding FZD and activating JNK via Dvl (mammalian homologue of drosophila dishevelled (Dsh), which is recruited to the plasma membrane through its DEP domain leading to activation of downstream components (shown in **Figure 13**B) (Moriguchi, Kawachi et al. 1999). This is a different mechanism from the involvement of Dsh in the canonical WNT pathway which occurs by binding of axin to the DIX domain of Dsh (Kishida, Yamamoto et al. 1999; Wallingford and Habas 2005). Activation of JNK ultimately leads to activation of transcription factors such as c-Jun and ATF-2 which are components of the AP-1 complex (Figure 13).

It has recently been shown that c-Jun plays a major role in joint development as loss of c-Jun led to disruption of the joint interzone (Kan and Tabin 2013). This was shown to be, in part, due to its ability to activate transcription of both WNT9a and WNT16. The Jun pathway is both upstream and downstream of WNT16 as JNK is a downstream target of WNT16 in keratinocytes

(Teh et al., 2007). It has also been linked to OA as higher levels of phosphorylated JNK were found in OA chondrocytes compared to controls (Clancy, Rediske et al. 2001).

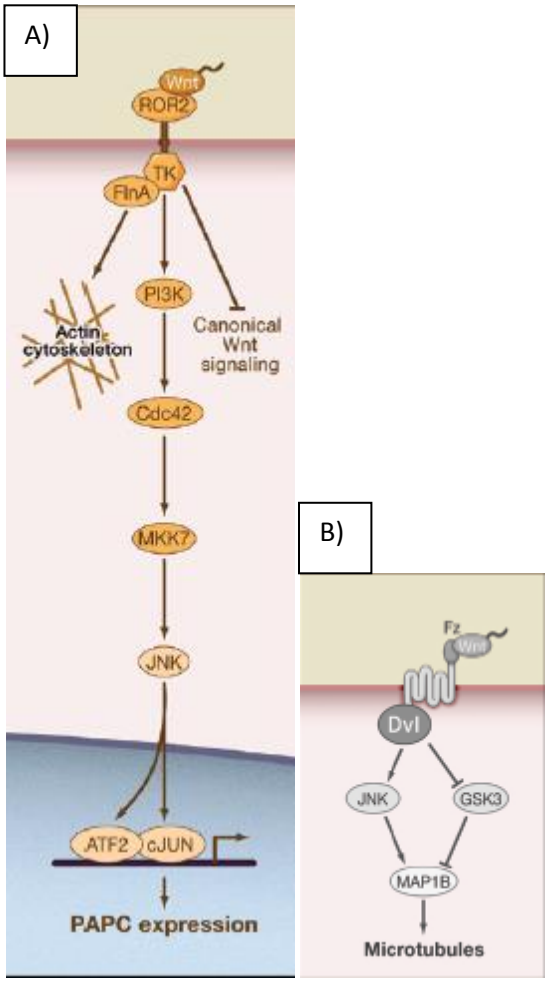

Figure 13: Representation of JNK signalling mechanisms (Semenov, Habas et al. 2007). A) Represents the activation of JNK via ROR2 receptor activation and B) through FZD receptor activation. Permission granted by Elsevier, licence number 3478120069059.

WNTs in development

During embryonic development WNT signalling controls several aspects of morphogenesis, from axis determination and organ morphogenesis. As discussed above, WNTs and WNT activated pathways play important roles in embryonic limb development and joint formation. Hartmann and Tabin reported that WNT4, WNT5a and WNT5b had distinct expression patterns within the developing limb and demonstrated that WNT9A is an early marker of the joint interzone preceding GDF5 (Hartmann and Tabin 2000). Soon after, the same group showed that WNT9a is a very early marker of joint formation, and its ectopic expression was sufficient to the formation of ectopic joint-like structures in developing chick limbs, characterised by the expression of Gdf5 (Hartmann and Tabin 2001). In spite of this, WNT9a is not required for joint formation as mice lacking the gene had almost normal joints (Spater, Hill et al. 2006) suggesting redundancy with other WNTs expressed within the joint interzone.

As well as WNT9a, WNT4 and WNT16 are also expressed in the developing joint and all three WNTs were shown to activate the canonical WNT pathway. In fact Guo et al. 2004, demonstrated that WNT canonical signalling was sufficient to trigger joint formation and also that it is required for joint formation, as cartilage-specific conditional deletion of β catenin in mice (Huelsken, Vogel et al. 2001) caused partial fusion or the complete absence of joints (Guo, Day et al. 2004). Conditional overexpression, (using a constitutively active form of β-catenin under the collagen type II promoter) showed a large reduction in cartilage formation and also exhibited joint fusions (Guo, Day et al. 2004). The observation of joint fusions in both gain and loss of function mutants is interesting and may highlight the importance of balanced activation between WNT pathways as too little or too much both have detrimental outcomes and that gradients of WNT signalling rather than mere activity or lack of it are necessary for patterning.

To further investigate the role of β-catenin in joint formation, a conditional β catenin knockout within the joint interzone was created by crossing β-catenin$^{fl/fl}$ mice with Gdf5-Cre mice (Koyama, Shibukawa et al. 2008). Although most joint appeared normal, joint fusions were observed in the wrists and a reduction was seen in GDF5 and lubricin expression (Koyama, Shibukawa et al. 2008). In keeping with these data, deletion of β-catenin (in tamoxifen inducible Col2CreER;β-catenin$^{fl/fl}$mice) also caused loss of lubricin in the knees of 7 week old mice, (Yasuhara, Ohta et al. 2011). Importantly, these experiments led to the discovery that the phenotype of the superficial cells of the developing cartilage is dependent on β catenin signalling: postnatal conditional β catenin deletion resulted in the inappropriate full

chondrocytic differentiation of superficial zone cells, loss of the specific phenotype of these cells and loss of their proliferative potential. Since this cell population represents the progenitor pool of the articular cartilage, this predictably led to the entire articular cartilage becoming hypocellular and with a disrupted architecture. Reciprocally, a postnatal pulse of conditional expression of constitutively active β catenin resulted in the expansion of this population and thickening of the articular cartilage. WNT-3A treatment of neonatal superficial zone cells induced lubricin upregulation in vitro and in vivo, after transplantation into athymic mice. Interestingly collagen type X expression, (a marker of hypertrophy) was lower in the WNT3a treated cells. In addition, cells from CagCreE;b-catenin$^{fl/fl}$ (tamoxifen inducible, cre recombinase system, under the chick β-actin promoter), treated with 1μM 4-hydroxytamoxifen or vehicle, and transplanted into in athymic mice showed that the resulting β-catenin deficient cartilage was characterised by strong collagen type X expression suggesting that β-catenin inhibits the maturation of chondrocytes towards hypertrophy, (Yasuhara, Ohta et al. 2011).

Collectively these data suggest an essential role for β-catenin in joint development and, at later stages, in maintaining the phenotype of the superficial zone cells and preventing hypertophic maturation of articular chondrocytes.

Finally, Spater et al. showed that a double knockout of WNT9A and WNT4 (both expressed in the joint interzone), resulted in synovial chondroid metaplasia suggesting that these WNTs, by suppressing chondrogenesis, drive progenitors to become synovial connective tissue, (Später, Hill et al. 2006).

Upstream of WNT9a and WNT16, transcription factor c-Jun also plays a pivotal role in both joint formation and lineage specification as conditional knockout of the gene had abnormal joints with joint fusion and irregular articular cartilage surfaces as well as missing ligaments, (Kan and Tabin 2013).

WNTs in adult joints and OA

Genetics studies in humans and mice have established the role of WNT signalling in OA.

In humans, loss of function polymorphisms sFRP3, a secreted WNT antagonist (Bi, Huang et al. 2009), are associated with an increased risk of OA (Loughlin, Dowling et al. 2004). This was confirmed in animal models, since sFRP3 deficient mice develop more severe cartilage damage in comparison to wild type littermates upon induction of OA by intra-articular injection of either collagenase, papain or methylated bovine serum albumin (Lories, Peeters et al. 2007).

In addition, our group have previously demonstrated that WNT canonical signalling is activated in OA and after injury (Dell'Accio, De Bari et al. 2006; Dell'accio, De Bari et al. 2008). However, both activation and the disruption of the pathway have been associated with cartilage degeneration in humans and in mice (Diarra, Stolina et al. 2007; Zhu, Chen et al. 2008; Zhu, Tang et al. 2009). Overexpression of constitutively active β-catenin in the cartilage of 6 month old mice with a tissue specific and inducible system (β-catenin$^{fx(Ex3)/fx(Ex3)}$ /Col2a1-CreER^{T2}) caused, after 2 months, destruction of the articular cartilage and formation of osteophytes, as well as acceleration of hypertrophy (Zhu, Tang et al. 2009). The same group also published that inhibition of β-catenin by overexpressing ICAT (which binds β-catenin and disrupts its interaction with TCF transcription factor) under the COL2a1 promoter resulted in cartilage destruction with complete loss of the cartilage surface by 12 months as well as an increase in chondrocyte apoptosis (Zhu, Chen et al. 2008). Therefore both too little and too much β-catenin leads to OA like changes in the articular cartilage, although this occurred via different mechanisms. Inhibition of β-catenin resulted in increased cell apoptosis while over activation led to premature chondrocytes maturation. Given these data the role of WNT signalling in OA pathogenesis was unresolved.

In 2011 however, our group showed that WNT3a (in a dose dependent manner) was able to induce both chondrocyte proliferation through the canonical WNT pathway and dedifferentiation through activation of the CaMKII-dependent pathway (Nalesso, Sherwood et al. 2011). These pathways were also shown to reciprocally inhibit one another, explaining why both exogenous WNT3A and blockade of the β catenin pathway resulted in de-differentiation: in the first case through direct activation of the CaMKII pathway, and in the second because the inhibitory effect of β catenin on CaMKII was removed (shown in **Figure 14**) (Nalesso, Sherwood et al. 2011).

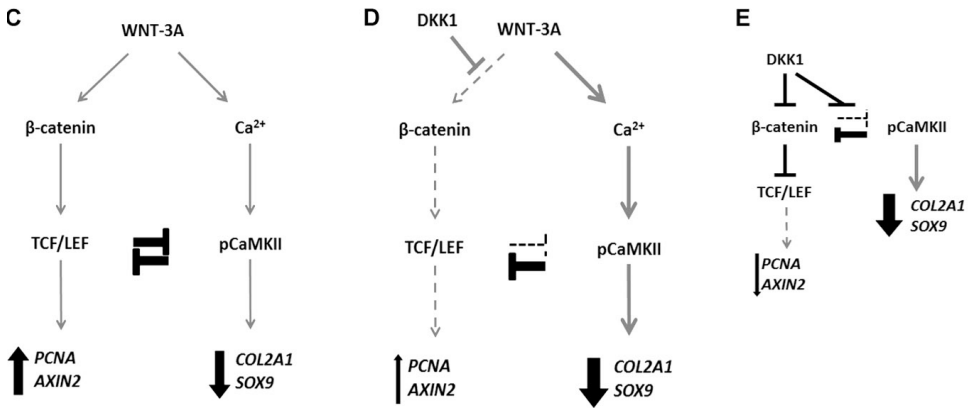

Figure 14: WNT3a activates both the canonical and CaMKII dependent pathway and these pathways reciprocally inhibit one another (Nalesso, Sherwood et al. 2011).Under permission form Rockerfeller university press.

This information increases our understanding of the extensive interactions between WNT pathways, and provides an explanation for WNT signalling paradoxes, for example, why activation and disruption of the canonical WNT pathway can both lead to the development of OA.

WNT16

WNT16 is one of the 19 human WNT proteins. Two alternative splice variants, WNT16A and WNT16B, have been described, which differ for the alternative use of the first exon driven from two alternative promoters (Fear, Kelsell et al. 2000). WNT16a was only expressed in the pancreas, while WNT16b, the more common variant, was more widely expressed. However detection of WNT16a has since not been replicated. A PCR analysis on the use of the alternatively spliced exon 1 demonstrated that chondrocytes indeed express only WNT16B (Nalesso et al. unpublished).

WNT16 is involved in both embryonic and adult processes. For example, single nucleotide polymorphisms in the WNT16 gene were associated with increased risk of forearm fracture and female $wnt16^{-/-}$ mice had thinner cortical bones, (Zheng, Tobias et al. 2012) suggesting the involvement of WNT16 in regulating bone density. WNT16 has also been linked to the specification of haematopoietic stem cells in zebra fish, (Clements, Kim et al. 2011), and to senescence in human fibroblasts, (Binet, Ythier et al. 2009).

With regards to its activity in synovial joints and its pathway activation profile, Guo et al., reported that WNT16 is expressed in the developing joint, and that its expression overlapped that of GDF5, WNT4 and WNT9A. Over expression led to activation of the TCF driven reporter assay (TOPflash assay) therefore showing that WNT16 is able to activate the canonical WNT pathway, in rat chondrocyte cell line, RCS (Guo, Day et al. 2004). WNT16 was later defined as being a specific marker of the superficial zone cells where β-catenin is known to be active (Yasuhara, Ohta et al. 2011). However, in other biological systems, WNT16 has been reported not to activate this signalling cascade, but instead to drive the phosphorylation of JNK and c-Jun in keratinocytes, (Teh, Blaydon et al. 2007). WNT16 was also shown to phosphorylate Vangl2 in CHO cells, and therefore, under some conditions, may also activate the PCP pathway (Gao, Song et al. 2011). These findings suggest that WNT16 might promote the activation of distinct signalling cascades in a cell context dependent manner.

Background work

WNT16 was found to be upregulated in articular cartilage in response to acute joint surface injury and in OA (Dell'accio, De Bari et al. 2008). Nalesso et al. also demonstrated that WNT16 deficient mice develop more severe OA compared to wild type littermates following DMM (Nalesso G, Thomas B et al. Manuscript in preparation) thereby suggesting a homeostatic function of WNT16 in cartilage homeostasis following injury. The identification of the cellular and molecular mechanisms and the signalling pathways that mediate such homeostatic effect and, in its absence, homeostatic failure is the subject of this study.

Hypothesis

Given the preliminary data showing a requirement of WNT16 in the homeostatic response to cartilage injury and the fact that in different cells and conditions, WNT16 can activate different signalling pathways, the central hypothesis of this work is that "WNT16 modulates chondrocyte phenotype and sub-lineage specification through β-catenin-dependent or/and independent pathways".

Aims

1. To investigate the biological effects of WNT16 in the articular cartilage.

WNT16 is expressed in the superficial chondrocytes during development (Yasuhara, Ohta et al. 2011) and is re-expressed in adulthood following injury and induction of OA (Dell'accio, De Bari et al. 2008). Wnt16 deficient mice are more susceptible to instability-induced arthritis. I have therefore explored the function of WNT16 both in adult and neonatal chondrocytes, with a focus on basic biological outcomes such as proliferation, differentiation, and lineage determination using both gain- and loss-of-function approaches.

2. To identify the signalling pathways activated by WNT16 in chondrocytes.

Wnt16 was shown to activate the canonical WNT pathway in a chondrocytic cell line and the JNK pathway in keratinocytes. I have therefore tested the activation of these pathways and other well characterised WNT dependent pathways using *in vitro* gain- and loss-of-function experiments.

3. To investigate what biological outcomes are dependent on particular signalling pathways activated by WNT16.

Our group previously showed that WNT-3A can activate multiple signalling pathways, eg. both the β-catenin and CaMKII pathways, simultaneously, and that each of these pathways are responsible for independent downstream effects. For example, the β-catenin pathway controlled cell proliferation while the CaMKII pathway caused loss of chondrocytes phenotype. Having discovered that WNT16 can also activate multiple signalling pathways, eg. the β-catenin pathway and the JNK pathway, I set out to investigate if these pathways specifically control particular outcomes, such as the upregulation of lubricin.

CHAPTER 2:

Materials and Methods

Solutions and buffers

Complete medium for eukaryotic cell culture

1x antibiotic-antimycotic solution (AA) (Gibco)

10% (v/v) foetal bovine serum (FBS) (Invitrogen)

In Dulbecco's modified Eagle medium/ Nutrient mixture F12 (DMEM/F12) with GlutaMAX^{TM} supplement (Gibco)

Freezing medium

7.5ml FBS

5ml DMSO (VWR)

12.5ml complete medium

Luria Broth (LB) medium

10g Tryptone (Sigma)

5g Yeast extract (Sigma)

10g NaCl (VWR)

To 1 litre dH_2O

LB agar

As above and including 15g Agar (Sigma)

Autoclave

RIPA Extraction buffer (SDS-PAGE)

150mM NaCl

1% (v/v) NP-40 (Fluka)

0.5% (w/v) Sodium deoxycholate (BDH)

0.1% (w/v) SDS (Biorad)

50mM Tris-HCl pH8 (Sigma)

Tris-Glycine Running buffer (SDS-PAGE)

25mM Tris-Base (Sigma)

192mM Glycine (Sigma)

0.1% (w/v) SDS

pH8.3

Tris-Glycine Transfer buffer (SDS-PAGE)

12mM Tris Base

96mM Glycine

pH8.3

5 X Laemmli Buffer (SDS-PAGE)

2.5g SDS

1.93g Dithiothreitol (BDH)

2.5ml Glycerol (VWR)

11ml 1M Tris-HCl pH6.8

5ml 0.2% (w/v) Bromophenol Blue in MeOH/EtOH (Sigma)

6.5ml dH_2O

pH6.8

Blocking solution (SDS-PAGE)

5% (w/v) Skimmed or semi-skimmed milk powder or BSA (Tesco)

0.1% (v/v) Tween in PBS (BDH)

Wash Buffer (SDS-PAGE)

0.1% (v/v) Tween in PBS

ECL

Solution 1:

1ml Luminol stock (0.88g/ 20ml DMSO) (Sigma)

0.44ml p-coumaric acid stock (0.29g/ 20ml DMSO) (Sigma)

10ml 1M Tris-base (pH8.5)

To 100ml dH_2O

Solution 2:

64µl 30% (v/v) H_2O_2 (Sigma)

10ml Tris-base (pH8.5)

To 100ml with H_2O

Mix solutions 1 and 2 in a 1:1 ratio prior to use.

Toluidine blue

0.2g Toluidine blue (Sigma)

100ml Acetate buffer (41ml 0.2M acetic acid + 9ml 0.2M sodium acetate to 100ml dH_2O pH4).

Rest for 1 week before use

Methodology

Generation of expression plasmids

Generation of WNT16 expressing plasmids was achieved either via conventional cloning or using the Invitrogen TOPO-TA cloning kit when cloning into pcDNA3.1, which utilises the actions of topoisomerase enzymes for the benefit of fast easy cloning.

Conventional cloning

Generation of the insert/ gene of interest

The insert (target gene) was either generated via polymerase chain reaction (PCR) or excised from another plasmid.

PCR was used to amplify the gene of interest from cDNA using specific primers that anneal in such way as to include the start and stop codons of the gene. The primers also contained at their 5' ends the appropriate restriction sites for convenient ligation into the destination vector at a later stage.

PCR reaction contains;

- 1-100ng DNA template
- 2.5pmol 5' and 3' primers
- 50µM dNTPs (Qiagen)
- 1x Enzyme buffer (Qiagen)
- 0.25units Taq polymerase (Qiagen)
- H_20 to a final volume (10 to 100µl).

Running conditions must include;

- Initial denaturation step (95°C – 5min).
- followed by 20-30 cycles of:
    - denaturation (95°C – 15 sec)
    - Primer annealing (50-65°C - 15 sec)
    - New strand synthesis (72°C – 30 sec).
- The reaction is completed with a final elongation step (72°C – 7min).

Digestion of DNA fragments is necessary to generate complementary ends between the insert and the plasmid, which is required for successful ligation. Therefore inserts, whether generated by PCR or digested from other plasmids, and the target plasmid, underwent digestion with appropriate restriction enzymes. Note that DNA solutions must be free from excess primer, and

PCR buffer prior to digestion reaction, therefore PCR products were isolated using agarose gel electrophoresis and purified using Qiagen QIAquick PCR purification kit according to manufacturer's instructions.

Digest reaction contain:

- 1-10µg DNA
- 1x Restriction Enzyme buffer (NEB)
- 1unit Restriction Enzyme (NEB)
- dH20 to final volume (between 10-20µ).

The samples were incubated for between 1 and 2 hours in a water bath at 37°C.

Following the reaction, digestion was confirmed via agarose gel electrophoresis, which also separates the fragments for ligation. The correct size band was then excised and DNA extracted using the QIAquick Qiagen gel purification kit according to manufacturer's instructions.

Ligation reaction. The ligation reaction allows for insertion of the gene of interest into the desired plasmid. If the plasmid is cut using restriction enzymes generating compatible ends, the plasmid must be dephosphorylated prior to ligation to prevent the un-ligated ends annealing to one another without insert.

The ligation reaction contains:

- Digested plasmid and insert at a 1:3 ratio (10-100ng)
- 1 X T4 DNA ligase buffer (NEB)
- 400 Units T4 DNA ligase (NEB)
- To 10-20µl dH_2O

The reaction was incubated at 16°C overnight.

The ligated product was used for transformation of heat competent E.coli (K12 strain) (NEB).

A 10µl aliquot of bacteria was thawed on ice and addition with of ~1µl of 1µg/µl ligated product (no clean up necessary) was added. The mix was incubated on ice for 30 minutes then transferred to 37°C for 1 minute.

Following this, 600µl of LB medium was added and the sample was incubated in a shaking incubator at 37°C for 45min, before plating the bacteria on an LB agar plate with appropriate antibiotics, and incubating at 37°C overnight. The following morning, bacterial colonies were selected, streaked on a gridded plate, and screened by PCR for the presence of the gene. For such PCR screening no DNA purification was necessary. Individual colonies were touched with a sterile toothpick, which was briefly dipped in the PCR reaction, streaked on a gridded plate, and

immediately added to a 5ml culture for plasmid preparation. Following agarose electrophoresis, a number of these were selected and sequenced to confirm the presence of the gene of interest.

TOPO-TA Cloning (invitrogen)

In their natural environment, topoisomerases create nicks in DNA, allowing it to be unwound for processes such as transcription to take place (Shuman, 1991). In this application, the enzyme exerts its actions on plasmid DNA. The topoisomerase cleaves the phosphodiester backbone, linearizing the plasmid. The energy from the break is maintained by transferring it into a covalent bond, between the 3' phosphate and a tyrosine on the enzyme. This bond is open to attack from a 5' OH of a similarly broken or open ended piece of DNA, such as the insert. Upon attack the reaction is reversed and the energy is transferred back into a phosphodiester bond now between the plasmid and the insert. This TOPO-TA technology greatly simplifies the cloning process. Once the gene of interest has been ligated into the plasmid the remaining steps are performed as above.

The protocol was carried out as per manufacturer's instructions. This involved incubating the PCR product with the supplied TOPO plasmid for 5 min at room temperature.

Note: Inserts for TOPO TA cloning require 3'A overhangs which are added by standard Taq polymerase during PCR amplification. These are complementary to the 5'T overhangs present on the linearised plasmid supplied with the kit and allow annealing of the insert to the plasmid.

Storing plasmid clones as bacterial stocks

Upon identification of positive clones, the respective colonies were picked and used to inoculate 5ml LB medium which was then incubated under shaking conditions at 37°C overnight. The following morning the bacterial culture was centrifuged at 5,000g for 5 minutes and the medium was removed. The pellet was gently re-suspended in a mix of glycerol and LB medium in a 1:4 ratio, and stored at -80°C. To re-amplify the bacteria, a sterile rod was scratched across the surface of the frozen stock, then streaked on an LB agar plate.

Plasmid amplification and purification form bacterial stock

For purification of a plasmid clone, a bacterial culture was established as above and the plasmid purified using the Qiagen QIAprep miniprep kit as per manufacturer's instructions.

Isolation of Mouse Articular Chondrocytes (MAC) (Optimised from Yasuhara et al, 2011)

The knee joints of neonatal mice, (3-5 days post natal) were exposed and the soft tissue, tendons and ligaments were carefully removed to expose the articular cartilage. Following this, the ends of the long bones were excised and incubated with trypsin (0.25% w/v) for 1 hour to remove any residual soft tissues, followed by digestion with collagenase type 1 (173U/ml) (Sigma) for 1.5 hours. This initial digestion separates the SZC chondrocytes from the matrix. These cells were filtered using a 20µm cell strainer then plated in culture dishes pre-coated with 0.1% (v/v) human plasma fibronectin solution (Sigma). One well of a 24 well culture plate was coated with 100µl of 0.1% (v/v) human plasma fibronectin for 2 hours, washed with PBS, blocked with 3% (w/v) BSA in PBS for 30 minutes then stored at 4°C for up to 1 week. The cells that did not adhere to the plates were washed out 20 minutes after plating. The deep chondrocytes were isolated by an additional overnight digestion of the remaining cartilage elements with 0.15% (w/v) collagenase type 1 (Yuasa et al, 2007), then filtered using a 20µm cell strainer and plated in cell culture vessels. After isolation cells were cultured in complete medium and passaged upon reaching confluency. Isolation was validated by real-time PCR for specific markers.

Isolation of Mouse Costal Chondrocytes (MCC) (Optimised from Gosset et al., 2008)

The anterior, cartilaginous part of the ribs were dissected from neonatal or adult mice. The soft tissues were removed and the skeletal elements were washed twice with PBS. An initial 45 minute incubation with collagenase P (1.2mg/ml) was performed at 37°C in a rotating incubator to remove any residual soft tissue. The ribs were washed with PBS before further digestion overnight with collagenase P (0.2mg/ml) (Roche) to break down the cartilage ECM and extract the cells. Following this, the cells were filtered using a 20µm cell strainer, and either plated in cell culture vessels and cultures in complete DMEM, or frozen down in complete medium.

Isolation of Human Articular Chondrocytes (HAC)

Human articular chondrocytes were extracted from the femoral condyles of osteoarthritic patients who had undergone knee replacement surgery and consented to donate samples. Surgical samples were placed immediately into a sterile container following surgery and processed the same day. Full thickness cartilage fragments were dissected from the underlying

mineralised cartilage and subchondral bone. Fragments were washed twice with complete medium containing 2% (w/v) antibiotic/antimitotic solution, before incubating with 1mg/ml pronase (Roche) for 30 minutes, at 37°C, under gentle rotation, followed by overnight digestion with 1mg/ml collagense P (Roche), under the same conditions, to release the cells. The following morning, cells were filtered using a 20µm cell strainer and plated in culture vessels with complete medium.

One explant of full thickness cartilage was not digested and instead processed for histological scoring. The explant was stored in 4% (w/v) PFA prior to embedding, sectioning and staining with toluidine blue to determine a histological score.

Histological scoring of cartilage tissue.

Histological scoring of human cartilage was achieved by staining with toluidine blue and analysis using a modified Mankin score (Mankin, Dorfman et al. 1971; van der Sluijs, Geesink et al. 1992). A score of 0 indicates normal cartilage and 13 is the maximum severity score (see Mankin score, table 1).

Mankin score (table 1)

Structure	Score
Normal	0
Slight disorganisation (cellular row absent, some superficial clusters)	1
Irregular surface, including fissures into the radial layer	2
Pannus	3
Superficial cartilage layers absent	4
Fissures into the calcified cartilage layer	5
Severe disorganisation	6
Cellular abnormalities	
Normal	0
Hypercellularity	1
Clusters	2
Hypocellularity	3
Matrix staining	
Normal	0
Staining reduced in radial layer	1
Staining reduced in inter territorial matrix	2
Only present in pericellular matrix	3
Absent	4
Total Mankin score	13

Table 1:Outlining scoring system for generating Mankin score for Cartilage.

Cell culture and expansion

All cells (primary and cell lines), where cultured as follows unless otherwise specified. Cells were cultured in complete medium (containing DMEM/F-12 with high glucose, 10% (v/v) FBS and 1% (v/v) antibiotic/antimitotic solution), at 37°C in humidified atmosphere containing 5% (v/v) CO_2. While the cells were in culture the medium was changed every 3-4 days and the cells allowed to reach 90% confluency before splitting in a 1 to 4 ratio. This was achieved by washing the cells once with PBS to remove medium before incubating with 0.025% (v/v) Trypsin:EDTA (Gibco) at 37°C for 3 minutes. Following gentle tapping to release cells, the trypsin was inactivated by addition of FBS. The cells were pelleted by centrifugation at 1500RPM (500g), and re-plated.

Freezing cells for storage

Cells not required immediately were suspended in complete medium at a concentration between 10^6 and 10^7 cells per ml. Half a ml of this suspension was added to 0.5ml of freezing medium, and immediately stored to -80°C freezer for 24 hours, before transfer to liquid nitrogen.

Cell counting

Cells were suspended and 10µl mixed with equal volume of trypan blue. This mixture was introduced into a Neubauer haemocytometer and counted. Those cells that showed uptake of trypan blue were excluded from counting and assumed dead (routinely <5%).

Micromass culture of cells

Cells were suspended at $2x10^7$ cells/ml in complete medium. Of this suspension, 20µl was plated in the centre of a well of a 24 well plate and allowed to adhere for 2.5 hours. One ml of complete medium was then gently added. The micromasses were left in the incubator for 24 hours before the addition of any stimuli and were then left in culture for up to 1 week. The medium/ stimuli were changed every 2 days.

Fixation of micromasses and alcian blue staining

After gentle washing with PBS, micromasses were fixed with 4% (v/v) PFA for 15 minutes at room temperature, washed with dH_2O, and 1ml of Alcian Blue dye at pH0.2 (0.5% (w/v) Alcian blue 8 GS) was added and left overnight at room temperature. The following morning, the excess dye was removed and the micromasses were washed thoroughly with dH_2O to remove any non-specific staining. Photographs were taken using a Leica DFC295 camera on a dissecting microscope. Alcian blue was extracted for quantification from the stained micromasses with 6M Guanidine HCl for 6 hours on a shaking platform at room temperature. The amount of extracted Alcian blue was measured by spectrophotometry at 630nm. Values were normalised either for protein content (Piarce BCA protein assay kit) or DNA content (SYBR Green I nucleic acid gel stain, Sigma).

Transfection of eukaryotic cells.

Cells were plated in a 24 or 6 well plate with complete medium and allowed to reach 50% confluency. At this stage the medium was changed to complete medium with 20% (v/v) FBS for 24 hours then the cells transfected according to the following protocols (which are designed for a single well of a 24 well plate).

Jet prime (Polyplus) reagent was used for transfecting cell lines and primary cells. For a single well of a 24 well plate, 50,000 cells were seeded and cultured in DMEM with 20% (v/v) FBS for 24 hours prior to transfection. Five hundred nanograms of DNA were added to 50µl of Jet Prime buffer, followed by the addition of 1µl of Jet Prime reagent. The mix was incubated at room temperature for 10 minutes, then added to 500µl of DMEM with 10% (v/v) FBS without AA. After 24 hours the medium was replaced with complete DMEM. eGFP was used to analyse transfection efficiency.

Lipofectamine. 1µg of plasmid DNA was added to 55µl of Optimem (GIBCO). Separate to this, 2µl of Lipofectamine 2000 (Invitrogen) was added to 55µl of Optimem and left to incubate for 5 minutes at room temperature, before addition to the first mixture containing the plasmid DNA. This solution was them incubated for a further 20 minutes at room temperature, then 100µl was added to 0.5ml DMEM (10% (v/v) FBS) and added to the cells for 24 hours, when it was replaced with complete medium.

Fugene. 1.5µl of Fugene was added to 94µl of Optimem and incubated for 5 minutes. Following this, 2µg of plasmid DNA was added and left to incubate for a further 30 minutes. 100µl was added to 0.5ml of DMEM (10% (v/v) FBS) on the cells.

Pathway analysis

Transfections for reporter assays were performed with Jet Prime reagent.

Super8XTOP/ FOP Reporter assay

Assay kit and reagent were form the Dual luciferase reporter assay system kit (Promega).

Cells were co-transfected with Super8XTOP or its mutagenised control, FOP -flash reporter plasmid (Kind gifts of Prof. Randall Moon, University of Washington, USA) and CMV-Renilla luciferase plasmid (Promega) in a ratio of 1:50. If using the WNT16 plasmid for overexpression, this (or its control plasmid), was also included in the mix in such proportion to ensure that the total amount of transfected DNA was maintained constant. After 24 hours the transfection

medium was removed and replaced with complete medium. Any stimulus was added at this point and the cells were left for a further 24 hours. Cells were harvested using 1x passive lysis buffer and incubated for 30 min at room temperature under gentle agitation. Following this, the cells were scraped from the plate and stored at -20°C. To perform the assay, 20µl of lysate was added to 100µl of firefly luciferase substrate and the luminescence recorded over a period of 15 seconds using a TD-20/20 luminometer (Turner Designs). Subsequently 100µl of Stop & Glo reagent was added which simultaneously quenches the firefly luciferase and provides a substrate for the renilla luciferase. Luminescence was recorded again as described above. Renilla luciferase activity was used to normalise for transfection efficiency.

Gene Expression Analysis

Extraction of total RNA from cells

Total RNA was extracted from single wells of a 24 well plate. The cells were washed with PBS and 1ml/well of TRIzol reagent (Invitrogen) was used to remove and lyse the cells. All further steps were performed on ice or at 4°C. Cells were sheared to ensure complete lysis using a needle and syringe and centrifuged for 10 minutes at 20,000g to remove cell debris. The supernatant was transferred to a new 1.5ml Eppendorf tube, and 200µl of chloroform was added, the tube was mixed vigorously for 20 seconds then returned to ice for 2 minutes. Samples were centrifuged at 10,000g for 15 minutes. The aqueous phase containing the RNA was transferred to a new tube and 500µl of ice-cold isopropanol added (additional phases include an intermediate layer containing genomic DNA and a lower phase containing proteins and the TRIzol reagent). If the yield of RNA is expected to be low 0.5µl of glycogen (Behoringer Mannheim Gmbh) was added with the isopropanol to maximize return. The samples were incubated on ice for 30 minutes to precipitate the RNA, then centrifuged for 30 minutes at maximum speed. The isopropanol was removed and the pellet washed with 70% (v/v) ethanol to remove salts. After an additional 5 minute centrifugation at maximum speed the ethanol was removed and the pellet was air dried and re-suspended in 6µl of Molecular biology grade water.

Concentration of RNA was determined using a Nanodrop spectrophotometer (Nanodrop 2000c from Thermo Scientific) at absorbance 260nm. 260/280 ratio should be between 1.8 and 2, indicating pure samples. Note that if glycogen was used in the precipitation process, the

concentration of the RNA cannot be determined and the maximum volume was taken forward for cDNA synthesis (see below).

Reverse transcription of mRNA

The Invitrogen thermoscript RT PCR system was used to synthesise cDNA.

Five hundred ng of total RNA was reverse transcribed from each sample using oligo dT primers. The reaction is performed in 2 steps:

Step 1 → Reaction mix A

- 0.5µl Oligo dT primer
- 1µl dNTPs
- 500ng total RNA
- To 6µl with H_2O
- Incubate for 5 minutes at 65ºC

Step 2 → Reaction mix B

- 2µl 5x Buffer
- 0.5µl Thermoscript (15 U/µl)
- 0.5µl DTT
- 0.5µl RNAse out (40 U/µl)
- 0.5µl H_2O
- Incubate for 1 hour at 50ºC followed by 5 minutes at 85ºC.

Subsequently 0.5µl of RNAse H (2 U/µl) was added to each sample and incubated at 37ºC for 20 min. Forty µl of Baxter water was added to each sample prior to PCR.

Real time polymerase chain reaction

Real time PCR was performed on an ABI 7900HT thermocycler.

Reaction for real time PCR contains:

- 1µl of cDNA sample synthesised above
- 2.5pmol 5' and 3' primers (a list of primer sequences can be found in table 2)
- 4µM dNTPs
- 1x hot start buffer
- 0.05µl hot start DNA polymerase (5 U/µl) (Qiagen)
- 0.1x SYBRGreen (Sigma)

- 0.2x Rox reference dye (Invitrogen)
- BaxterH_20 to 10µl.

Running conditions include:

- 2 minutes at 50°C followed by an initial denaturation step (96°C – 15min), which also activates the hot start polymerase.
- This is followed by 40 cycles of;
    - Template denaturation (96°C – 15 sec)
    - Primer annealing (50-65°C - 15 sec) as needed for optimal primer annealing
    - New strand synthesis (72°C – 30 sec).

Cycling conditions were optimised to achieve maximum specificity and synthesis from each set of primers. Following cycling, a melting curve was performed from 90 to 72 degrees, which allowed for quality controlling the reaction and identification of those wells that had undergone non-specific amplification. Gene expression was calculated using a standard curve generated using a 1/100,000 dilution of PCR product. Standard curve dilutions were 1:1, 1:32, 1:1000. A water control was also included to identify contamination. The first time a new set of primer was used, the amplicon was checked for size by agarose gel electrophoresis. Relative gene expression was calculated using a standard curve spanning 2 log scales generated on every plate with a positive control. All genes were normalised for housekeeping gene, actin. (see below Primer information table).

Primer sequences (table 2)

Gene	Sense Primer	Antisense primer	Amplicon length	PCR conditions
Mouse/human β-actin	TGACGGGGTCACCCACACTGTGCCCATCTA	CTAGAAGCATTTGCGGTGGACGATGGAGG	661	3 step 55
Human aggrecan	GTTGTCATCAGCACCAGCATC	ACCACACAGTCCTCTCCAGC	509	2 step 68
Human COL2A1	CTGCTCGTCGCCGCTGTCCTT	AAGGGTCCCAGGTTCTCCATC	432	2 step 68
Human sox9	GAACGCACATCAAGACGGAG	TCTCGTTGATTTCGCTGCTC	361	3 step 55
Human Lubricin	TCACAGTTGTTATTGTTTACAGACC	GGGTAAGTGAATACACTAGTTTTGA	152	3 step 60
Human Axin2	TACCGGAGGATGCTGAAGGC	CCACTGGCCGATTCTTCCTT	345	3 step 55
Human COL10A1	AATCCCTGGACCGACTCGAATTTC	TTGATGCCTCGCTGTCCTGGAACC	267	3 step 55
Human PCNA	GGAGAACTTGGAAATGGAAAC	CTGCATTTAGAGTCAAGACCC	548	3 step 55
Mouse aggrecan	GAAGAGCCTCGAATCACCTG	ATCCTGGGCACATTATGGAA	132	3 step 55
Mouse COL2A1	CATTGTTGGTCTGCCTGGTC	TTCTCTCTCTGCCCTAAGCC	750	3 step 55
Mouse sox9	TATGTGGATGTGTGCGTGTG	CCAGCCACAGCAGTGAGTAA	137	3 step 55
Mouse Lubricin (prg4)	TGGAGTGCTGTCCTGATTTCAAGAG	GGTGATTTGGGTGAGCGTTTGGTA	256	3 step 55
Mouse Matrilin1	CCGTGGCAGACCACTACTTT	ACTCACAAGCACAGGGGTCT	108	2 step 68
Mouse WNT16	GCCACTACCACTTCCACCC	GAGCCACCATTCTGCAAGG	188	3 step 60
Mouse Axin2	AGCGCCATCGACAGCGAGTT	CAGGCGGTGGGTTCTGGGAA	182	3 step 50
Mouse sox2	CCAGGAGAACCCCAAGATGCACAA	TCATGCTGTAGCTGCCGTTGCTC	341	3 step 60
Bovine actin	AGCAGTCGGTTGGATCGAGCA	GGGAAGGCAAAGGACTTCCTGTAAC	137	3 step 55
Bovine aggrecan	GATGCTTCTATCCCAGCCTCCGC	CGGTCCGGGAAGTGGCGGTAA	125	3 step 60
Bovine COL2A1	ACGTCCAGATGACCTTCCTG	GGATGACCAGAGCCTTCTTG	126	3 step 55
Bovine sox9	ACTCTGGGCAAGCTCTGGAGACT	GGCGCGGCTGGTACTTGTAGTCC	121	3 step 60
Bovine Lubricin	GGAGATGTGGGGAAGGGTAT	TCTGAGATGCTCCTGGAGGT	288	3 step 55
Bovine WNT16	GCCCAAGAGCTAAGGCAATA	GCCATTTTGGCAGGAAATAC	145	2 step 60
Bovine Axin2	GAAATAGCGGTCCTGGTCCT	GTCTTCCCAAAGCTGTCTGC	119	3 step 55

Table 2: Outlining all primer sequences and their conditions used in this thesis.

Protein Analysis

Western Blotting

For cell lysates, cells were washed with PBS and lysed with 120µl 1x RIPA buffer containing phosphatase and protease inhibitors (Roche). A cell scraper was used to ensure complete

removal of all cells, and samples were incubated on ice for 30 minutes, vortexing every 10 minutes. In some occasions the cell lysates were stored at -80°C at this stage.

In the case of liquid samples such as supernatants, samples were either run on a gel in a ratio of 4:1 with standard Laemmli buffer or concentrated as outlined below.

Forty to sixty µg of protein (determined by BCA assay- see above) was prepared for each sample and brought to 40µl with PBS and 10µl of 5x Laemmli buffer was added. The samples were heated to 95°C for 5 minutes then loaded on Tris-glycine gels and run at 130v (constant voltage) in 1x Tris-glycine running buffer (diluted in dH_2O), until the leading edge reached the bottom of the gel. Proteins were transferred to a nitrocellulose membrane at 100v (constant voltage) for between 1–2 hours depending on the size of the protein of interest. All elements were immersed in 1x Tris-glycine transfer buffer (25xTris-glycine transfer buffer, 5% (v/v) Methanol, diluted in dH_2O). Following transfer membranes were blocked for 3 hours in blocking solution, and the primary antibody left overnight at 4ºC or at room temperature for 1 hour (diluted in blocking solution). A list of antibodies can be found in table 3. Following washing (3x5 minutes + 1x45 minutes in wash buffer), the HRP-conjugated secondary antibody diluted in blocking buffer was applied and left at room temperature for 45 minutes. Subsequently the membrane was washed again then exposed to HRP substrate (ECL solutions 1 and 2 in a 1:1 ratio, incubated for 5 minutes, Biorad), and developed using Hyperfilm ECL (GE healthcare, Amersham).

Antibodies used (table 3)

Antibody	**Raised in**	**Dilution (WB)**	**Blocking solution**	**Company**
β- actin	Mouse	1/5000	5% milk	Sigma (A5441)
Lubricin	Rabbit	1/500	5% milk	Abcam (ab28484)
β-catenin	Rabbit	1/1000	5% milk	Cell Signalling Technology (9562)
Phospho c-Jun	Rabbit	1/1000	5% BSA	Cell Signalling Technology (9164)
Total c-Jun	Rabbit	1/1000	5% BSA	Cell Signalling Technology (9165)
WNT16	Mouse	1/4000	5% milk	BD bioscience (552595)
Secondary AB				
anti mouse	Goat	1/2000	5% milk	Santa Cruz biotechnology (Sc 2005)
anti rabbit	Goat	1/2000	5% milk	Santa Cruz biotechnology (Sc 2004)

Table 3: Outlining all antibodies and WB conditions used in this thesis. Antibodies were used according to manufacturer's instructions.

Protein precipitation from medium for WB

Tricholroacetic acid (TCA) precipitation of proteins.

TCA precipitation was used to concentrate proteins and also to facilitate the solubilisation of WNT16.

One volume of 100% (w/v) TCA was added to 3 volumes of supernatants (the final TCA concentration will be 25% (w/v)) and incubated at -20°C for 5 minutes. The samples were centrifuged at 100g for 10 minutes. The supernatant was removed and the pellet washed with 200µl ice-cold acetone by tilting gently. The samples were centrifuged again at 100g for 5 minutes. After one additional wash in acetone the pellets were dried at room temperature for 15-30 minutes. The protein pellet was re-suspended in PBS and Laemmli buffer (to a final concentration of 1x), incubated for 5 minutes at 95° and loaded on a polyacrylamide gel for western blotting as above.

Concentration of proteins using beads

Strata Clean resin (Agilent technologies) was used to pull down proteins from solution. This is a solid phase silica-based resin containing hydroxyl groups which bind and separate proteins from the solution.

The resin solution was vortexed to re-suspend the product. The volume of resin solution required is equal to the square root of the volume being purified. The resin was added to the cell media, vortexed thoroughly, then incubated at room temperature for 10 minutes. Laemmli buffer was added to each sample to a final concentration of 1x. The samples were denatured at 95°C and loaded on a polyacrylamide gel for western blotting as described above.

Statistical analysis

Statistical tests used are outlined in the figure legends. P values were shown as follows; $p<0.05$ - *, $p<0.01$ - **, $p<0.001$ - ***. Data with p values higher than 0.05 were considered not significant.

CHAPTER 3:
Biological effects of WNT16 in chondrocytes

Introduction

WNT16 is expressed in the superficial chondrocytes during development (Yasuhara, Ohta et al. 2011). It is not expressed in healthy adult cartilage but is re-expressed following injury and induction of OA in both mice and humans (Dell'accio, De Bari et al. 2008). In addition Wnt16 deficient mice are more susceptible to instability-induced arthritis. Therefore the aim of this chapter is to explore the function of WNT16 both in adult and neonatal chondrocytes, with a focus on basic biological outcomes. To achieve this I have assessed proliferation, differentiation, and lineage determination in a number of cell lines and primary cells using both gain- and loss-of-function approaches.

Early gain-of-function experiments were particularly challenging because of the relatively low expression levels achieved upon plasmid transfection. This became evident only 18 months later, when recombinant WNT16 became available. At that stage it was clear that the dose-responses achieved with the plasmid overlapped with the low end of the dose responses obtained with the recombinant protein. Eventually, it became evident that WNT16 has a biphasic effect depending on the concentration: the overexpression experiments only revealed the low concentration effects, but not the high concentration effects, which where those that were seen *in vivo* in a parallel study conducted by Dr Giovanna Nalesso. For completeness, I will report hereafter the most important experiments of the entire investigation in a chronological way and I will summarise at the end how apparent contradictions can be reconciled. A number of optimization experiments have been reported in the appendices to this thesis.

Results

WNT16 is expressed by HAC after isolation from cartilage tissue.

To determine whether WNT16 is secreted in the supernatant and whether transfection with a plasmid encoding WNT16 could significantly increase WNT16 expression in primary HAC I compared the endogenous expression levels and those after transfection in the supernatant and the cell lysates by western blotting (**Figure 15**). A WNT16 expression plasmid was kindly donated by Professor Teh (Queen Mary University of London) within the backbone of a BABE retroviral vector, in a HA tagged form. I then subcloned WNT16 into the pcDNA3.1-His mammalian transfection vector, and inserted a stop codon at the end of the open reading frame to prevent the expression of the His tag.

WNTs are notoriously difficult to demonstrate by western blotting because of the posttranslational modifications. In the blot shown below, therefore, I also demonstrated how TCA precipitation improved its detectability.

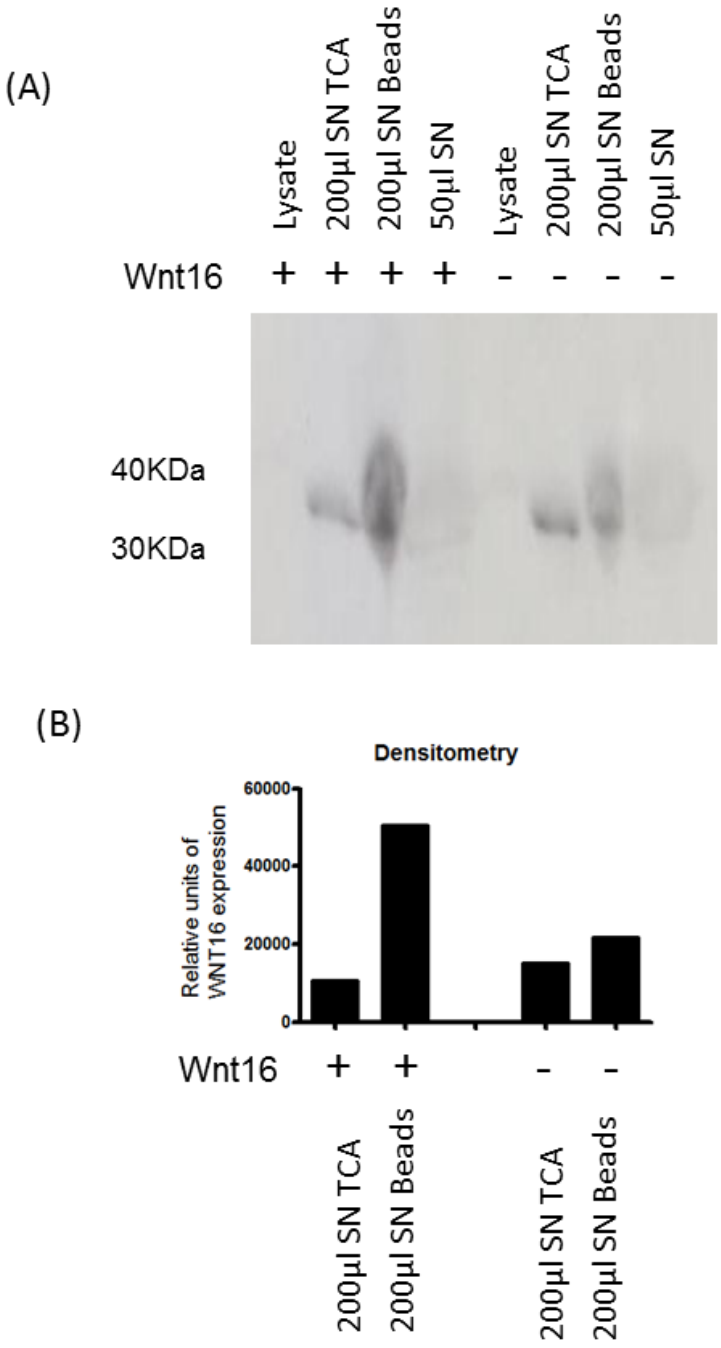

Figure 15: WNT16 was expressed by HAC after isolation from cartilage explants.

(A) Subconfluent P0 HAC, were transfected with either empty plasmid (EP) or WNT16 expression plasmid. Lysate and supernatant (SN) were harvested following culture in complete medium with serum, for 48 hours after transfection. The SN was either TCA precipitated, concentrated using beads or left untreated before western blotting. Equal concentrations (60µg) of lysate were loaded into the gel. (B) Densitometry analysis of WNT16 band in (A). N=1.

This experiment (shown in **Figure 15**), confirmed that HAC from this arthroscopy patient expressed high endogenous levels of WNT16. The protein was only detected in the supernatant of cells and not in the lysates, indicating that it is efficiently secreted. A slight increase in expression was observed upon transfection with WNT16 expressing plasmids, but this requires confirmation in multiple samples. However, although HAC from one patient only have been tested, the results are in keeping with those seen by Dell'accio at al., in 2008, where real-time PCR and immunmohistochemical analysis of cartilage samples from different donors showed an upregulation of WNT16 in OA cartilage compared to samples from preserved areas (Dell'accio, De Bari et al. 2008).

Interestingly, secreted WNT16 run as a smear on acrylamide gels. This was corrected by TCA precipitation and re-suspension (shown on western blot, **Figure 15**), and therefore it is unlikely to be caused by glycosylation, but rather by WNT16 being associated with complex multimolecular structures or secreted within extracellular vesicles, which may facilitate its transport.

WNT16 plasmid transfection had no significant effect on mRNA expression of phenotypic markers in HAC.

I explored whether the increase in WNT16 expression seen upon plasmid transfection was sufficient to determine downstream events (**Figure 16**). I transfected HAC with this WNT16 expression plasmid and analysed differences in gene expression by RT-PCR. At this stage we had not yet identified an adequate readout for WNT16 activity. I therefore included in this initial screening, cartilage differentiation markers such as sox9, col2a1, aggrecan, col10a1 (a marker of chondrocyte hypertrophy also expressed in OA cartilage), and PCNA (a marker of proliferation). Note that all data are displayed with standard error bars.

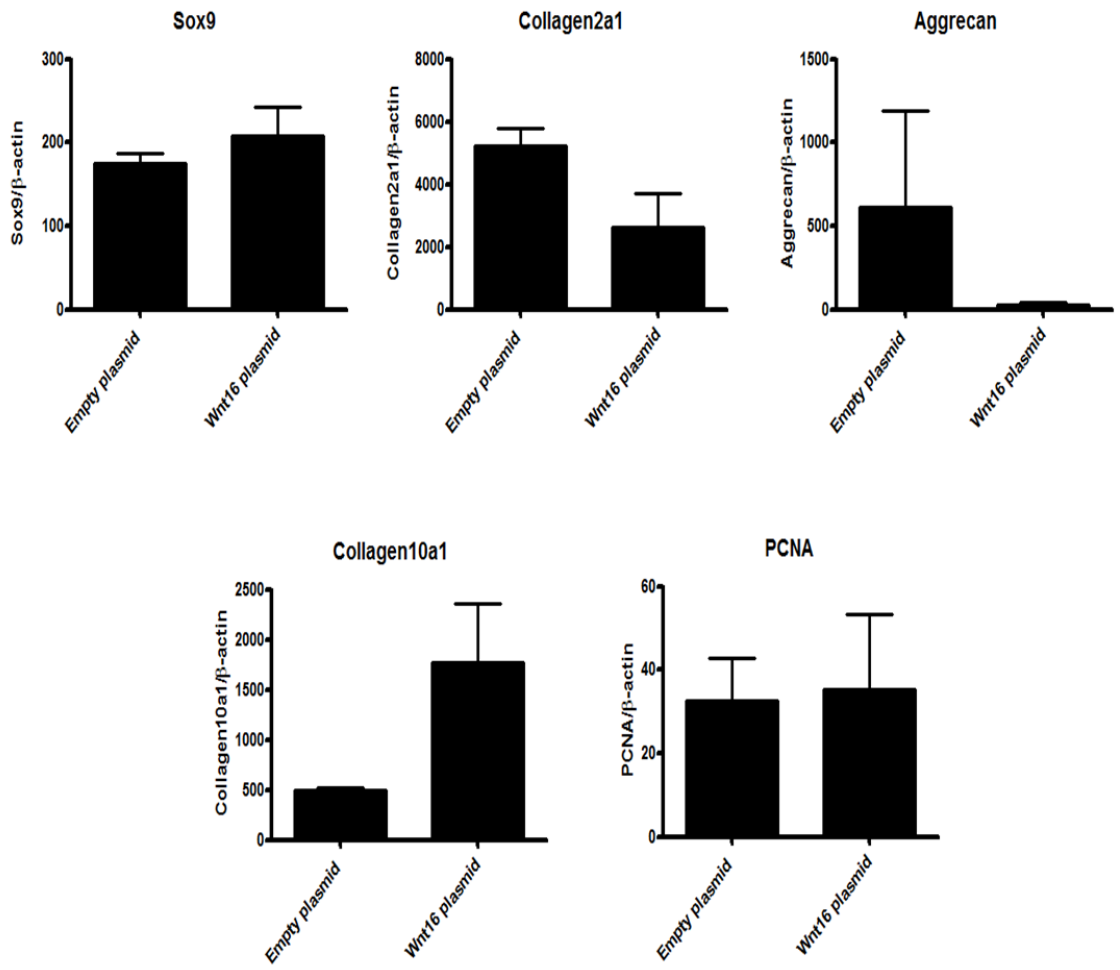

Figure 16: WNT16 overexpression had no effect on gene expression in HAC

P0 HAC from a single arthroscopy patient were transfected with empty plasmid or WNT16 expression plasmid and harvested for gene expression analysis by RT-PCR following culture in complete medium containing serum, 48 hours later. Values were normalised for β-actin. Graphs are representative of one experiment (n=4 per group). An unpaired t test conducted for statistical analysis.

No statistically significant differences were observed in the expression of differentiation markers following WNT16 overexpression in HAC (**Figure 16**). Other than the possibility that WNT16 has no function in HAC a number of other reasons, such as patient variability and high endogenous levels of WNT16 may explain why no effect was seen in this experiment. These are discussed at the end of this chapter.

WNT16 overexpression had no significant effect on the phenotype of bovine primary articular chondrocytes.

Unlike HAC, Primary bovine articular chondrocytes are readily available, stable in culture, and, for a primary cell, easy to transfect. In addition, we can consider them 'healthy' cells as they are from relatively young animals.

For these reasons I continued my investigations into the function of WNT16 in these cells and performed an overexpression experiment using the WNT16 expression plasmid (**Figure 17**). I felt relatively confident using my plasmid expressing human WNT16 due to the degree of conservation between human and bovine WNT16, which is 94% at amino acid level. As a readout, in addition to the classical chondrocytic marker genes as in

Figure 16 I also included lubricin, a marker of the superficial zone of the articular cartilage (WNT16 is expressed here during development (Yasuhara, Ohta et al. 2011)), and axin2 a transcriptional target and validated readout of the canonical Wnt pathway (of which WNT16 is an activator in a rat chondrocytic cell line (Guo, Day et al. 2004)).

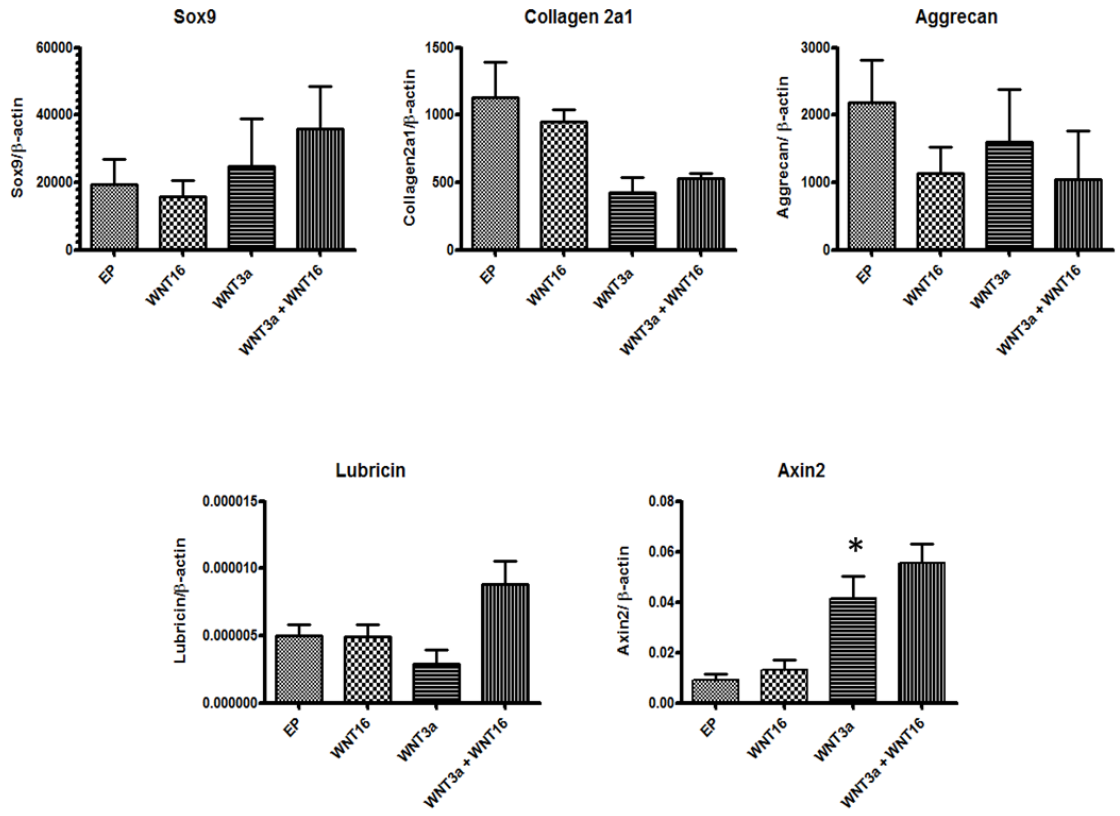

Figure 17: WNT16 overexpression had no significant effect on bovine primary chondrocytes.

P0 primary bovine articular chondrocytes were transfected with empty plasmid or WNT16 expression plasmid, and treated with either 100ng/ml WNT3a recombinant or vehicle. Cells were harvested for real time analysis by RT-PCR following culture in complete medium containing serum, 24 hours later. Values were normalised for β-actin. Graphs are representative of one experiment (n=4). An unpaired t-test was used for statistical analysis.

No statistically significant differences were observed upon plasmid transfection of WNT16 in primary bovine articular chondrocytes when compared to control (**Figure 17**). However WNT3a, a well-known activator of the canonical WNT pathway, upregulated axin2 as expected (Nalesso, Sherwood et al. 2011). As with HAC, the lack of effect seen by WNT16 may be due to a number of factors, for example, endogenous WNT16 expression may be masking the effect of exogenous WNT16.

WNT16 plasmid transfection had no statistically significant effects on the mRNA expression of phenotypic markers in mouse costal chondrocytes.

Bovine primary articular chondrocytes are abundant and easy to manipulate in vitro. However, as I had access to *wnt16*$^{-/-}$ mice, I decided to investigate whether chondrocytes from Wnt16 knockout mice, having no endogenous WNT16, would be a better model for WNT16 overexpression experiments. To achieve this, I isolated costal chondrocytes from adult mice (greater than 6 weeks of age, isolation of articular chondrocytes from adult mice gives a poor yield of cells), and transfected cells with the WNT16 expression plasmid (mouse WNT16 shares 90% homology at amino acid level with human WNT16). In this analysis (**Figure 18**), as well as chondrocytic markers (sox9, col2a1 and aggrecan), I also included lubricin, a marker of the SZC that express WNT16, and matrilin1, a marker of the epiphyseal chondrocytes during development, which do not express WNT16. Lineage tracking experiments have demonstrated that these two populations, and their respective markers, therefore, represent two separate differentiation lineages within the developing skeleton, the former giving rise to the articular cartilage (Warman 2014), and the latter to the epiphyseal lineage ultimately destined to be replaced by bone (Hyde, Dover et al. 2007).

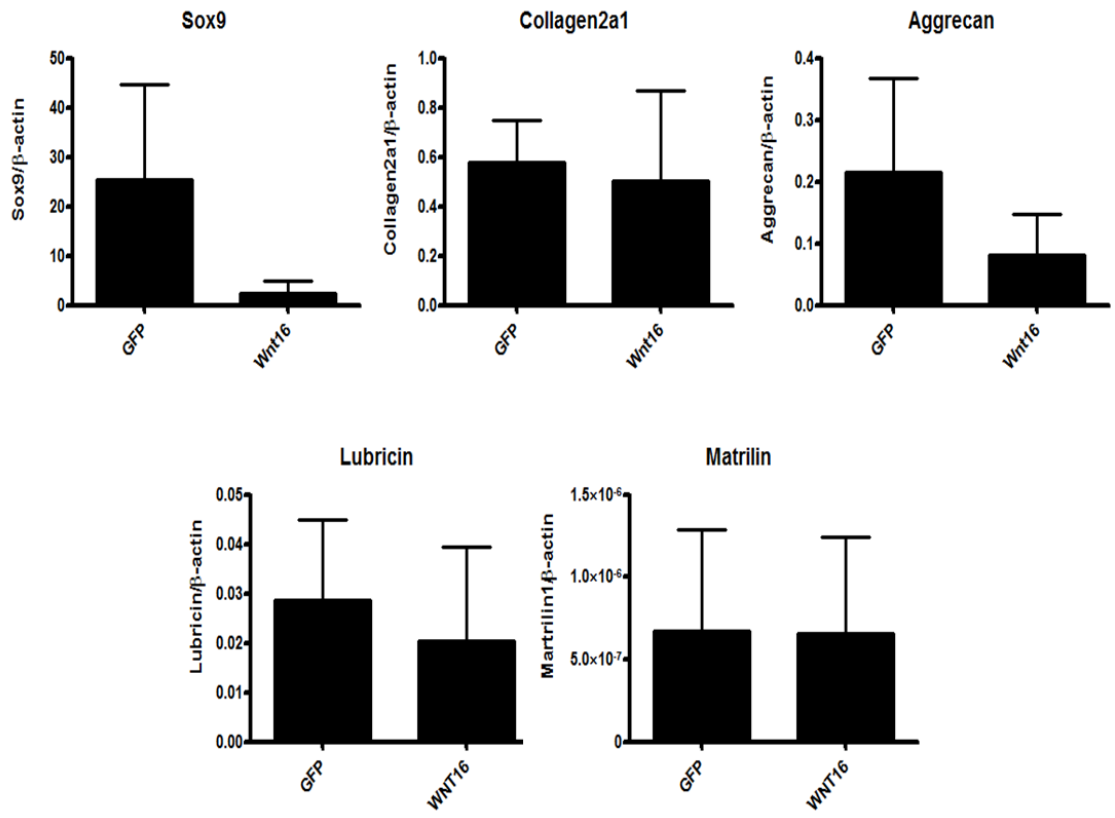

Figure 18: WNT16 overexpression had no statistically significant effect on mouse costal chondrocytes.

P1 mouse costal chondrocytes were transfected with either empty plasmid or WNT16 expression plasmid and harvested following culture in complete medium containing serum, 24 hours later for gene expression analysis by RT-PCR. Values were normalised for β-actin. Graphs are representative of one experiment (n≥2). An unpaired t test was performed to measure statistical significance.

No statistically significant differences were seen between cells transfected with control plasmid and WNT16 expression plasmid (**Figure 18**).

To conclude this section, thus far my gain of function experiments using the WNT16 expression plasmid generated no statistically significant data regarding the biological activity of WNT16 in HAC, bovine primary articular chondrocytes, or mouse costal chondrocytes and a discussion regarding possible explanations can be found at the end of this chapter. In all three cell types, however, I did see a trend towards downregulation of chondrocytic marker genes but this needed further confirmation.

Loss-of-function analysis by comparison of wild type and *wnt16*$^{-/-}$ cells from the superficial zone (SZ) of the cartilage of neonatal mice.

As a parallel approach to identify the effects of WNT16 in chondrocytes, I compared the expression of phenotypic markers in superficial zone chondrocytes (SZC), from wild type and *wnt16*$^{-/-}$ mice, in an attempt to investigate loss-of-function of WNT16.

Dr Giovanna Nalesso, in our laboratory, previously explored the possibility of isolating articular chondrocytes from neonatal mice (Gosset, Berenbaum et al. 2008). At this age the secondary ossification centre has not formed yet and therefore, although the cell yield is very high, most chondrocytes are of epiphyseal origin. Dr Nalesso found no difference in mRNA expression of chondrocyte specific genes when comparing cells from the whole neonatal epiphysis of wild type and wnt16 knockout mice (data not shown). Since WNT16 is expressed only in the superficial zone of the articular cartilage (Yasuhara, Ohta et al. 2011), cell preparations obtained from whole immature epiphyses will contain only a very small minority of WNT16 expressing cells. Therefore, the effect of WNT16 deletion may be very difficult, if not impossible to detect.

Therefore I took advantage of a recently described method for separating SZC from deep zone chondrocytes (DZC) from neonatal mouse joints (Yasuhara, Ohta et al. 2011). In this method a first enzymatic digestion releases predominantly SZC, which are subsequently further enriched by differential adhesion to fibronectin (Yasuhara, Ohta et al. 2011).

Protocol validation for enriching SZC cultures.

The use of neonatal mice for this protocol means that the physiology of the joint is neither that of mice during development/embryogenesis nor that of adult mice. The SZC correspond to the same SZC seen during the late stages of joint development and is marked by the expression of lubricin, although the expression of some other markers such as WNT16 is lost (Dell'accio, De Bari et al. 2008). In neonatal mice, however, the DZ also includes a portion of the underlying epiphysis, which, in adulthood, is replaced by bone. The most superficial part of the DZ, instead, both in adulthood and in neonatal mice, pertains to the articular lineage. This is now uncontroversial, since lineage tracking experiments where bacterial β galactosidase expressed by a LacZ cassette marks the progeny of the SZC, in adult life, and extends to include the deep zone of the articular cartilage, all the way to the subchondral bone (Warman 2014), and lineage tracking of Matrilin-expressing chondrocytes (epiphyseal) shows that the progeny of those cells do not contribute to the articular cartilage (Hyde, Dover et al. 2007).

In order to validate and quality control the SZC enrichment in my hands, I utilised lubricin as a marker of the SZC and matrilin-1 as a marker of DZC. Rare samples where lubricin and/or matrilin1 were not enriched in the SZC and DZC cultures respectively, were excluded from further analysis. The expression of Lubricin and Matrilin1 in each compartment following isolation and exclusion of samples is shown in **Figure 19**.

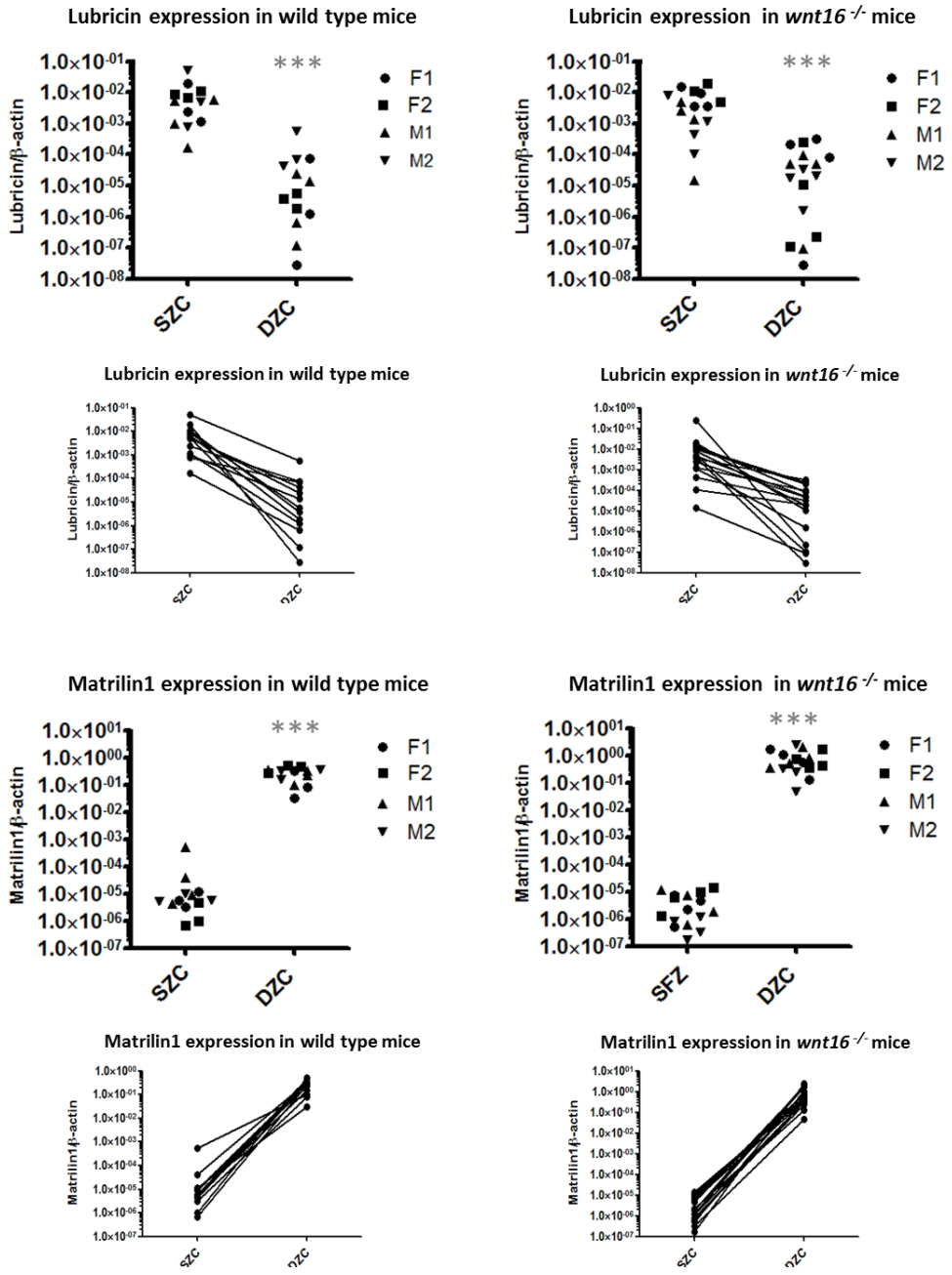

Figure 19: lubricin and matrilin1 were enriched after separation of SZC and DZC.

Chondrocytes from neonatal mouse epiphyses were isolated from the knees of 3 day old wild-type and Wnt16 knockout (*wnt16*$^{-/-}$) mice as indicated, and SZC and DZC culture were established as previously described (Yasuhara, Ohta et al. 2011). Cells were cultured in serum containing medium until cells reached 90% confluency (P0), and were then harvested for gene expression analysis by RT-PCR. All paired samples where lubricin and/or Matrilin1 were not enriched in the SZC and DZC cultures respectively were excluded from all future analysis (smaller graphs are a repeat of data to show paired samples of SZC and DZC from each mouse). This analysis was conducted on cells from two female and 2 male mice (F1/2, M1/2), n≥3 per mouse. Graphs are representative of a single isolation. Mann-Whitney test was used to test for statistical significance.

Following exclusion of paired samples where lubricin and/or matrilin1 were not expressed as expected, additional markers were analysed by Q-PCR and comparisons were made between SZ and DZ regions in wild type and *wnt16*$^{-/-}$ mice to further confirm successful enrichment (**Figure 20**).

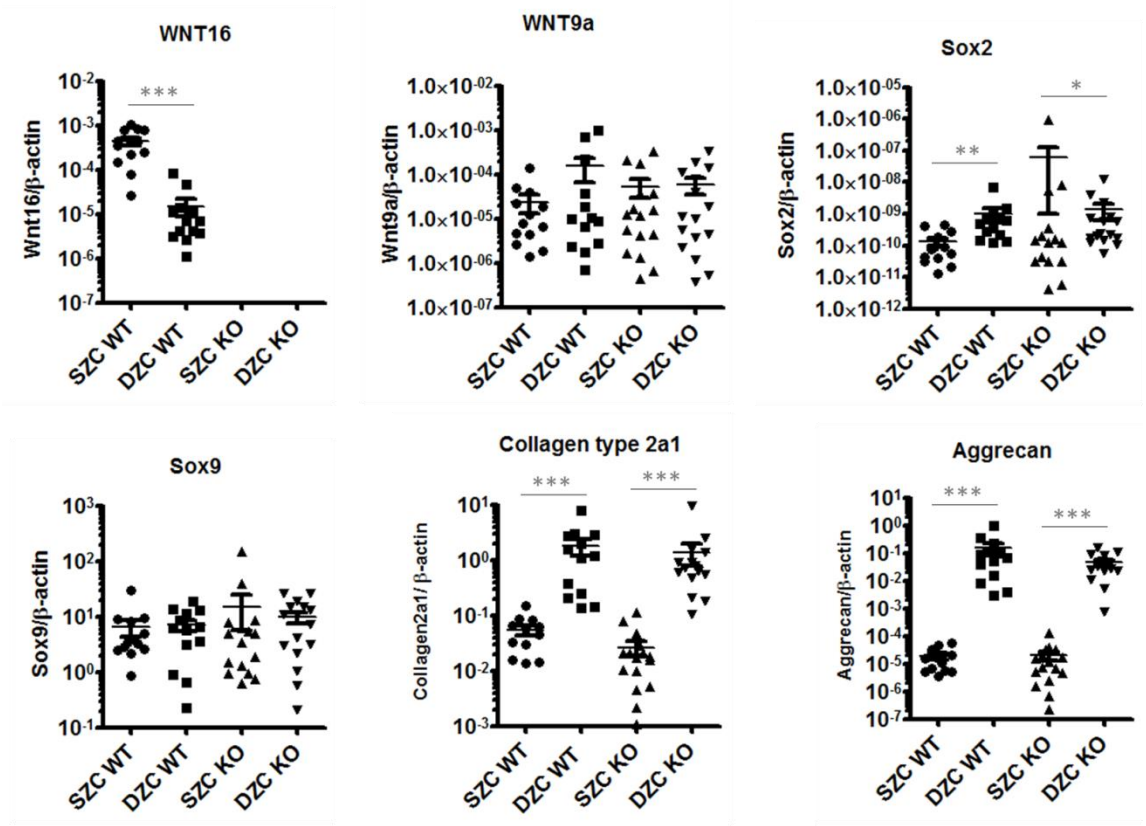

Figure 20: In addition to lubricin and matrilin1, other SZC and DZC specific markers were enriched as expected.

SZC and DZC were isolated from the knees of 3 day old mice as previously described (Yasuhara, Ohta et al. 2011). Cells were cultured in serum containing medium until cells reached 90% confluency (P0), then harvested for gene expression analysed by RT-PCR. This analysis was performed after the exclusion of paired samples based on lubricin/ matrilin1 expression as described. Values were normalised for β-actin. Graphs represent a single isolation containing cells from 4 mice (2male and 2 female as in figure 19). N≥3 per mouse. Mann-Whitney test was used to test for statistical significance between SZC and DZC from wild type (WT) and wnt16 knock out (KO) mice respectively.

Figure 20 shows that, as expected (Yasuhara, Ohta et al. 2011), Wnt16 was enriched in the SZC preparation, whereas col2A1 and aggrecan expression were higher in the DZC. Sox9 and wnt9A were not modulated. However, the expression of the stem cell marker sox2, previously reported to be expressed in SZC (Yasuhara, Ohta et al. 2011), was not enriched in my cultures. This may be due to strain specificity or experimental conditions, in addition, in my hands, sox2 detection levels were so low that they may be considered negligible. Further investigation into the regulation of this marker is required to understand what is occurring in my system.
In summary, isolation of enriched SZC cultures in my hands was confirmed by the expression of SZC markers lubricin and wnt16 in SZC cultures, and matrilin1, col2a1 and aggrecan in the DZC cultures.

Following isolation and in vitro culture to P0, SZC and DZC from wildtype and *wnt16*$^{-/-}$ mice were photographed and assessed for any obvious morphological differences (**Figure 21**). SZC had a more fibroblast like shape as expected compared to the characteristic rounded shape of mature chondrocytes seen with the DZC. However no clear differences were seen when comparing wild type and *wnt16*$^{-/-}$ cells.

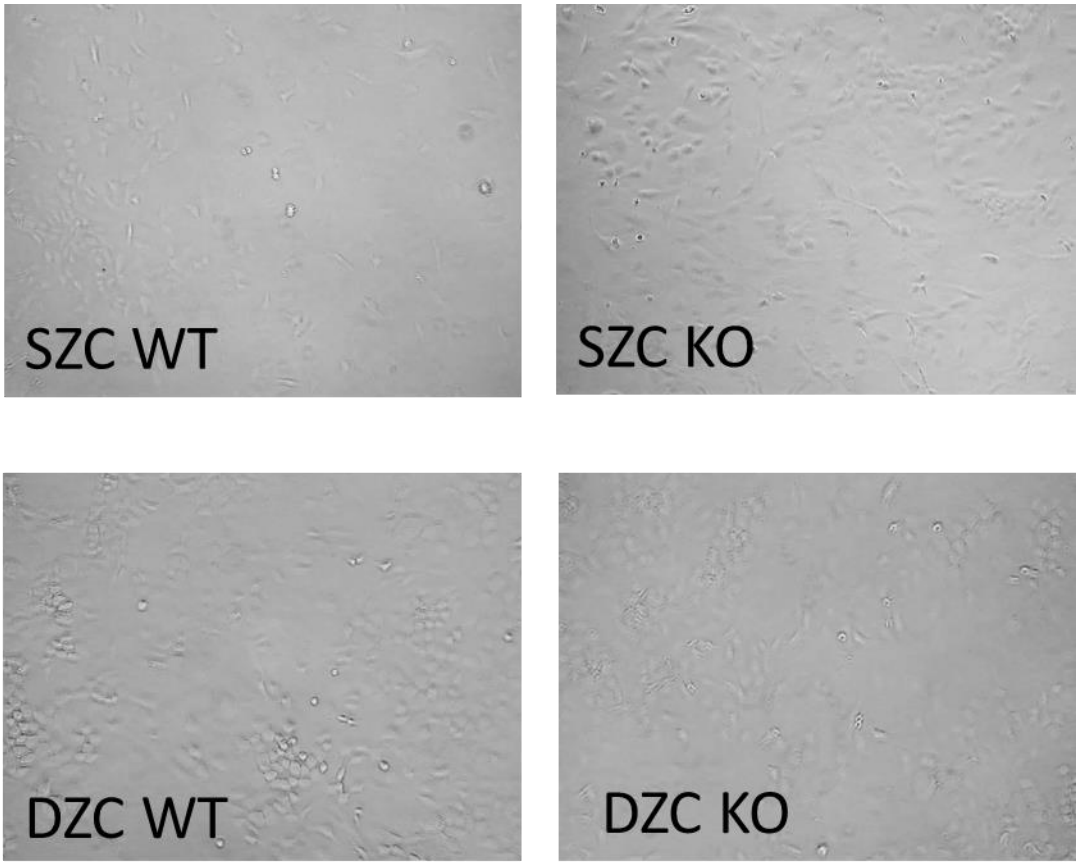

Figure 21: No obvious differences were observed between the morphology of wild type and wnt16 knockout chondrocytes.

SZC and DZC were isolated from the knees of 3 day old mice as previously described (Yasuhara, Ohta et al. 2011), and cultured in serum containing medium until cells reached 90% confluency (P0). Photographs were taken at 10x magnification with an inverted microscope. The figure shows representative images.

Wnt16$^{-/-}$ chondrocytes displayed no difference in proliferation rate compared to wild type chondrocytes.

In order to investigate whether WNT16 affected the growth rate of SZC or DZC, I monitored their proliferation in culture (results shown in **Figure 22**). Proliferation rate was calculated as the number of days required to reach 90% confluency.

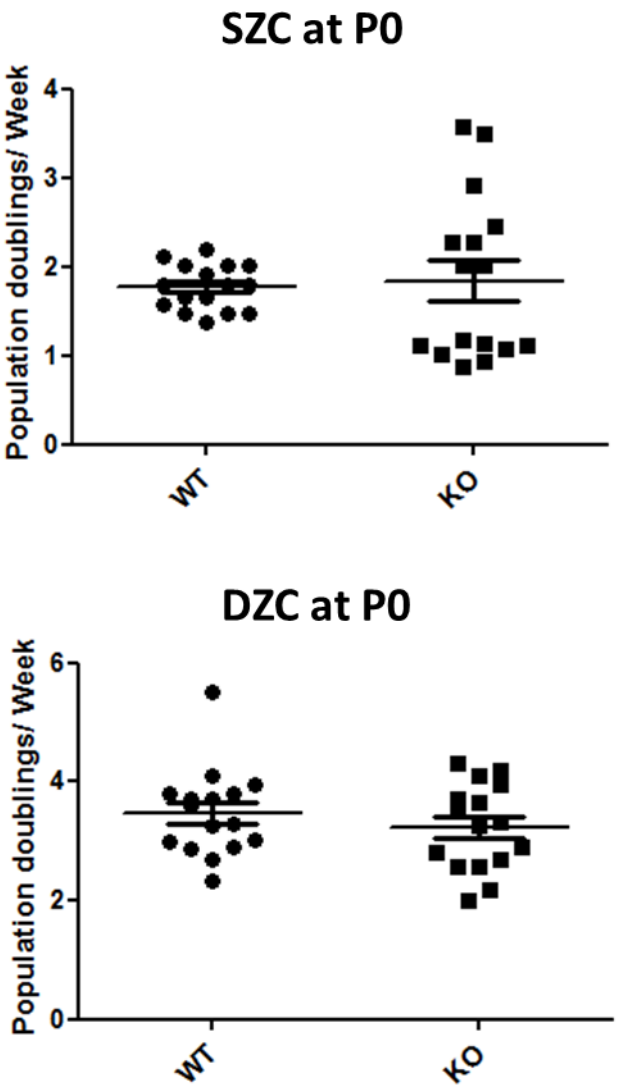

Figure 22: No statistically significant differences were observed in the proliferation rates between wild type and knockout SZC or DZC.

SZC and DZC were isolated from the knees of 3 day old mice as previously described (Yasuhara, Ohta et al. 2011). Cells were cultured in serum containing medium. Cells were counted, plated and allowed to reach 90 % confluency (P0), then counted again. Population doubling time was calculated by considering the change in total cell number between plating and reaching 90% confluency against time taken for this to occur. Graphs represent a single experiment. N=16 (4 mice, 4 replicates per mouse). Mann-whitney test was used to test for statistical significance.

No significant difference was seen between the proliferation rate of wild type and knockout cells in either the SZC or DZC (**Figure 22**).

Wnt16$^{-/-}$ SZC micromasses produce more abundant glycosaminoglycan-rich ECM than wild type SZC.

In order to investigate whether WNT16 affected the chondrogenic potential of SZC, P0 SZC were plated in micromass. Following 1 week in culture the micromasses were fixed and stained with alcian blue (pH0.2). Results are shown in **Figure 23**.

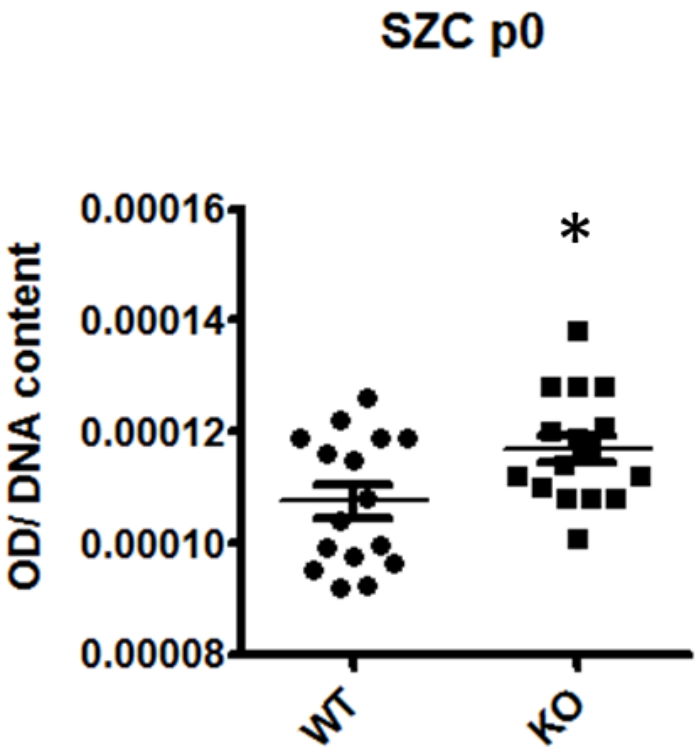

Figure 23: Loss of function of WNT16, increased the chondrogenicity of SZC.

SZC were isolated from the knees of 3 day old *wnt16*$^{-/-}$ mice as previously described (Yasuhara, Ohta et al. 2011). Cells were expanded to P0 then plated in micromass and cultured for 1 week in complete medium containing serum. At this stage micromasses were fixed and stained with alcian blue. Alcian blue content was measured following extraction with 6M guanidine using a spectrophotometer and normalised for DNA content. Results represent a single experiment, (n=16). Mann-whitney test was used for statistical comparison, error bars represent standard error of the mean.

Data from **Figure 23** shows that, In the absence of WNT16 SZC produce more GAG-rich ECM. The SZC retain an "immature" phenotype in response to endogenous Wnts (Koyama, Shibukawa et al. 2008; Yasuhara, Ohta et al. 2011). Therefore we can hypothesise that WNT16 supports the SZC phenotype by preventing their full differentiation into mature articular chondrocytes and in the absence of WNT16 SZC begin to differentiate. It is possible that after a longer time point we would see a greater difference between wild type and *wnt16*$^{-/-}$ cells. These data were in keeping with those showing that the SZC express less col2A1 and aggrecan than DZC.

No significant differences in the expression of common chondrocyte phenotypic markers were observed between SZC from wild type and wnt16*$^{-/-}$ *mice.

In order to investigate further the differences between SZC from wild type and knockout mice I compared the expression of SZC and DZC markers by RT-PCR (**Figure 24**).

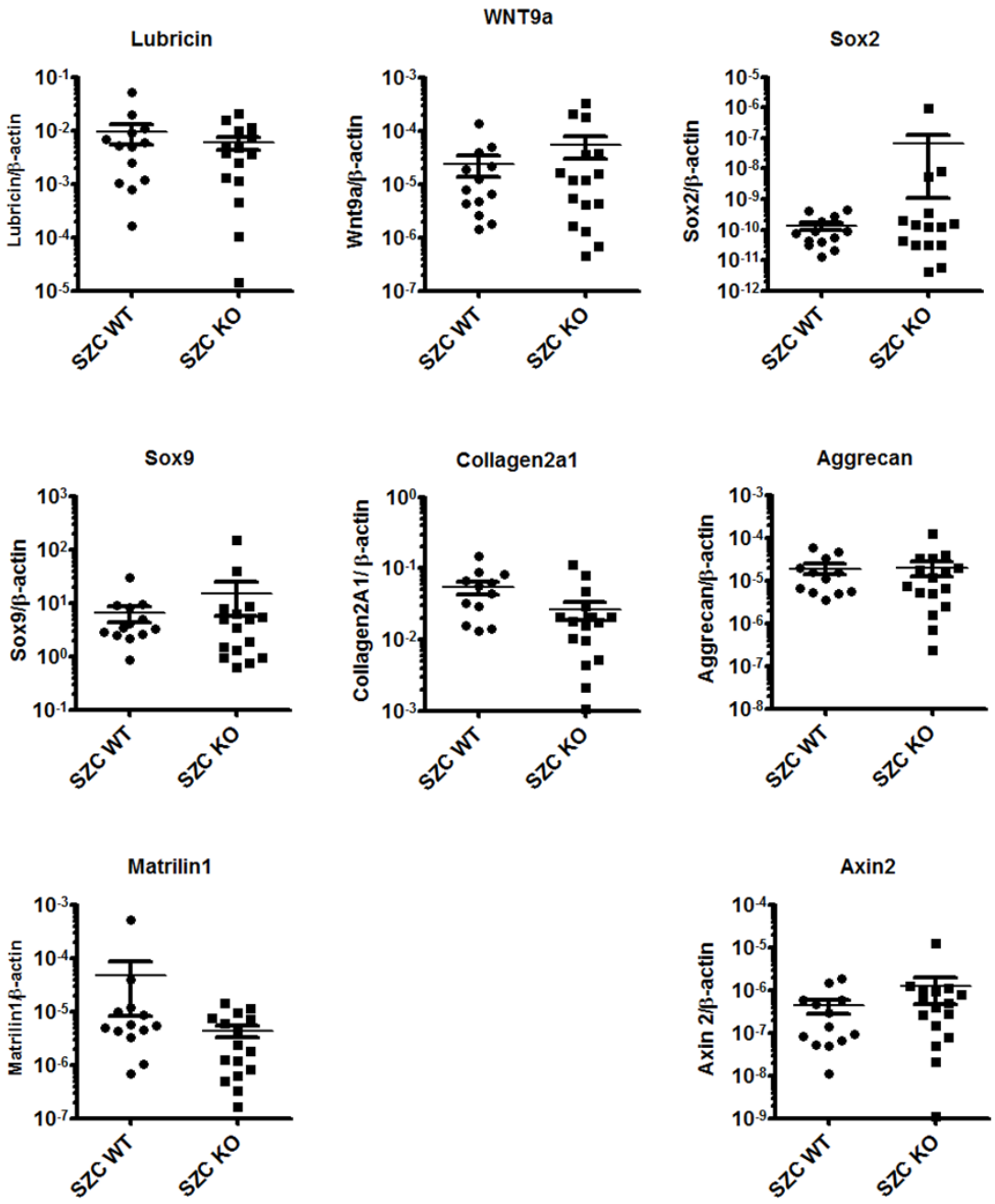

Figure 24: No significant differences in gene expression of chondrocyte specific markers were observed between SZC from wild type or wnt16$^{-/-}$ mice.

SZC were isolated from the knees of 3 day old mice as previously described (Yasuhara, Ohta et al. 2011). Cells were expanded to P0 in complete medium containing serum and harvested for gene expression analysis by RT-PCR. All values were normalised for β-actin. Data is representative of a single isolation, also shown in ***Figure 20***. Here, data are presented to compare wild type and *wnt16*$^{-/-}$ SZC. In ***Figure 20***, data is presented to highlight differences between SZC and DZC. Man-whitney test was used for statistical comparison, error bars represent standard error of the mean.

No significant differences were detected in the expression of SZC and DZC specific markers, between wild type and knockout SZC (**Figure 24**). Data from **Figure 23** showed that loss of WNT16 caused an increase in the proteoglycan content of SZC. Therefore we might have expected an increase in chondrocytic markers sox9, col2a1 and aggrecan. Therefore mechanisms other than transcriptional regulation of matrix components may explain the GAG accumulation, including stability, post-transcriptional processing of mRNA and translation rate and post translational modifications, including addition of sidechains etc. In addition we must also consider the rate of degradation of the ECM by catabolic enzymes.

Gain-of-function experiments for WNT16

Dose response using a WNT16 expression plasmid.

This first experiment was conducted before the availability of the recombinant protein. Therefore, my approach to generate a dose response curve by overexpression was to dilute the WNT16 expressing plasmid with empty plasmid so as to maintain the total amount of transfected DNA constant (1μg). The experiment was performed in wild type mouse costal chondrocytes which were harvested after 48 hours. The results are shown in **Figure 25**.

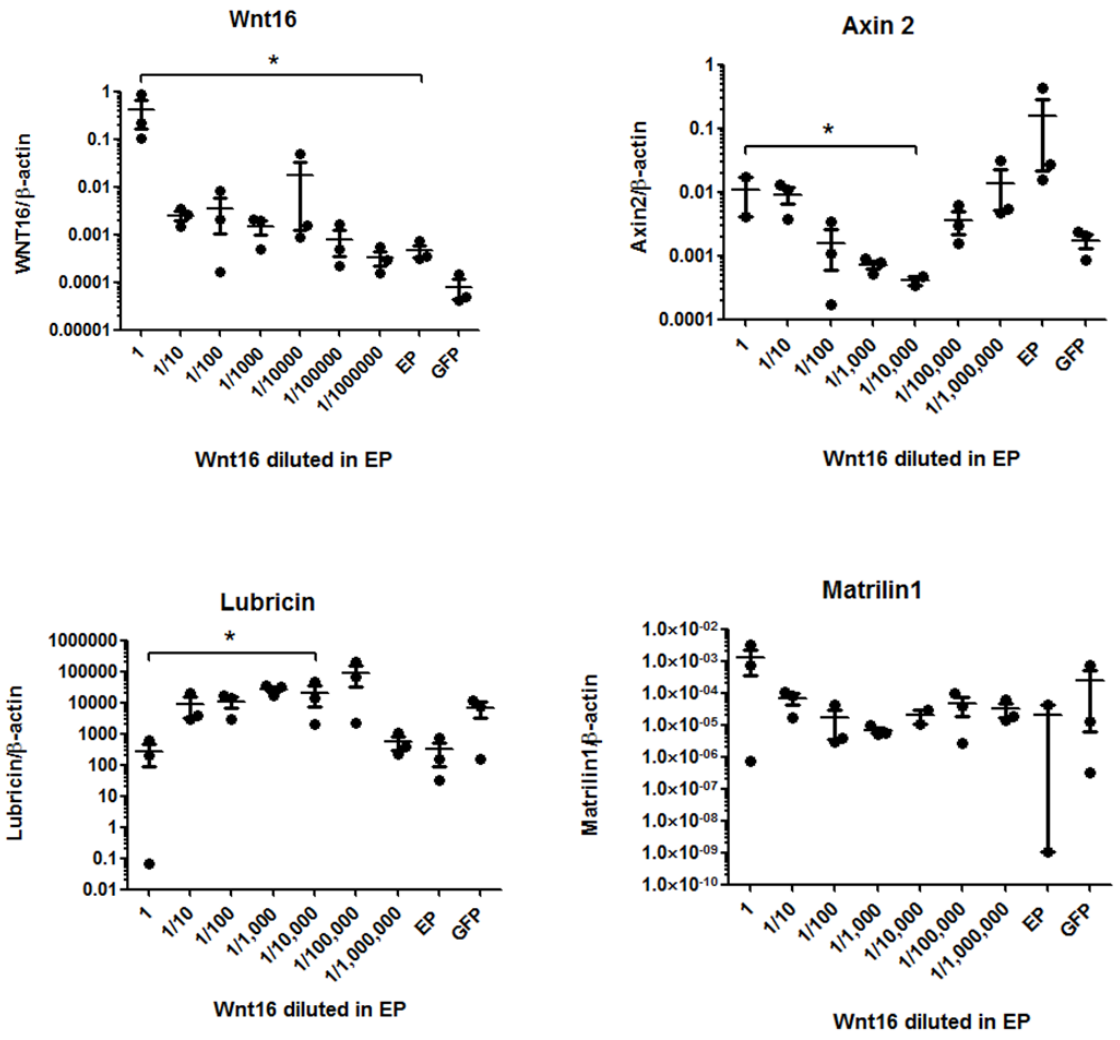

Figure 25: WNT16 dose response was achieved by dilution of wnt16 expression plasmid in EP.

Wild type mouse costal chondrocytes were transfected with decreasing amounts of WNT16 expression plasmid (diluted in empty plasmid, EP). (1) represents undiluted wnt16 plasmid, (1/10) represents 1 part wnt16 plasmid to 9 parts empty plasmid etc. Total concentration of plasmid DNA was kept at 1µg/ml. Stimulated cells were harvested for gene expression analysis after 48 hours culture in complete medium containing serum. Values were normalised for β-actin. The ANOVA analysis with post test for linear trend between mean and column number was used to test for significance. * represents results of the post test for indicated data groups. Data are representative of a single experiment (n=3).

As shown in **Figure 25**, a dose response with WNT16 was successfully achieved using this method. At low WNT16 concentration the WNT/β catenin target gene axin 2 was inhibited compared to control. Higher concentrations of WNT16 progressively increased axin 2 expression. However, under these experimental conditions, axin 2 never exceeded the original levels.

The results suggest that the activity of WNT16 is concentration-dependent, with a relatively narrow window when effects are detectable. This may explain why I had seen no significant results in previous overexpression experiments (**Figure 18** is equivalent to (1) in this experiment). First, as 1μg/ml of wnt16 expression plasmid (seen here labelled as (1)), generated no change in the expression of the genes tested and differences were only seen at lower concentrations, and second, as plasmid transfection is unlikely to be entirely consistent between wells, resulting in variable WNT16 concentration and variable results. Differences between empty plasmid and GFP are likely caused by GFP itself which was expressed to high levels in the cells.

In order to improve the expression of WNT16 using the plasmid I generated a perfect Kozak sequence using PCR cloning. The Kozak sequence is recognised by the ribosome and helps to initiate translation of mRNA to protein. However when I compared expression levels, there was no detectable difference between the expression of WNT16 generated from either plasmid (data not shown). Therefore optimization of the Kozak sequence made no difference to the expression levels of WNT16.

Exogenous recombinant WNT16 supports the expression of SZC phenotypic markers in primary bovine articular chondrocytes.

At this stage I reached a turning point in my studies when recombinant WNT16 became available (R&D systems), and allowed efficient dose response experiments and stimulations with high concentrations.

To confirm the results obtained in **Figure 25**, I performed a dose response experiment for WNT16 in primary bovine articular chondrocytes, results are shown in **Figure 26**.

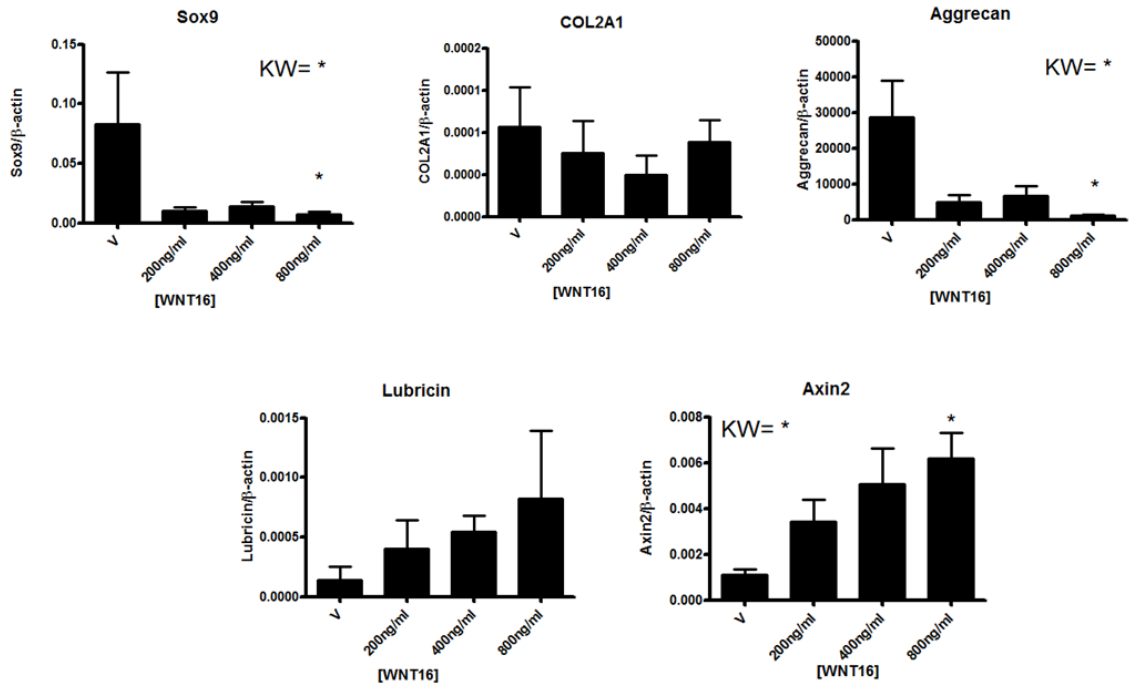

Figure 26: Recombinant WNT16 supports the SZC phenotypic marker profile in Primary bovine articular chondrocytes.

P0 bovine chondrocytes were plated in micromass and cultured for 24 hours in complete medium before treatment with recombinant WNT16 (ng/ml). Micromasses were harvested for gene expression analysis by RT-PCR after 6 days in culture in complete medium containing serum. Values were normalised for β-actin. Data are representative of a single experiment (n=4). Kruskal-wallis test with the Dunn's multiple comparisons post-test was used to asses significance. KW represents results of the kruskal-wallis test. Individual * represent the results of the Dunn's poet-test.

The data in **Figure 26** show that aggrecan and sox9 were significantly downregulated upon WNT16 stimulation. Additional chondrocytic marker, col2a1 also showed a trend towards downregulation. Lubricin on the other hand, showed a trend towards upregulation. This is in keeping with data from **Figure 23** showing that, in SZC, WNT16 loss of function resulted in a higher proteoglycan content and strengthens the hypothesis that WNT16 maintains the phenotype of the SZC.

Axin2, a validated readout for the activation of the canonical Wnt pathway, was dose-dependently upregulated upon WNT16 stimulation. This indicates that, at high concentrations (≥200ng/ml), WNT16 activates the canonical pathway. At a first look, this trend is in contrast with that seen in **Figure 25** which showed that WNT16 inhibited axin2 expression. However, if we compare the trends more carefully, we see that in **Figure 25**, after an initial downregulation at low concentrations of WNT16, axin2 expression increases in a linear fashion as WNT16 concentration increases (although never above control in this experiment, highlighting the limitation of plasmid transfection in reaching high concentrations of WNT16). We can therefore hypothesise that WNT16 inhibits the canonical WNT pathway at low concentrations but activates the pathway at high concentrations and that the concentrations achieved with plasmid transfections never reached the concentrations required to activate the canonical Wnt pathway. This was later confirmed in **Figure 28** are high doses biologically relevant? It is tempting to dismiss the high concentration effects as "off-target", however a number of considerations must be made: Although Wnts are usually considered "morphogens" and therefore signal over long distances (a typical example of this signalling modality is in the Drosophila imaginal disks where wingless-producing cells control the morphogenesis of the wings through long-distance signalling), in many other contexts, Wnts signal through cell-to-cell contact (Clevers and Nusse 2012). In these cases, Wnts are concentrated through binding to extracellular matrix proteoglycans. Therefore, concentrations of 200-800 ng/ml are likely to be physiological, locally. In keeping with this, *in vivo* data obtained by Dr Nalesso confirmed, first, that Wnt16 is retained and accumulated in the pericellular matrix in chondrocytes, and, second, that *wnt16*$^{-/-}$ mice failed to upregulate β catenin following induction of experimental OA, thereby suggesting that, *in vivo,* Wnt16 can signal through the canonical Wnt pathway, which, in my experiments, was activated only at concentrations >200 ng/ml.

One consideration is that this experiment was conducted in micromass over 6 days, whereas monolayer experiments are conducted over shorter time points, which may account for some

variation in results.

For the analysis of WNT16 function, in all subsequent experiments I used 200ng/ml of WNT16 as this was the lowest concentration which consistently elicited a biological response.

Exogenous recombinant WNT16 supports the expression of SZC phenotypic markers in wnt16$^{-/-}$ mice

In order to confirm the results seen in primary bovine articular chondrocytes, I performed a gain of function experiment using recombinant WNT16 on *wnt16*$^{-/-}$ SZC (**Figure 27**). I used 200ng/ml of recombinant WNT16 and harvested cells for gene expression analysis after 24 hours.

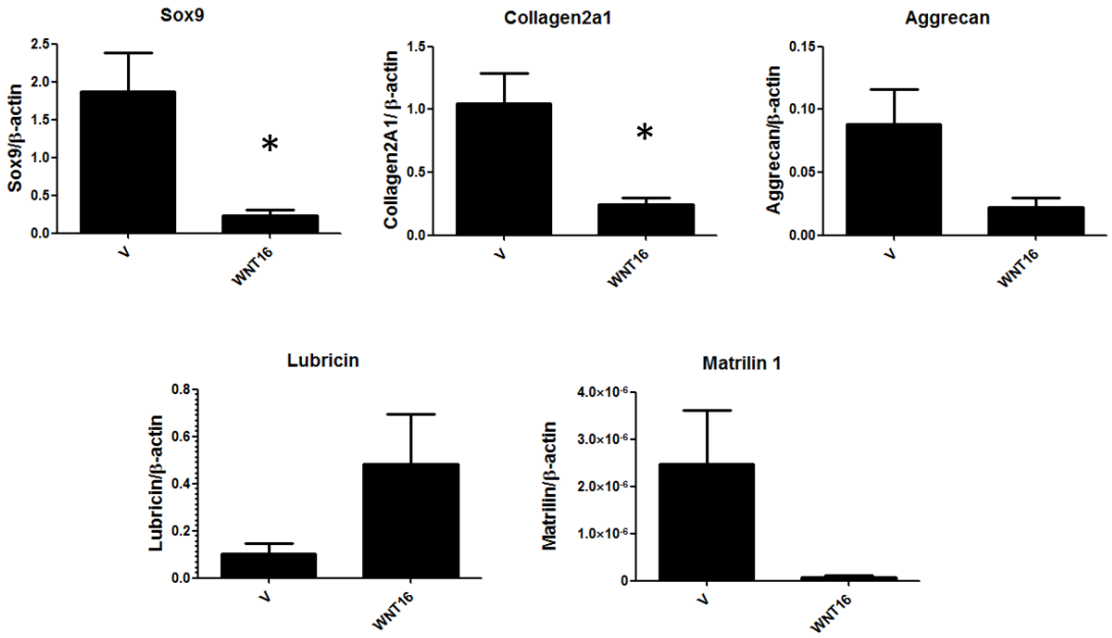

Figure 27: Recombinant WNT16 supports the SZC phenotypic marker profile in wnt16$^{-/-}$ SZC.

SZC were isolated from the knees of 3 day old mice as previously described (Yasuhara, Ohta et al. 2011). Cells from *wnt16*$^{-/-}$ mice were expanded to P0 and stimulated with 200ng/ml of recombinant WNT16 for 24 hours in complete medium containing serum, before harvesting for gene expression analysis by RT-PCR. Data are representative of a single experiment (n=4). All values were normalised for β-actin. Unpaired students T-test was performed for statistical comparison.

Figure 27 shows that recombinant WNT16 significantly downregulated the expression of sox9 and col2a1. There was a trend towards downregulation of aggrecan (P=0.10), whereas SZ marker lubricin showed a trend towards upregulated upon WNT16 stimulation (P=0.09). These results were mostly in keeping with those seen in **Figure 26**, which exhibited the same trends, and confirm that WNT16 functions to maintain the SZC phenotype, by upregulating SZC markers and preventing chondrocytic maturation. This is also in keeping with data from **Figure 23**, which showed that SZC from *wnt16*$^{-/-}$ mice had increased proteoglycan content when compared to cells from wild type mice. Slight differences may be accounted for by variations in experimental conditions (micromass/monolayer, and 6 days/24hours). However no differences were seen in **Figure 24**, were gene expression was compared between wild type and *wnt16*$^{-/-}$ SZC. This may be due to compensatory mechanisms that occur in the absence of WNT16 in vivo.

In conclusion WNT16 activity supports the SZC phenotype and inhibits chondrocytic maturation.

Discussion

One major problem throughout my studies was the unreliable availability of human primary articular chondrocytes. In addition, even when available, samples from human patients expressed variable levels of endogenous WNT16 (Dell'accio, De Bari et al. 2008). In fact we know that expression levels vary not only between patients, but also within a single joint (Dell'Accio, De Bari et al. 2006; Dell'accio, De Bari et al. 2008). It became clear therefore that I needed cells or cell lines that were readily available and consistent in their capacity to express WNT16. In preliminary experiments summarised in the appendix, I selected the human chondrocytic cell line C28/I2 as a suitable model to studying the mechanistic effects of WNT16. This human chondrocytic cell line had the best marker profile and the lowest endogenous expression of WNT16, however some problems arose when conducting WNT16 experiments to look at chondrogenicity as WNTs require serum for their activity but these cells require serum free conditions to differentiate (summarised in the appendix). Therefore throughout my studies I also used other sources of primary chondrocytes including bovine articular chondrocytes, mouse costal chondrocytes and neonatal mouse superficial zone cells (SZC).

As noted earlier in this chapter the initial stages of my project were challenging and overexpression of WNT16 yielded no results in HAC, bovine articular chondrocytes or mouse costal chondrocytes. There are a number of reasons that may explain why this happened. At this stage I did not have an established readout for WNT16 activity, which represented a major problem when attempting to interpret results and one possibility is that I was not analysing the correct genes. As well as variability related to transfection efficiency, high or variable levels of endogenous WNT16, due to variability between donor samples, may have masked the effects of exogenous WNT16. In addition some of these experiments contained a low number of replicates which along with that discussed above, will have contributed to a low statistical power of this analysis.

Early gain-of-function experiments where a dose response was attempted with the WNT16 plasmid, pcDNA3.1WNT16, suggested that WNT16 exhibits a dose dependent effect and some of these results later proved to be in keeping with experiments using the recombinant. Given that the activity of WNT16 is dose dependent we can assume (as we cannot accurately administer specific doses using plasmid transfections), that where results were not in keeping with later experiments that concentrations of WNT16 were not sufficient to see a response.

I continued my investigation using a loss-of-function approach and compared SZC, which express WNT16, from wildtype and *wnt16*$^{-/-}$ mice. SZC marker lubricin was enriched in SZC cultures and DZC markers matrilin1, aggrecan and collagen type 2a1 were enriched in DZC cultures indicating successful isolation of SZC and DZC separately and is in keeping with results seen by Yasuhara et al., 2011 (Yasuhara, Ohta et al. 2011). Sox2, a stem cell marker was not differentially expressed in my system. This may indicate that a population of cells were lost during the isolation or culturing as the levels of sox2 was very low. Repeating the experiment an additional few times, as well as analysing cell populations immediately following isolation rather than following *in vitro* culture to P0, would provide insight into any differences seen between my results and those published. Nevertheless, those cells expressing wnt16 were enriched in the SZC as expected, providing a platform for loss-of-function analysis when compared to those isolated in parallel from *wnt16*$^{-/-}$ mice.

No obvious morphological differences were seen between SZC and DZC from wild type and *wnt16*$^{-/-}$ mice, **Figure 21**, and no differences were seen in proliferation, **Figure 22**. Proliferation was calculated by measuring population doublings up to P0 over a period of time, however confirmation with other routine methods, such as BrdU incorporation or analysis of

proliferating cell nuclear antigen (PCNA), Ki-67 and phosphor-histone H3 (which are markers of proliferation), would confirm this result.

Measuring of proteoglycan content between wild type and *wnt16*$^{-/-}$ SZC showed that knock out cells cultured in micromass, had a higher matrix content than wild type cells, **Figure 23**. We know that WNT16 exerts a chondroprotective effect in vivo, as mice lacking WNT16 developed a more severe cartilage breakdown, therefore we might expect that cells exposed to WNT16 would produce more matrix than those not exposed to WNT16. However gene expression analysis following gain-of-function using recombinant WNT16 was in keeping with my results in micromass cultures and showed that WNT16 inhibited the expression of chondrocyte transcription factor, sox9, and two of its target genes, matrix components, collagen type 2a1 and aggrecan, **Figure 26** and **Figure 27**. In addition to downregulating the expression of mature chondrocyte markers, WNT16 upregulated the expression of lubricin, a marker of the SZC. These data suggest that WNT16 maintains the phenotypic marker profile of the SZC and regulates their differentiation into mature chondrocytes.

CHAPTER 4:

Pathway activation profile of WNT16

Introduction

The next chapter of my project involved investigating more systematically the pathway activation profile of WNT16. WNT proteins are known to activate a number of different pathways both canonical (the β-catenin dependant pathway), and non-canonical pathways. A number of the non-canonical pathways are calcium dependant e.g. CaMKII and Calcineurin, while others are not, eg. the JNK and PCP pathways. These non-canonical pathways are not as well studied as the canonical branch of WNT signalling, however as mentioned in the introduction they play important roles in both development and adulthood.

Results

Activation of the Canonical Wnt Pathway

WNT16 has been shown to activate the canonical WNT pathway in a rat chondrocyte cell line (Guo, Day et al. 2004). In addition, my previous results showed that WNT16 modulates the canonical WNT pathway readout axin2. Therefore, I began by investigating more thoroughly the effect of WNT16 on this pathway.

WNT16 modulates Axin2 mRNA expression in a dose dependent manner

Axin 2 is a transcriptional target and a well validated readout for activation of the canonical WNT pathway. Data from **Figure 26**, showed that concentrations of WNT16 ≥200ng/ml consistently upregulated axin2 expression. However, some early experiments conducted with the plasmid, suggest that low concentrations of WNT16 inhibit axin2 expression.

To confirm the biphasic effect of WNT16 on the canonical WNT pathway I performed a dose response experiment on P0 bovine primary articular chondrocytes using recombinant WNT16, and covered a wide range of concentrations from 10ng/ml to 400ng/ml (**Figure 28**).

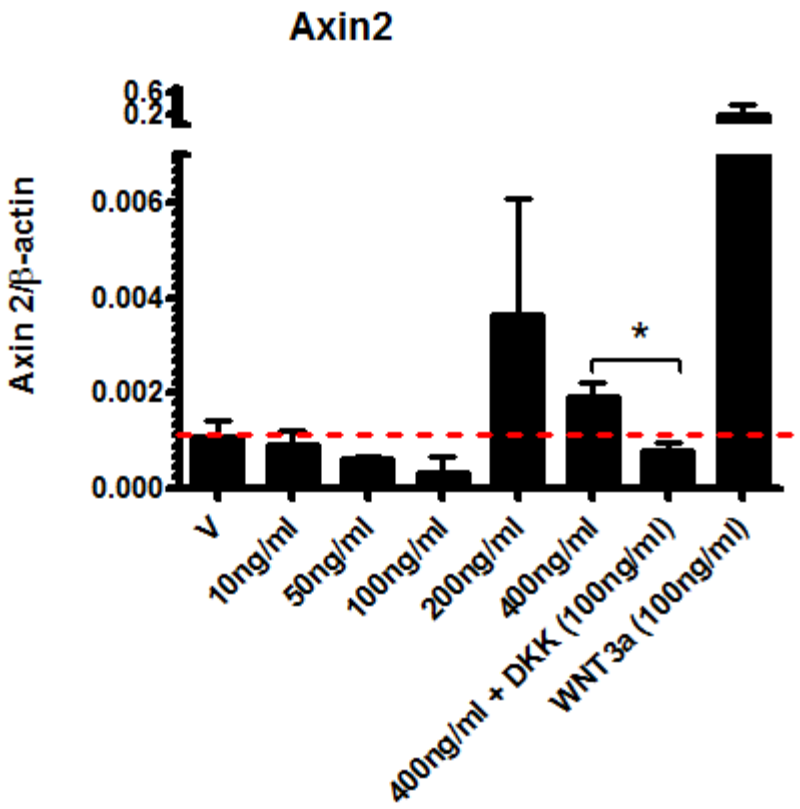

Figure 28: WNT16 dose dependently modulated the canonical WNT pathway.

P0 Bovine primary articular chondrocytes were treated for 24 hours with WNT16, with or without inhibitor DKK1 (100ng/ml). WNT3a (100ng/ml), was used a positive control for canonical activation. Experiment was conducted in complete medium containing serum. Gene expression was analysed by RT-PCR. Values were normalised for β- actin. Data represent a single experiment (n=3). Upregulation of axin2 by 200ng/ml WNT16 shown in 3 separate experiments (see also **Figure 33**, and data not shown). Unpaired students T test or ANOVA with post-test for linear trend between mean and column number was used for statistical comparison. Red dotted line represents control level of axin2 expression.

Data from **Figure 28** show that at low concentrations of WNT16 (50ng & 100ng) axin2 expression was downregulated compared to vehicle, suggesting that these concentrations inhibit the canonical WNT pathway. At higher concentrations (>200ng/ml), WNT16 upregulated axin2 expression compared to vehicle. As expected, Axin2 was strongly upregulated upon stimulation with WNT3A and downregulated by DKK1 an inhibitor of the canonical Wnt pathway. This results are in-keeping with repeats of this experiment. This confirms my previous hypothesis that low concentrations of WNT16 inhibit the canonical WNT pathway and higher concentrations (≥200ng/ml) activate the pathway.

Further investigation into the optimal time point for analysis of axin2 as a readout for canonical activation may yield greater differences in results. For example, a dose response between 100ng/ml and 200ng/ml conducted over a time course would allow for further investigation into the mechanisms of action of WNT16.

WNT16 stimulation results in β-catenin accumulation.

In order to confirm these results, I repeated the same experiment and monitored accumulation of β catenin as an alternative readout for activation of the canonical WNT signalling (**Figure 29**).

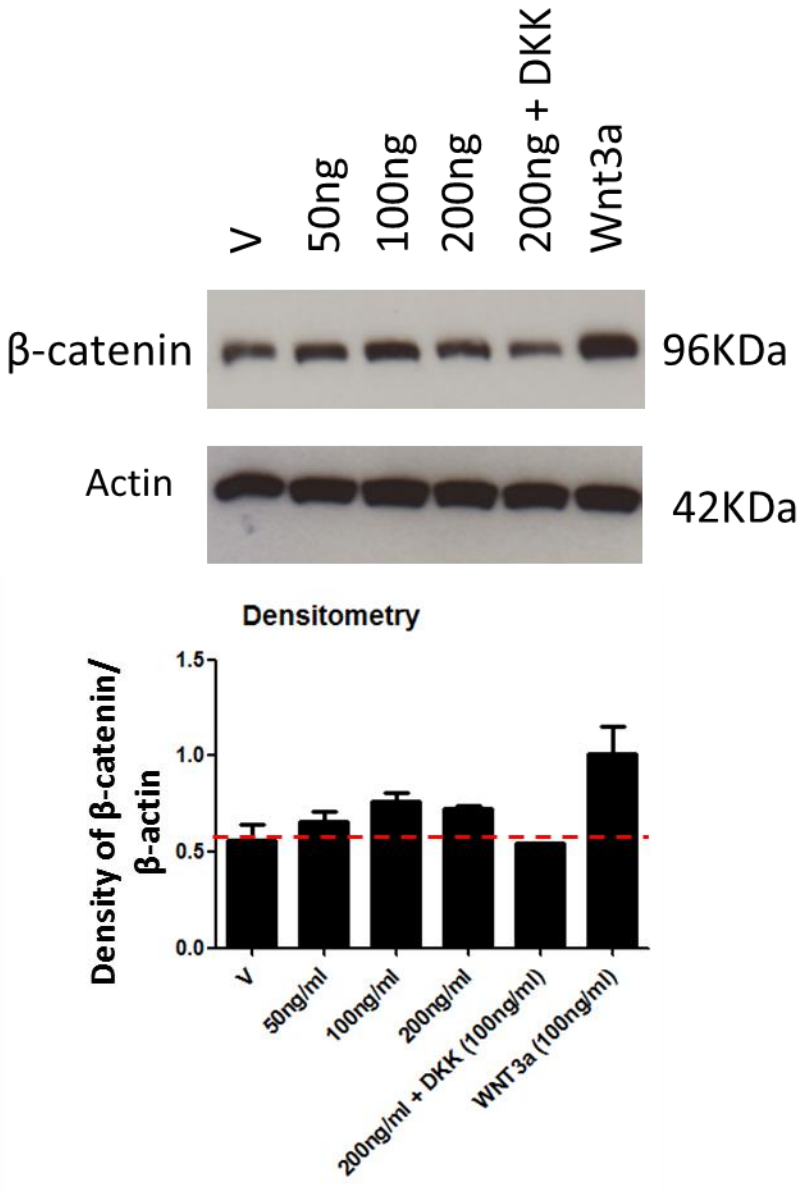

Figure 29: WNT16 increased total β-catenin levels.

Bovine primary articular chondrocytes were treated for 48 hours with WNT16 (ng/ml), with or without inhibitor DKK1 (100ng/ml). WNT3a (100ng/ml), was used a positive control for canonical activation. Experiment was carried out over a 48 hour time point in complete medium containing serum, then harvested with RIPA buffer to preserve protein from the cell lysate. Total β-catenin levels were analysed by western blot for β-catenin on whole cell lysates. Values were normalised for β- actin. Western blot image is of a representative blot. Densitometry calculation is including 2 repeats. Bars represent standard error of the mean.

The results showed that WNT16 increased total β-catenin levels in the cell at all concentrations, indicating the WNT16 activates the canonical WNT pathway (**Figure 29**). The densitometry values represent combined results of 2 blots run with different experimental repeats. 48 hour time point was used as standard for analysis of protein levels. B-actin was used as a loading control. It is possible that too much protein was loaded on the gel, resulting in very heavy bands. Less protein may allow for better representation of differences between conditions.

Discrepancies between these results and those in **Figure 28** are possibly due to a regulatory mechanism between the accumulation of β-catenin in the cytoplasm and its transcriptional activity. Therefore it may be that at the receptor level, WNT16 activates the canonical WNT pathway at all concentrations, but other mechanisms activated within the cell exert an inhibitory effect on the canonical WNT pathway at low levels of WNT16, similarly to that seen with WNT3a (Nalesso, Sherwood et al. 2011). With this in mind I investigated which other WNT pathways were activated by WNT16 in an attempt to dissect the mechanism. Comparison of cytoplasmic and nuclear levels of β-catenin would also provide further insight into the mechanism of action of WNT16 and at which level the inhibition of axin2 occurs.

The PKA pathway is not modulated by WNT16

The protein kinase A (PKA) pathway is known to be activated by WNT5a and is involved in processes such as regulation of apoptosis and chondrogenic differentiation (Torii, Nishizawa et al. 2008; Noguchi, Watanabe et al. 2010).

The PKA or CREB reporter assay monitors the activity of PKA/cAMP in cells by expressing the firefly luciferase gene under the control of a promoter containing cAMP response elements.

Both WNT16 expression plasmid and recombinant WNT16 were used for comparison. The human immortalised chondrocyte cell line C28/I2 was transfected then stimulated 24 hours later for a further 24 hours before harvesting cell lysates for the reporter assay (**Figure 30**).

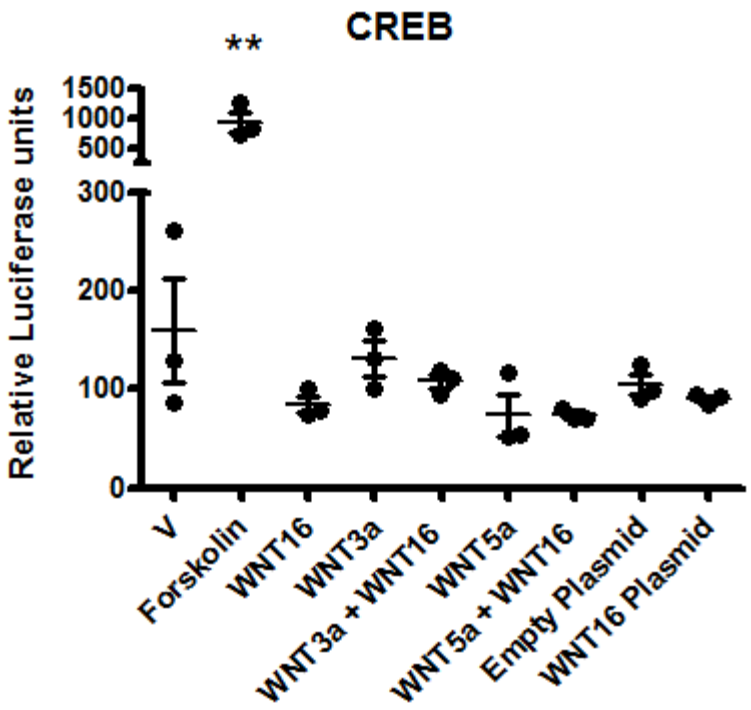

Figure 30: WNT16 did not activate the PKA pathway.

C28/I2 cells were transfected with reporter plasmids and indicated groups were also transfected with either WNT16 expression plasmid or empty plasmid (last 2 columns). 24 hours later cells were stimulated with either WNT16 (200ng/ml), WNT3a (100ng/ml) and WNT5a (100ng/ml), or Forskolin as positive control (100µM) as indicated in the graph (Those transfected with WNT16 or empty plasmid were not stimulated). Experiment was left for a further 24 hours then cell lysates were harvested for analysis of luciferase levels as a readout for pathway activation. Values were normalised for renilla luciferase. Data are representative of a single experiment (n=3). An unpaired students t-test was used for statistical analysis.

WNT16 did not induce luciferase activity compared to controls and therefore does not activate the PKA pathway in C28/I2 cells (**Figure 30**). Like WNT16, WNT3a did not activate the pathway. Unexpectedly, WNT5a, a reported activator of the pathway, did not induce luciferase activity in these cells which may be due to cell specificity. However, as the positive control (Forskolin) successfully activated the reporter we can assume that the assay was functioning correctly.

The Calcineurin pathway is not modulated by WNT16

I also investigated if WNT16 can activate the calcineurin pathway (**Figure 31**). This reporter construct expresses the firefly luciferase gene under the transcriptional control of a minimal CMV promoter with NFAT binding sites. NFAT is a family of transcription factors downstream of calcineurin which is known to regulate both bone formation and chondrogenesis.

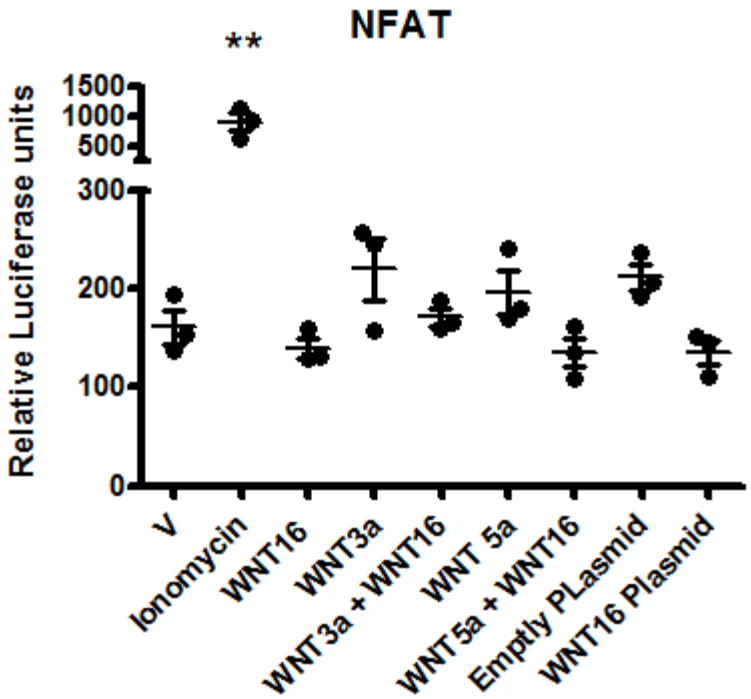

Figure 31: WNT16 did not activate the Calcineurin pathway.

C28/I2 cells were transfected with reporter plasmids and indicated groups were also transfected with either WNT16 expression plasmid or empty plasmid (last 2 columns). 24 hours later cells were stimulated with either WNT16 (200ng/ml), WNT3a (100ng/ml) and WNT5a (100ng/ml), or Ionomycin as positive control (1µM) as indicated in the graph (Those transfected with WNT16 or empty plasmid were not stimulated). Experiment was left for a further 24 hours then cell lysates were harvested for analysis of luciferase levels as a readout for pathway activation. Values were normalised for renilla luciferase. Data are representative of a single experiment (n=3). An unpaired students t-test was used for statistical analysis.

WNT16 did not activate the NFAT reporter assay and therefore does not activate the calcineurin pathway. WNT3a and WNT5a showed the same trend. The positive control Ionomycin, activated the reporter.

WNT16 activates the JNK pathway

WNT16 is known to activate the JNK pathway in keratinocytes (Teh, Blaydon et al. 2007). To investigate whether WNT16 activates the pathway in chondrocytes I treated primary bovine articular chondrocytes with WNT16 and looked for activation of c-Jun, a transcription factor downstream of JNK (**Figure 32**).

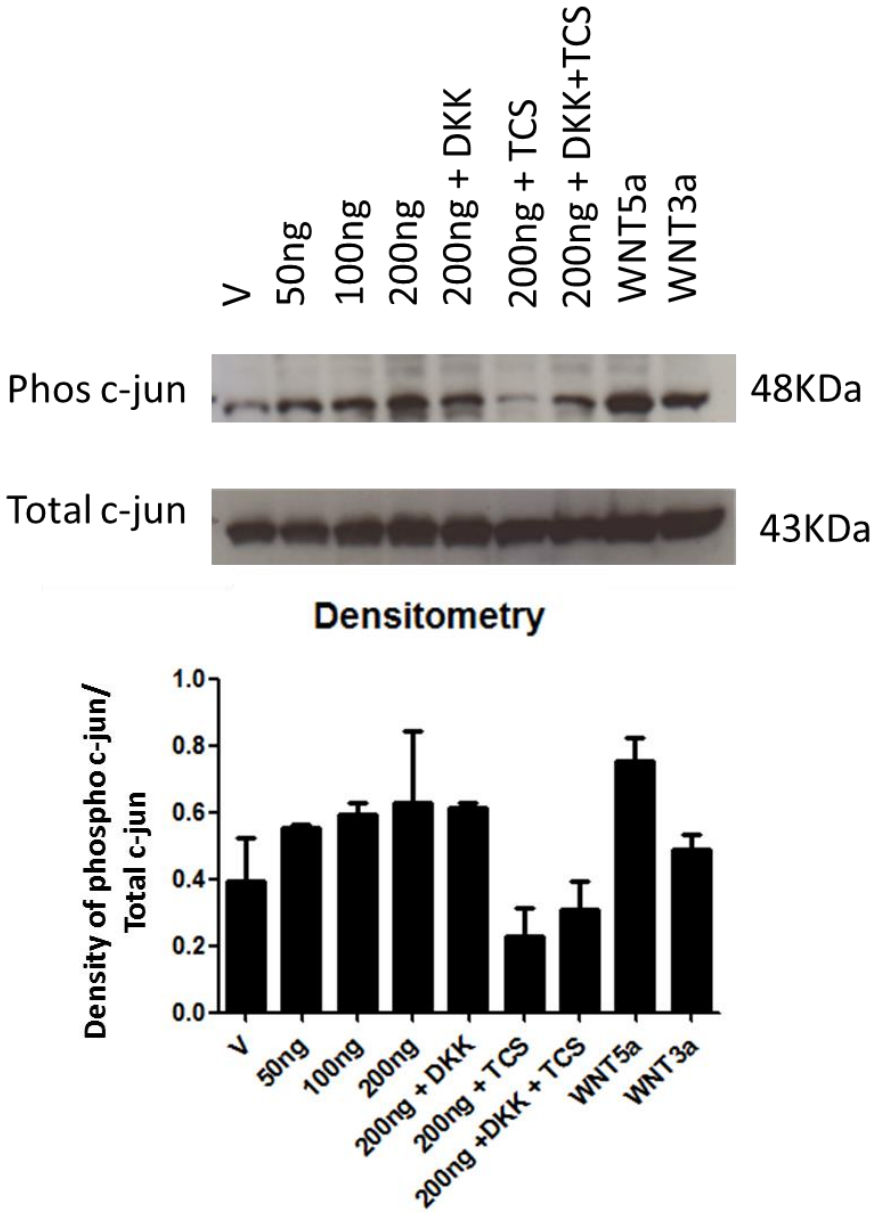

Figure 32: Recombinant WNT16 activated the JNK pathway.

WNT16 dose dependently phosphorylated transcription factor c-jun. P2 Bovine articular chondrocytes were plated, left to attach, then treated with increasing concentrations of WNT16 (ng/ml), DKK1 (100ng/ml), WNT5a (100ng/ml), WNT3a (100ng/ml) and (TCS-10µM) and harvested after 30 minutes using RIPA buffer to preserve lysates for western blotting. 60µg of sample was loaded for each condition. Densitometry represents 2 samples normalised for control. Error bars represent standard error of the mean.

WNT16 upregulated phosphorylation of c-Jun (**Figure 32**). This indicates that WNT16 activates the JNK pathway. Blocking JNK activity with the inhibitor TCS (Szczepankiewicz, Kosogof et al. 2006; Kauskot, Adam et al. 2007), inhibited c-Jun phosphorylation as expected. Inhibitor should display >1000fold selectivity for JNK1,2, and 3 over other kinases such as ERK2 and p38. WNT5a, a known activator of the pathway, successfully induced c-Jun phosphorylation, as did WNT3A, but to a lesser extent than WNT16.

30 minute time point was shown in the literature to be optimal for JNK phosphorylation, however a time course with WNT16 (200ng/ml) would optimise the outcome for my own system.

Therefore, we can conclude that WNT16 is able to activate both the canonical Wnt and the JNK pathways in a dose dependent manner.

Inhibition of the JNK pathway also inhibits the canonical Wnt pathway

In order to investigate the crosstalk between the JNK pathway and the canonical WNT pathway, I stimulated bovine articular chondrocytes with WNT16, with and without JNK inhibitor, TCS, and looked at axin2 mRNA expression and total β-catenin protein levels (**Figure 33**).

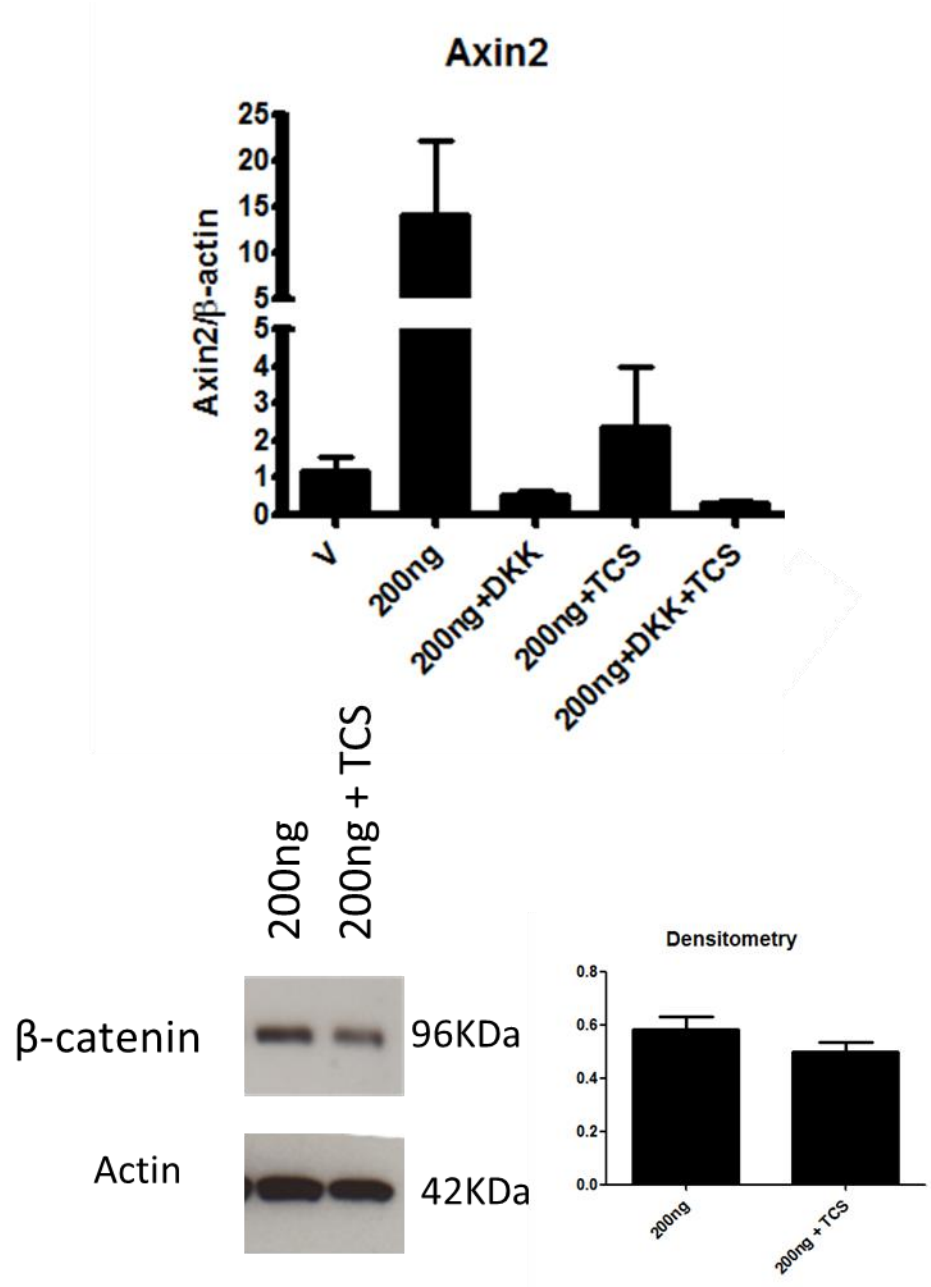

Figure 33: Blocking the JNK pathway following WNT16 stimulation also downregulated the canonical WNT pathway.

Bovine articular chondrocytes were treated with WNT16 (200ng/ml), DKK (100ng/ml), and (TCS-10μM) and harvested after 24 hours for gene expression analysis by RT-PCR (A), or at 48 hours with RIPA buffer for western blot (B). Experiments were conducted in complete medium containing serum. (A) represents a single experiment (n=4), however the experiment was repeated and results were inkeeping with the above data (data not shown). (B) Image shows a representative blot, densitometry represents n=2. Unpaired students t test was used to analyse significance. Error bars represent standard error of the mean.

The data from **Figure 33** suggest that, in the presence of WNT16, inhibition of the JNK pathway also partially inhibits the canonical WNT pathway. Although the decrease in axin2 is not significant, the trend is confirmed by the decrease in β-catenin protein levels.

IT would be interesting to gain more information into the interaction between these two patwhays, for example, knock down of an essential JNK component, eg. c-jun, by siRNA, would provide greater insight into this and the mechanism of activity of WNT16.

Discussion

Results from chapter 3 suggested that WNT16's activity on the WNT canonical pathway is biphasic, inhibiting the pathway at low concentrations and activating the pathway at higher concentrations. This was confirmed in **Figure 28** of this chapter where concentrations lower than 200ng/ml inhibited expression of axin2, a validated WNT canonical readout, compared to control, and concentrations greater than 200ng/ml increased axin2 expression. The activation of the WNT canonical pathway by WNT16 was confirmed by β-catenin accumulation in **Figure 29**. This is used as a measure of WNT canonical pathway activation. In the inactive state, β-catenin is degraded. Following binding of a canonical WNT to receptors, the degradation complex is interrupted, and β-catenin accumulates in the cytoplasm before translocating to the nucleus to activate transcription. This result indicated that WNT16 caused accumulation of β-catenin and thus, WNT canonical pathway activation at all concentrations (50-200ng/ml), this is not in keeping with previous results that showed concentrations of WNT16 <200ng/ml inhibiting the pathway (based on axin2 expression). This may be due to a regulatory mechanism following β-catenin accumulation in the cytoplasm that affects pathway activity further downstream. For example, interactions with other pathways such as the JNK pathway which was activated by WNT16 at all concentrations (50-200ng/ml, based on c-jun phosphorylation, a validated readout for JNK activation, **Figure 32**).

Interaction between these two pathways has already been described (Saadeddin, Babaei-Jadidi et al. 2009). As well as having some common target genes, such as c-myc, cyclinD1 and CD44, there are a number of other links between the two pathways. For example, Dvl and axin are important elements in both pathways. Dvl is able to activate both pathways through different domains. In mice, the DEP domain in the C-terminal half of the protein was sufficient and necessary to activate the JNK pathway, whereas the DIX domain was not required. However for

β-catenin activation, the DIX and PDZ domains are required but not sufficient as removal of the DEP domain abolished signalling. Interestingly a mutation in the DEP domain at lys438 which abolished JNK signalling did not affect canonical activation, indicating the DEP domain plays a different role in the activation of the canonical WNT pathway to that which it does in the activation of JNK (Moriguchi, Kawachi et al. 1999). In Drosophila however the removal of the c-terminal region of Dsh (the Drosophila homologue of Dvl), including the region corresponding to the mouse DEP domain, did not affect the ability of the protein to elevate Armadillo levels (β-catenin homologue), and therefore seemed to not be required for canonical WNT signalling, at least in drosophila. The region corresponding to the PDZ domain however, is required (Yanagawa, van Leeuwen et al. 1995; Lee, Ishimoto et al. 1999). As well as Dvl, axin a well-known antagonist of the canonical WNT pathway has also been shown to activate the JNK pathway. This occurs by complex formation and activation of MEKK1 through separate domains to those which act on the canonical WNT pathway (Zhang, Neo et al. 1999). It is possible therefore, that a single WNT ligand can activate both pathways and that the switch may occur further downstream than the receptors at the level of these intracellular proteins, which offers an explanation as to how WNT16 might activate both the canonical WNT and JNK pathways.

As well as upstream components, also downstream transcription factors for both pathways, TCF4 (HMG transcription factor) and β-catenin in the case of the canonical WNT pathway and c-Jun (an AP-1 transcription factor) in the case of JNK, can form a complex on the c-Jun promoter to cooperatively activate transcription (Nateri, Spencer-Dene et al. 2005). Complex formation between the transcription factors is dependent on JNK mediated phosphorylation of c-Jun (Nateri, Spencer-Dene et al. 2005).

JNK also directly regulates components for canonical activation. The tcf4 promoter is a target for phosphorylated c-Jun (Hayakawa, Mittal et al. 2004), and JNK phosphorylates β-catenin at Serine 191 and 605, facilitating nuclear localization. Inhibition of total JNK activity prevented nuclear accumulation of β-catenin without affecting its accumulation in the cytoplasm, and abolished the Lef1-luciferase activity induced by WNT3a, this seemed to be more dependent on JNK2 than JNK1. Upsteam of JNK in this mechanism is Rac1 (a member of the Rho family of small GTPases), which is essential for WNT3a induced JNK2 phosphorylation and lef1-luciferase activity, as a dominant negative form of the protein abolished transcriptional activation. In addition mutant mouse embryos lacking Rac1 in the developing limb bud (Msx2-Cre;$Rac1^{n/c}$), had identical phenotypes to mice lacking β-catenin from the same regions, with complete loss

of hind limbs and truncated forelimbs (Wu, Tu et al. 2008). These data indicate that the Rac1 pathway, including JNK activity is essential for β-catenin translocation. This data supports my own findings that inhibiting the JNK pathway also inhibits axin2 expression (**Figure 33**).

With regard to the inhibition of the canonical WNT pathway at low levels of WNT16, if JNK is essential for canonical activation and JNK activation by WNT16 is dose dependent, then we might consider that low JNK activity seen at low levels of WNT16 is not sufficient to translocate necessary β-catenin levels to activate transcription of axin2. Further experiments are necessary to confirm this, including blocking the JNK pathway at low levels of WNT16 and investigating cytoplasmic versus nuclear levels of β-catenin, which can be achieved via western blotting. However, one limitation in analysis of cell fractions is that pathway activation does not require translocation of all β-catenin molecules to the nucleus, and if total cell levels of the protein are high, comparison of cytoplasmic versus nuclear fraction may not be representative of pathway activation/ inhibition, as a few molecules may be sufficient for activity. Having said that, a change in the proportion of translocated β-catenin would provide information regarding the point at which WNT16 modulates the pathway. Independently from the interference of other pathways, further experiments looking at WNT canonical activation through different avenues (such as luciferase reporters or additional transcriptional targets), would confirm that the inhibitory effect on axin2 is a true reflection of pathway activity or if it is an effect specific to the axin2 promoter.

CHAPTER 5:

Biological outcomes of WNT16 pathway activation

Introduction

Disruption of Wnt16 resulted in increased susceptibility to instability induced OA (Nalesso, Thomas et al., manuscript in preparation). My data so far indicate that lubricin is a target of WNT16. Lubricin is an essential protein for joint homeostasis, as mice lacking the prg4 gene develop spontaneous OA (Coles, Zhang et al. 2010). Therefore it is likely that the chondroprotective effect of WNT16 is mediated through lubricin expression. Therefore I investigated more thoroughly the mechanism by which lubricin is upregulated by WNT16.

Results

Activation of the canonical WNT pathway is required for the WNT16-induced upregulation of lubricin in SZC

To investigate if the activation of the canonical WNT pathway was required for the WNT16-induced upregulation of lubricin, SZC from *wnt16*$^{-/-}$ mice were stimulated with WNT16 in the presence or in the absence of DKK1 and compared lubricin expression both at mRNA and protein levels (**Figure 34**).

(A)

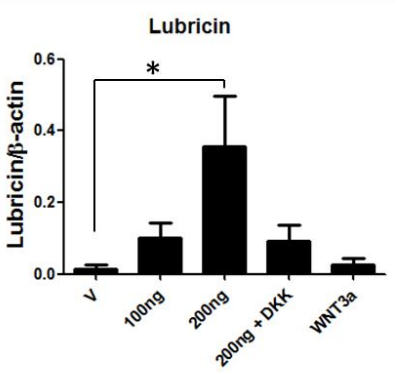

(B)

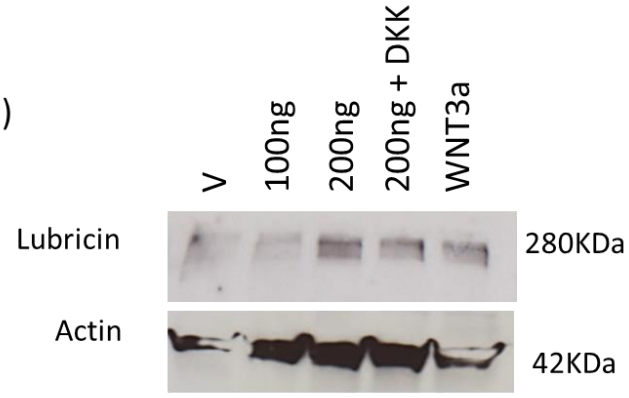

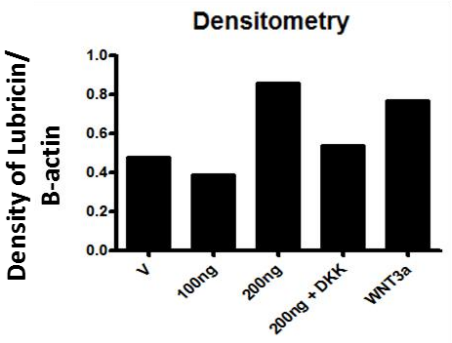

Figure 34: WNT16-induced lubricin expression was mediated by activation of the canonical WNT pathway in SZC.

SZC were stimulated with recombinant WNT16 (ng/ml), DKK1 (100ng/ml) and WNT3a (100ng/ml) then harvested 24 (A), or 48 (B) hours later for gene and protein expression analysis. Experiment was conducted in complete medium with serum. (A) Data represents a single experiment (n=4). (B) Image is representative blot, experiment was repeated and results show the same trend (data not shown). Values were normalised for β-actin. The ANOVA analysis with the Tukey post-test for comparing all pairs of columns was used to check significance of the data.

WNT16 induced lubricin expression at both mRNA and protein level, while addition of DKK1, showed a trend towards inhibition of this upregulation (p=0.1) (**Figure 34**). In addition, WNT3a a more potent activator of the canonical WNT pathway was not able to upregulate lubricin to the same extent as WNT16. Therefore the canonical WNT pathway is involved in the WNT16 upregulation of lubricin as DKK reduced this effect, however given the poor effect of strong canonical WNT activator, WNT3a, on lubricin expression, other pathways are likely involved in the activity of WNT16.

Activation of the canonical WNT pathway is required for the WNT16-induced upregulation of lubricin in Primary Bovine articular chondrocytes

In order to confirm the results seen in SZC (**Figure 34**), I repeated the experiment in bovine articular chondrocytes (**Figure 35**).

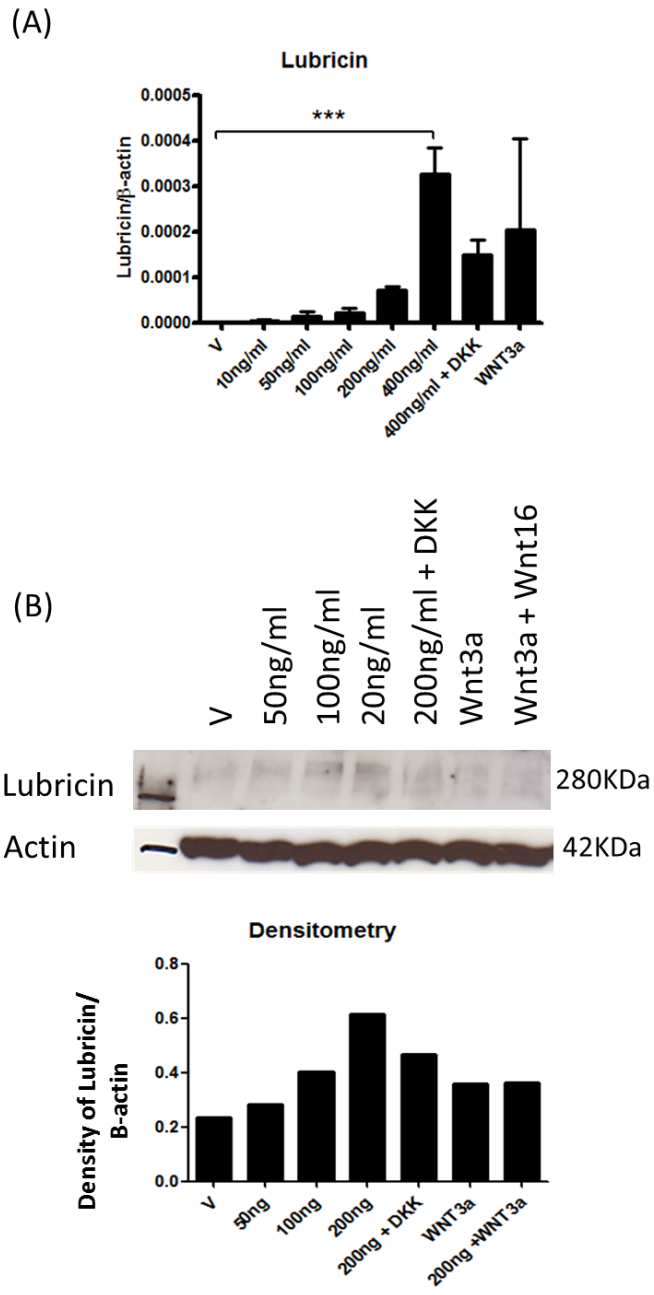

Figure 35: WNT16 upregulation of lubricin is mediated through the canonical WNT pathway in BAC.

Bovine articular chondrocytes (<P1), were stimulated with recombinant WNT16 (ng/ml), Dkk1 (100ng/ml) and WNT3a (100ng/ml). Cells were harvested for gene expression analysis following 24hours. (A), or for western blot analysis following 48 hours of stimulation (B). Experiment was conducted in complete medium containing serum. Values were normalised for β-actin. (A) represents data from one single experiment (n=3). Experiment was repeated 3 times in total and results are inkeeping (**Figure 36** and data not shown). (B) Image is a representative blot, experiment was repeated and results are in keeping (data not shown). An ANOVA analysis with post-test for linear trend between mean and column number was used to test for statistical significance between V and increasing concentrations of WNT16. The ANOVA, with tukey post-test was used for all other comparisons.

The results show that WNT16 upregulated lubricin expression and that inhibition of the canonical WNT pathway downregulated WNT16 induced lubricin expression (p=0.054) (Results shown in **Figure 35**). This is in keeping with **Figure 34** and confirms the requirement of canonical WNT pathway activation for WNT16-induced lubricin expression.

Interestingly, in both SZC and bovine articular chondrocytes, WNT3a, a more potent activator of the canonical WNT pathway, was not able to upregulate lubricin to the same levels as WNT16, a weaker activator of the canonical WNT pathway. This indicates that there may be an additional step to the mechanism by which WNT16 upregulates lubricin expression, as it not the result of the canonical activation alone.

Upregulation of lubricin by WNT16 also requires activation of the JNK pathway

WNT16, as well as activating the canonical WNT pathway, is also able to activate the JNK pathway. Therefore, I investigated whether this pathway was involved in the mechanism of lubricin upregulation by WNT16 (**Figure 36**).

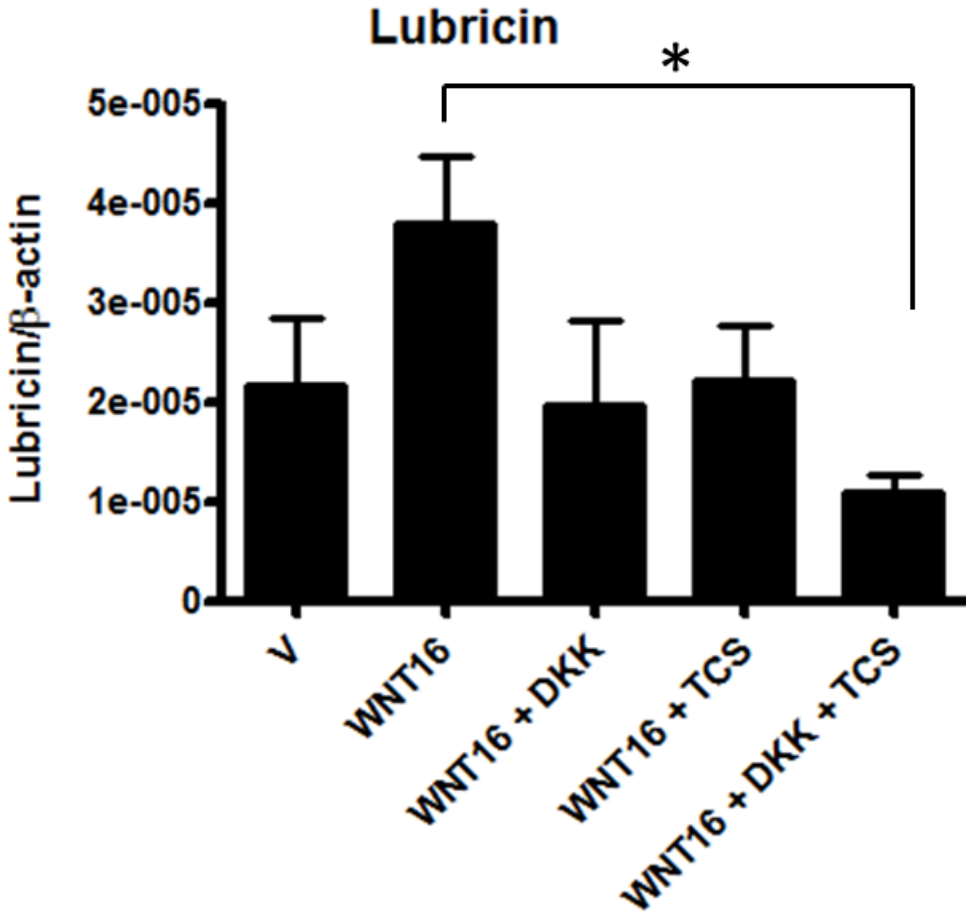

Figure 36: WNT16-induced lubricin expression was also dependent on activation of the JNK pathway.

Inhibition of the JNK pathway downregulated WNT16 induced upregulation of lubricin. Bovine articular chondrocytes were stimulated with recombinant WNT16 (200ng/ml), DKK1 (100ng/ml), and TCS (10µM) and harvested after 24 hours for gene expression analysis by RT-PCR. Experiment was conducted in complete medium containing serum. Values were normalised for β-actin. Data represent one single experiment (n=3). Experiment was repeated and results were inkeeping. An unpaired students T-test was used for statistical comparison between WNT16 and WNT16+inhibitor.

The results from **Figure 36** showed that inhibition of the JNK pathway showed a trend towards downregulation of lubricin expression. However, simultaneously inhibiting both pathways had a cumulative effect and reduced lubricin expression to below that of controls. Therefore, both the canonical WNT and the JNK pathways are required for WNT16 upregulation of lubricin.

The requirement of the canonical WNT pathway for lubricin upregulation is in keeping with data from Yasuhara et al., 2011, showing that loss of β-catenin in vivo reduced lubricin expression in the SZC of 2 week old mice, and constitutively active β-catenin increased its expression (Yasuhara, Ohta et al. 2011). The observation that lubricin expression was not completely lost upon loss of canonical activation however, may be due to the remaining JNK activity in the cartilage.

Similarly to WNT16, WNT3a was also able to activate both the canonical and JNK pathways (**Figure 28** and **Figure 32**), therefore, it is interesting that WNT3a did not upregulate lubricin expression to the same extent as WNT16. However, WNT3a was shown to be a specific activator of JNK2 with activation being dependent on Rac1 (Wu, Tu et al. 2008). It may be that lubricin upregulation requires JNK1 or that JNK activation is achieved by a different mechanism specific to WNT16 activation. It would be interesting in the future to dissect the mechanism further and study activation of pathway components and of different protein isoforms.

This upregulation of lubricin by WNT16 may be involved in the protective effect of WNT16 seen *in vivo* following DMM in mice (Nalesso, Thomas et al. OARSI and manuscript in preparation), as we already know that lubricin is essential for cartilage homeostasis (Coles, Zhang et al. 2010). WNT16 cannot be the only modulator of lubricin however, as *wnt16*$^{-/-}$ mice do not develop spontaneous OA, but is likely to be part of a specific response following injury as this is when WNT16 is expressed (Dell'accio, De Bari et al. 2008).

Discussion

This chapter provides evidence that lubricin is a direct target of WNT16 in primary bovine chondrocytes and mouse SZC. This occurs, in part through activation of the WNT canonical pathway as blockade of the WNT canonical pathway reduced the upregulation of lubricin. However levels did not return to that of control and WNT3a, a more potent activator of the canonical pathway, was not able to upregulate lubricin to the same levels as WNT16, indicating

the involvement of other pathways. It transpired that the JNK pathway, also activated by WNT16 was involved in this mechanism, as blockade of the pathway led to a decrease in lubricin expression and blockade of both the WNT canonical pathway and the JNK pathway simultaneously had a cumulative effect. In summary lubricin expression is directly induced by WNT16 and requires activation of both the WNT canonical and JNK pathways. One limitation of this observation is that the data are for mRNA levels only, confirmation of this at protein level would provide a higher level of certainty in the result.

CHAPTER 6:

WNT16 can act as an antagonist of WNT canonical signalling

Introduction

Given the biphasic activity of WNT16 on canonical WNT pathway activation seen *in vitro,* and in order to investigate the biological relevance of this, we investigated the outcome of pathway activation *in vivo,* using the well validated Xenopus Laevis axis duplication assay outlined below. We speculated that the inhibition of the canonical WNT pathway by WNT16 may be due to basal WNT signalling in control samples, therefore, as well as looking at the effect of WNT16 alone, we also investigated the effect of WNT16 in combination with other more potent canonical WNTs.

Results

The effect of WNT16 in the Xenopus axis duplication assay

In order to investigate pathway activation by WNT16 *in vivo* we utilised a well validated Xenopus assay, in which complete axis duplication is seen upon over-activation of the canonical WNT pathway. This involved injecting a single ventral blastomere at the 4 cell stage of the developing embryo with WNT16 RNA. I first sub cloned WNT16 into the CS2+ vector (provided by Dr Leslie Dale, UCL) which contains the SP6 promoter enabling the generation of capped RNA. Dr Leslie Dale at UCL performed the injections and the analysis of the results, shown in **Figure 37**.

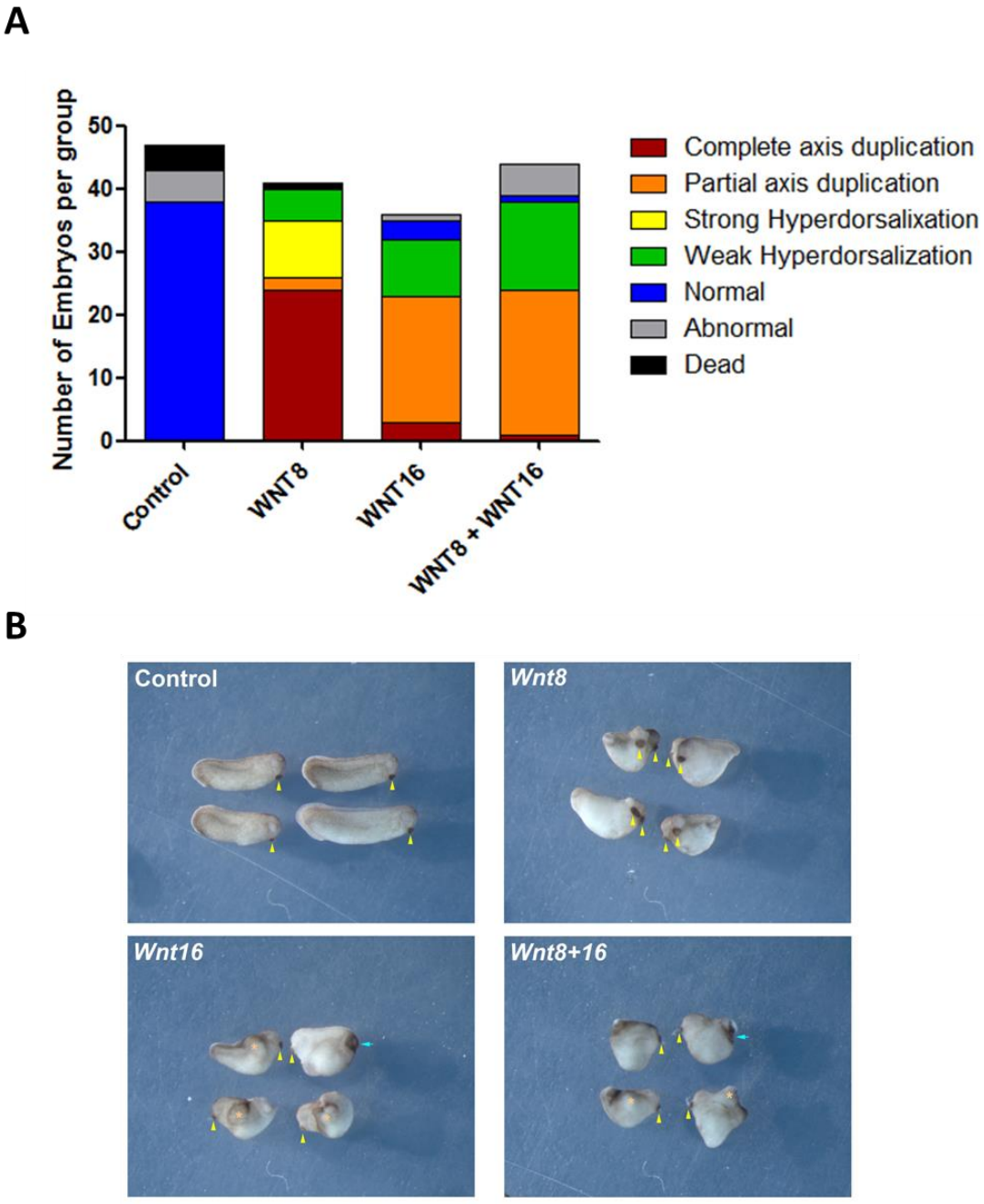

Figure 37: WNT16 inhibited WNT8 induced axis duplication in Xenopus Laevis embryos.

Xenopus Laevis embryos were injected ventrally with either 0.02ng/µl WNT16 or 0.002ng/µl WNT8 (as previously optimised) RNA at the 4 cell stage and left for 2 days to develop before analysis of results. (A) graphical representation of results, (B) representative images. Yellow arrowheads highlight cement glands, which are duplicated in the WNT8 injected embryos. Orange asterix, indicates a 'bump' found in the WNT16 injected embryos and indicates a partial secondary axis. Blue arrowheads highlight a defect found in only the WNT16 injected embryos. Data are representative of a single experiment (n≥36). Experiment was repeated and results were in keeping. Injection and analysis was conducted by Dr. Leslie Dale, UCL.

The results (**Figure 37**), showed that, as expected, WNT8 induced the formation of a complete secondary axis, shown by duplication of the cement glands (Yellow arrowheads) and hyper-dorsalization. WNT16 induced a partial secondary axis, shown by the enlargement but not duplication of the cement gland. This indicates a weak activation of the canonical WNT pathway. This is in keeping with my *in vitro* data that showed that WNT16 upregulated Axin2 mRNA but not to the same extent as strong canonical activator, WNT3a (**Figure 28**). Most interestingly embryos co-injected with WNT16 and WNT8 were indistinguishable from WNT16 injected embryos, indicating that WNT16 activity overcame WNT8 activity leading to inhibition of canonical pathway activation by WNT8. Control embryos developed normally.

Therefore WNT16 *in vivo*, at this concentration, is a weak activator of canonical WNT pathway, but also inhibits the activity of other more potent canonical WNTs. This may occur through blocking the binding of canonical WNTs at a receptor level, or further downstream through activation of a second pathway by WNT16 which interacts with the canonical pathway.

In vitro validation of WNT16 as an agonist of the canonical pathway

In order to further investigate the results discovered in **Figure 37**, where WNT16 was able to inhibit WNT8 activity, *in vitro* competition assays were carried out. HEK293 cells transfected 24 hours previously with SUPER8TOPFlash reporter plasmids, were stimulated with WNT16 and a strong canonical activator (WNT3a), simultaneously, then left for a further 24 hours before harvesting for assay (**Figure 38**). The SUPER8TOPFlash reporter plasmids contains TCF/LEF promoter elements (TCF and LEF are transcription factors that form complexes with β-catenin to activate transcription), followed by the luciferase gene. Therefore upon activation of the WNT canonical pathway, β-catenin forms a complex with these transcription factors and activates transcription of luciferase, the quantity of which is measured by addition and rate of cleavage of its substrate which results in energy release in the form of luminescence.

A

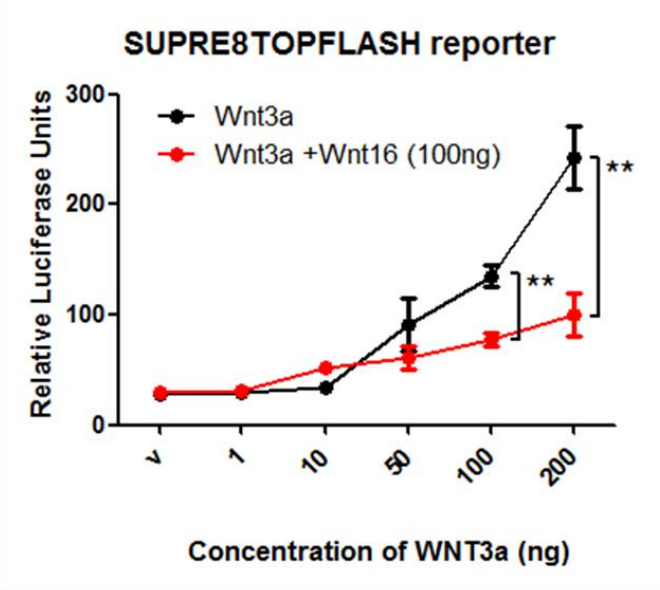

B

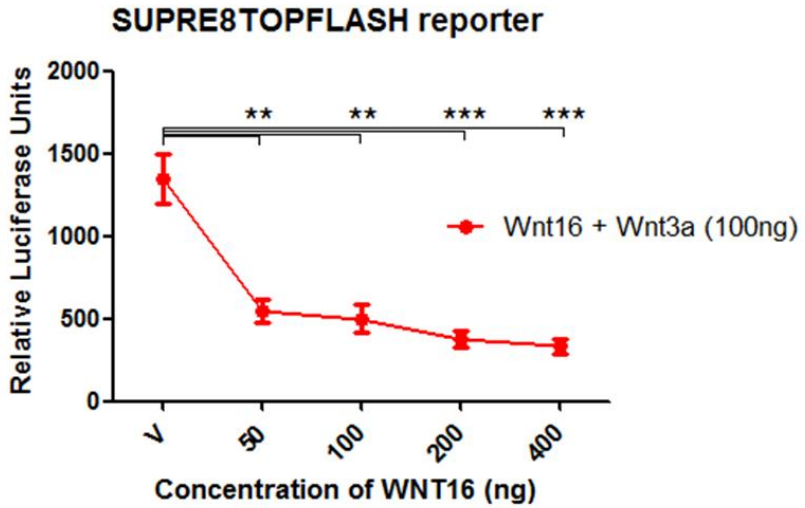

Figure 38: WNT16 inhibited WNT3a activation of the WNT canonical pathway.

HEK293 cells transfected with SUPER8TOPFlash reporter plasmids 24 hours prior to stimulation with either WNT16, WNT3a, or WNT16 and WNT3a in combination. Following a further 24 hours, cell lystaes were harvested for quantification of luciferase levels as a readout for pathway activation. Experiments were conducted in complete medium containing serum. (A) Variable levels of WNT3a (ng/ml), were combined with constant level of WNT16 (100ng/ml). (B) Variable levels of WNT16 (ng/ml), were combined with constant levels of WNT3a (100ng/ml). (A and B) are results from 2 separate experiment, each with n=4 per condition. An unpaired students t-test was used for statistical analysis.

In keeping with **Figure 37**, WNT16 inhibited canonical activation by potent canonical WNT, WNT3a. Simultaneous stimulation with equal concentrations (100ng/ml) of WNT3a and WNT16 resulted in significant down regulation of WNT canonical pathway activity when compared to WNT3a alone **Figure 38 A**. In fact half the amount of WNT16 (50ng/ml) was also able to inhibit WNT3a (100ng/ml) induced pathway activation **Figure 38 B**.

Discussion

Data from **Figure 37** and **Figure 38** suggest that, as well as being a weak activator of the WNT canonical pathway (chapter 4), WNT16 can also inhibit strong activation of the pathway by other more potent WNT ligands, such as WNT3a and WNT8. This is in keeping with *in vivo* data from Giovanna Nalesso, which showed that, 7 days following surgical induction of OA in mice, *wnt16*$^{-/-}$ mice had a higher expression of axin2 mRNA (Nalesso, Thomas et al., Manuscript in preparation). Literature has already shown that a balanced activation of WNT signalling is essential for normal joint homeostasis as both too much and too little WNT canonical signalling led to OA in mice (Zhu, Chen et al. 2008; Zhu, Tang et al. 2009). It is possible that WNT16 may act as a "buffer" of WNT canonical signalling, maintaining a low level of activation but preventing excessive activity and therefore may be the essential molecule regulating the level of activity in the joint following injury. If this is the case, WNT16 is first reported WNT ligand that acts in this way and would begin to explain how WNT signals are able to maintain their delicate balance *in vivo*.

In order to better understand the 'buffering' mechanism of WNT16, the next experiments would include investigating at which stage in the pathway WNT16 is acting and whether the inhibition is direct (e.g. through blocking of canonical frizzled receptors), or indirect (e.g. through activation of another pathway which acts on the canonical WNT pathway).

CHAPTER 7:

General discussion and Conclusions

I have discovered that WNT16 supports the phenotype of the superficial zone chondrocytes, through maintenance of their progenitor phenotype, including the upregulation of lubricin expression. This occurred through a balanced and dose-dependent activation of the canonical WNT pathway and JNK pathway by WNT16. In particular, the modulation of the canonical WNT pathway by WNT16 showed a biphasic effect, as high concentrations caused a weak activation of the pathway and low concentrations, inhibited pathway activation compared to control. In addition, WNT16 showed the ability to inhibit strong activation of the canonical WNT pathway by other more potent canonical WNTs, an entirely novel function in the field of WNT signalling and unique amongst WNT ligands.

The superficial zone chondrocytes (SZC) are a pool of chondrocyte progenitors that contribute to the response to injury (Seol, McCabe et al. 2012); (Dowthwaite, Bishop et al. 2004). Loss-of-function experiments showed that SZC from *wnt16*$^{-/-}$ mice had a higher proteoglycan content, suggesting that they undergo a "premature" chondrocytic differentiation and fail to retain their specific phenotype. Conversely, gain-of-function experiments using recombinant WNT16, inhibited the expression of mature chondrocyte markers, suggesting a function for WNT16 in inhibiting maturation of these cells and maintaining the pool in their progenitor state. If SZC are required in the injury response to repopulate damaged areas of cartilage, the function of WNT16 upregulation following injury may be to prevent/limit the differentiation of the entire population at once, and thus loss of the progenitor pool of cells. The maintenance of the SZC phenotype by WNT16, is further supported by the upregulation of lubricin, a specific marker of SZC but also a molecule essential for cartilage homeostasis. We know that loss of Lubricin leads to spontaneous OA in mice (Coles, Zhang et al. 2010), and that lubricin treatment led to decreased cartilage damage in rats (Flannery, Zollner et al. 2009). *In vivo* work in our lab has shown that *wnt16*$^{-/-}$ mice develop a worse outcome of disease following surgical induction of OA; this was associated with decreased lubricin expression and a higher instance of apoptosis in the superficial zone of the articular cartilage (Nalesso, Thomas et al., manuscript in preparation). Therefore it is likely that the chondroprotective effect of WNT16 is through both, upregulation of lubricin which is essential for cartilage homeostasis, and maintenance of the SZC population.

Having said that, *wnt16*$^{-/-}$ mice still express normal levels of lubricin in unchallenged conditions and do not develop spontaneous OA. Therefore the effect is a specific response which occurs after injury that is likely through a specific mechanism. This phenomenon is not unique to WNT16. An example of this is the deletion of SOX9. SOX9 is strictly required for cartilage formation (Bi, Deng et al. 1999), however, postnatal deletion of SOX9 did not result in osteoarthritis even in mice aged for nearly 2 years (Henry, Liang et al. 2012). Although collagen type II and aggrecan expression were drastically reduced in those mice, as expected by the direct activation of transcription of these genes by SOX9, no structural damage was detected in the cartilage (Henry, Liang et al. 2012). Of course the limitation of these conditions is that the husbandry of laboratory mice is not representative of "life in the wild" where mice represent pray to other animals and their joints are more challenged. Interestingly, SOX9 is strongly upregulated after cartilage injury and osteoarthritis and therefore, in adulthood, represents an injury-driven response gene involved in cartilage homeostasis (Dell'accio, De Bari et al. 2008).

With 19 WNTs present in human and mice, why do we specifically need WNT16? In chapter 4, WNT16, at doses equal to, or higher than 200ng/ml caused an upregulation of axin2, a validated readout of canonical WNT activation. At doses equal to or less than 100ng/ml, axin2 expression was inhibited compared to control. WNT ligands are known to form concentration gradients *in vivo* and exert dose dependant activities (Li, Ahrens et al. 2011; Nalesso, Sherwood et al. 2011), however WNT16 is the first reported WNT to have agonistic activity and specifically inhibit pathway activation by other WNT ligands. WNT16 was able to inhibit pathway activation *in vitro* by WNT3a, as well as *in vivo* by WNT8, in a well validated model in Xenopus Laevis, where axis duplication is seen upon canonical WNT pathway activation. Therefore my results indicate that WNT16 functions to "buffer" the degree of activation of WNT signalling to physiological levels, thereby preventing excessive activation, known to drive chondrocyte hypertrophy and cartilage breakdown (Zhu, Tang et al. 2009), or excessive inhibition which would cause cartilage breakdown by failing to support progenitor populations (Zhu, Chen et al. 2008; Yasuhara, Ohta et al. 2011). Further work is required to determine whether this occurs directly (e.g. through direct competition for receptor binding) or indirectly (e.g. through activation of an inhibitory molecular mechanism). Some of these experiments are currently ongoing in our laboratory. For instance, we are investigating whether WNT16-induced activation of ROR2 has a role in the inhibitory mechanism. Competition studies would also

provide insight into the mechanism, however they are more complicated, due of the complexity of the receptor repertoire and the multimerization required. In addition, WNTs bound to the receptor complexes are rapidly internalized in endosomes and multivescicular bodies, (Taelman, Dobrowolski et al. 2010), making these studies very challenging.

This discovery that WNT16 behaves as a partial agonist may provide some explanation for discrepancies between some of my earlier results regarding axin2 mRNA expression (**Figure 28**), and β-catenin protein levels (**Figure 29**) as a measure of canonical WNT pathway activation. Axin2 expression was increased or decreased compared to control depending on the concentration of WNT16 administered, but β-catenin levels were higher at all concentrations of WNT16. It is important to note that, even in control samples, some basal WNT signalling was present, therefore the apparent inhibition of canonical WNT signalling by WNT16 is dependent on the starting levels of pathway activity for that experiment.

However, as mentioned in the discussion at the end of chapter 2, it is possible that secondary mechanisms are in place that regulate pathway activity further downstream of β-catenin accumulation to affect transcriptional activity specifically or even that promoters of specific transcriptional targets are specifically targeted by WNT16 and are not an accurate readout of general canonical activation in this case. These points could be addressed by looking at some additional transcriptional targets of β-catenin (OPG etc.), particularly as axin2, although a validated readout of activation, is an antagonist of canonical WNT signalling. In addition, the SUPER8TOPFlash reporter assay is a reliable measure of pathway activation, however some difficulties with transfection of reporter plasmids in chondrocytes is limiting, and no stable reporter lines exist in chondrocytic cells lines. In the future, generation of a stable reporter line in chondrocytes would prove beneficial.

A limitation of my data is that a large proportion of my outputs are measured by mRNA expression, which although is an accurate measure of transcriptional regulation within the cell, mRNA do not always correlate to protein as post transcriptional/translational regulation etc. can affect the final outcome. Further analysis into the resulting biological effect of WNT16 *in vivo* would strengthen and add biological relevance to my data. As mentioned previously, we know that *wnt16*$^{-/-}$ mice have a worse outcome of OA following surgical induction of OA. This

correlated with decreased lubricin expression in the articular cartilage of *wnt16*$^{-/-}$ mice and increased apoptosis in the SZC specifically (Nalesso, Thomas et al., manuscript in preparation). However further investigation into change in specific marker expression *in vivo* following injury, particularly those of the progenitor population, would add weight to my results, and prove that WNT16 is able to efficiently maintain this population *in vivo*. Most importantly, gain of function experiments *in vivo* would show if delivery of WNT16 following injury is able to improve the outcome of disease and highlight whether there is potential for WNT16 as a therapeutic in OA. In addition rescue with lubricin in the *wnt16*$^{-/-}$ mice following injury would identify if the upregulation of lubricin by WNT16 is sufficient to rescue the phenotype.

As well as the potential benefits of WNT16 in cartilage, my results highlight the advantages of WNT16 in a broader sense. It is interesting that this partial activation of canonical WNT signalling was conserved across the species and in different biological contexts including primary axis formation in Xenopus Laevis. This degree of conservation suggests that this "buffering" function of WNT signalling has a biological relevance that is far broader than that related to cartilage homeostasis following injury, and may be important (and used) in all those situations where a controlled degree of WNT activation is required including regeneration and embryonic morphogenesis.

The importance of a tight control of WNT signalling in regeneration has been exemplified in the elegant studies by Kawakami et al. who demonstrated that subtle differences in the way WNT signalling is modulated are of crucial importance in the outcome of regeneration. They showed, in fact, that subtle modulation of the temporal dynamics of WNT activation following wing amputation in the chick embryo (a species that does not regenerate at this stage of development) resulted in nearly complete wing regeneration. In their words "*variations in the concentration and/or spatiotemporal distribution of molecules involved in tissue generation during embryogenesis may be the raw material upon which evolution has granted some animals the ability to regenerate*" (Kawakami, Rodriguez Esteban et al. 2006). The implication, for me, is that understanding and controlling such variation is the key to understanding and controlling such ability therapeutically.

While modern stem cell research is supplying more and more systems and cells for the biological repair of damaged organs, it is the understanding of the molecular mechanisms underpinning the tight control, in the intensity, time, and space, of these morphogenetic signalling events that will be necessary to achieve the level of control over proliferation, differentiation, patterning and morphogenesis required for reparative organogenesis.

CHAPTER 8:

Additional data and future directions

Results

WNT16 loss of function affects male and female mice differently

Comparing the proliferation rate of wild type and knockout SZC cells revealed that as a whole, there was no significant difference between the two genotypes. However, a more careful analysis revealed that when the gender was taken into account, there were clear differences. Data are shown in **Figure 39**.

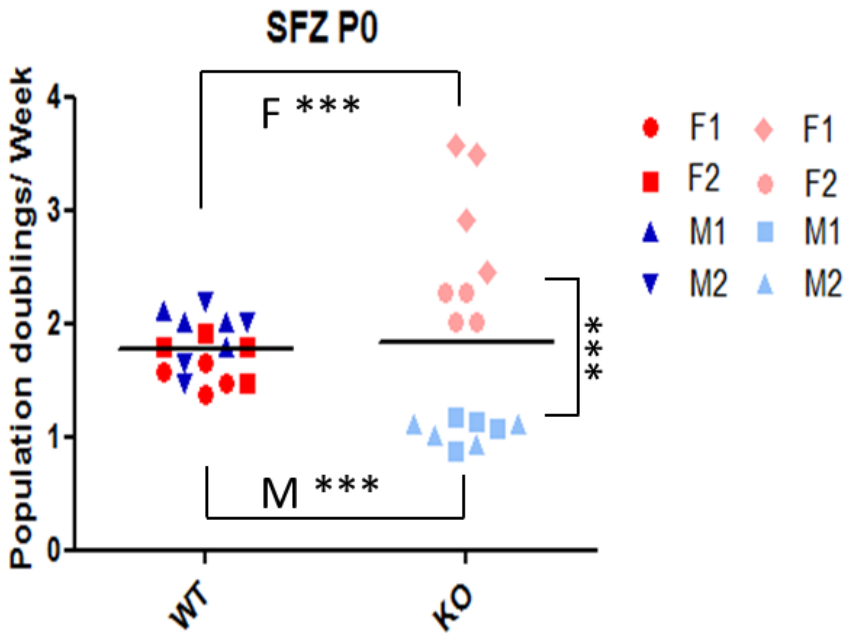

Figure 39: Loss of function of WNT16 affects the proliferation of males and females differently.

SZC and DZC were isolated from the knees of 3 day old mice as previously described (Yasuhara, Ohta et al. 2011). Cells were cultured in serum containing medium. Cells were counted, plated and allowed to reach 90 % confluency (P0), then counted again. Population doubling time was calculated by considering the change in total cell number between plating and reaching 90% confluency against time taken for this to occur. Graphs represent a single experiment. N=16 (4 mice, 4 replicates per mouse). Data seen also in **Figure 22** but are represented with males and females separated. An unpaired t-test was used for statistical comparison.

In the interest of clarity the females are represented in red (wild type) and pink (knockout), and the males in blue (wild type) and light blue (knockout). Although no differences were seen between the sexes in wild type mice, in the knockout cells there is a clear grouping of cells from male and female mice. Cells from female mice lacking in WNT16 proliferate faster than cells from males that lack the gene. In-fact, loss of WNT16 caused cells from female mice to proliferate faster than wild type cells while cells from male mice responded by proliferating slower than wild type cells.

Interestingly, although there was no significant difference between the genders in terms of lubricin expression, the proliferation rate in the individual samples correlated with lubricin mRNA expression. Correlation plots are shown in **Figure 40**.

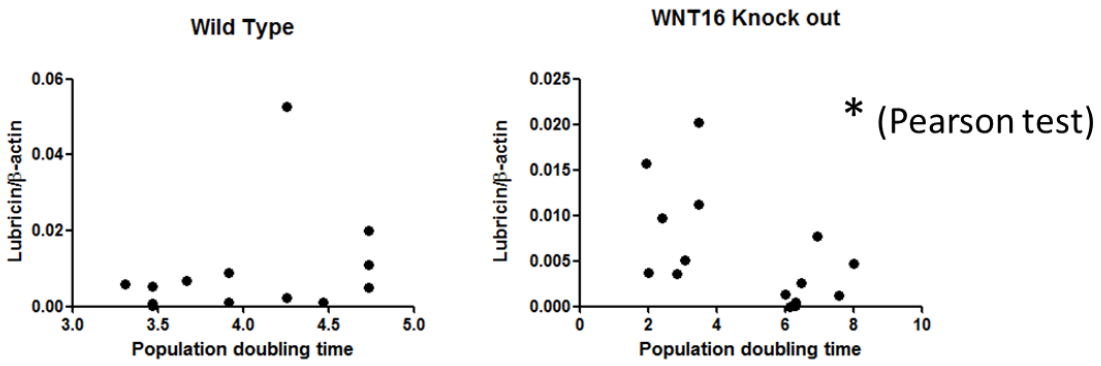

Figure 40: Lubricin expression in cells from male and female wnt16$^{-/-}$ mice, correlated with proliferation rate in these groups.

SZC and DZC were isolated from the knees of 3 day old mice as previously described (Yasuhara, Ohta et al. 2011). Growth rate data from **Figure 22**/**Figure 39** and corresponding lubricin mRNA expression from **Figure 19**/**Figure 24** for each mouse was plotted for analysis of correlation. Both experiments were conducted in complete medium containing serum. Data from each experiment are representative of a single experiment (n≥12). The pearson test was conducted to test for a significant correlations.

The results from **Figure 40**, show that the differential proliferation rate in cells from male and female *wnt16*$^{-/-}$ mice correlated with lubricin mRNA expression within these groups. However no correlation was found in the wild type cells. This is tantalizing because it is well known that OA is more prevalent in post-menopausal females, however, before menopause, OA is more prevalent in males (Paradowski, Bergman et al. 2006). This, and experimental data in ovariectomised mice (Ma, Blanchet et al. 2007), suggest a hormonal influence on the mechanisms of disease. My data offer an opportunity to study the molecular basis of this observation.

WNT16 and Inflammation

Upstream of WNT16

WNT16 upregulation, in OA, takes place only in the early phase of disease, when local inflammation is also present (Nalesso, Thomas et al. OARSI and manuscript in preparation). Therefore, I investigated whether inflammatory cytokines influenced WNT16 expression (**Figure 41** and **Figure 42**).

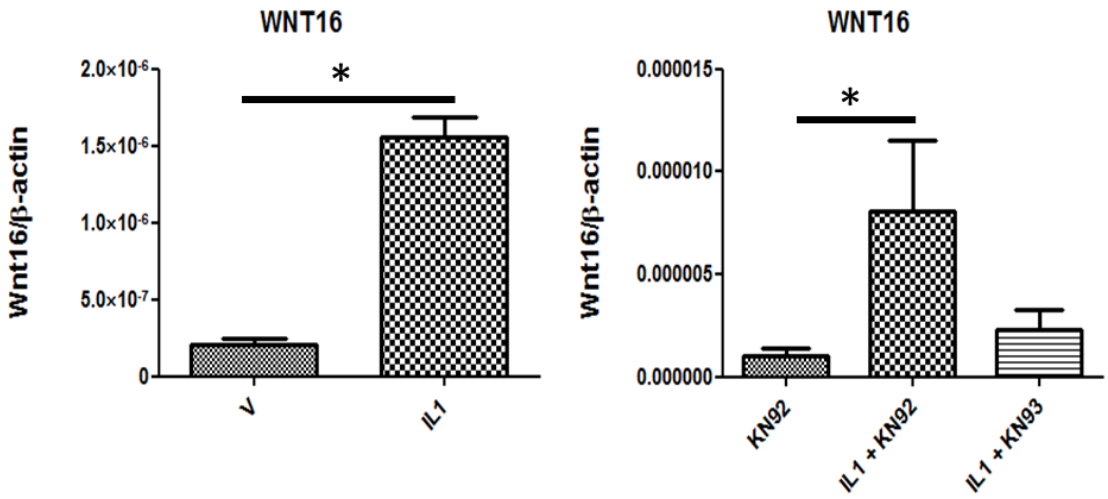

Figure 41: WNT16 mRNA expression is upregulated by IL-1 in a CaMKII dependent manner.

P0 HAC were stimulated with vehicle or 10ng/ml IL-1β, and 10μM KN93 (CaMKII inhibitor) or its control, KN92 and harvested for gene expression analysis by RT-PCR 24 hours later. Experiment was conducted in complete medium containing serum. Data are representative of a single experiment (n=4). An unpaired T test was used for statistical comparison.

IL-1 treatment of HAC significantly increased WNT16 expression. In a different system, MyD88, a co-receptor for IL-1, is necessary for the activation of CaMKII. This offered an interesting molecular link between IL-1 signalling and WNT signalling. Indeed, induction of WNT16 by IL-1 was abolished upon blockade of the CaMKII pathway (using inhibitor KN93 when compared to its control KN92).

From the literature we know that c-Jun is a transcriptional activator of the WNT16 promoter and is necessary for its expression in the developing mouse embryo (Kan and Tabin 2013).
Therefore I decided to investigate further whether there was any relationship between these two pathways and WNT16 expression.

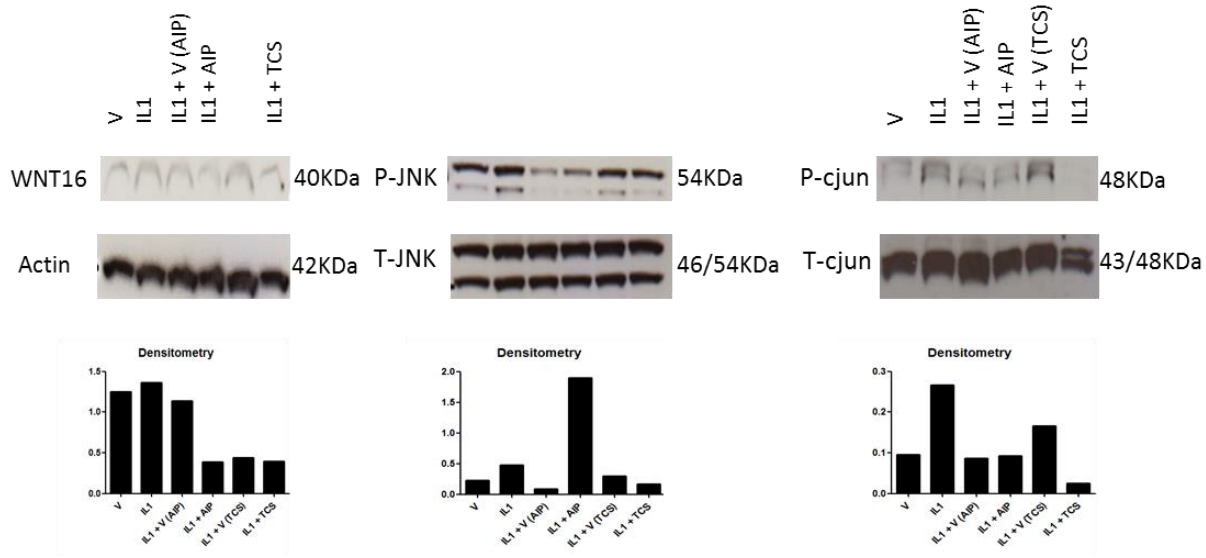

Figure 42: Pathway analysis upstream of WNT16

Bovine articular chondrocytes were stimulated with 10ng/ml IL-1β, with or without 5μM AIP (CaMKII inhibitor), or 10μM TCS (JNK Inhibitor). Cells were harvested after 24 hours for WNT16 analysis or 30 min for phospho-protein analysis. Experiment was conducted in complete medium containing serum. Images are representative of a single experiment (n=1) and will need confirmation. Densitometry analysis was conducted by measuring the intensity of the WNT16 band or both bands in the case of phosphorylated c-jun and JNK and normalising for their respective loading controls (both bands take in the case of total c-jun and JNK).

Data in **Figure 42** requires validation before drawing conclusions as western blots have been run on single samples. However we are able to speculate at the link between the CaMKII pathway, the JNK pathway and WNT16 expression. CaMKII blockade reduced WNT16 expression at protein level. This is in keeping with **Figure 41**. In addition IL-1 activated the JNK pathway as expected (Li, Commane et al. 2001), and CamKII blockade increased IL-1 induced JNK phosphorylation (**Figure 42**), indicating that there may be a link at between the two pathways at this stage. Further analysis is required however, in order to draw any solid conclusions.

These results are important because they show a molecular link between post-traumatic inflammation and the homeostatic phenomena that take place following injury, and therefore suggest that this inflammatory phase is not necessarily pathogenic, but could have essential functions in the activation of repair mechanisms. Indeed, there is overwhelming evidence, in other contexts, that controlled and self-limiting inflammation is an essential component of regeneration and wound healing (Benowitz and Popovich 2011).

Appendix

Selection and optimisation of cell lines for investigating the function of WNT16

In order to understand the function of WNT16 in chondrocytes, I needed to choose the optimal cell line for in vitro experiments. Therefore, I selected 3 human chondrocytic cell lines: C28/I2, immortalised human costal chondrocytes; JJ012; and SW1353, two chondrosarcoma cell lines, for comparison and analysed their chondrocytic capacity as well as their basal expression of WNT16, which would allow me to identify candidate cells for gain- and loss-of-function experiments.

C28/I2 chondrocytic cell line have the greatest capacity to form cartilage extracellular matrix in vitro

To compare the chondrogenic potential of different human chondrocytic cell lines in culture and identify the best culture conditions, I selected c28/I12, JJ012, and SW1353, as well as HAC, and compared their capacity to accumulate GAGs in different serum conditions (***Figure 43***). Cells were plated and cultured in micromass, in the presence of FBS (10%v/v or 1%v/v).

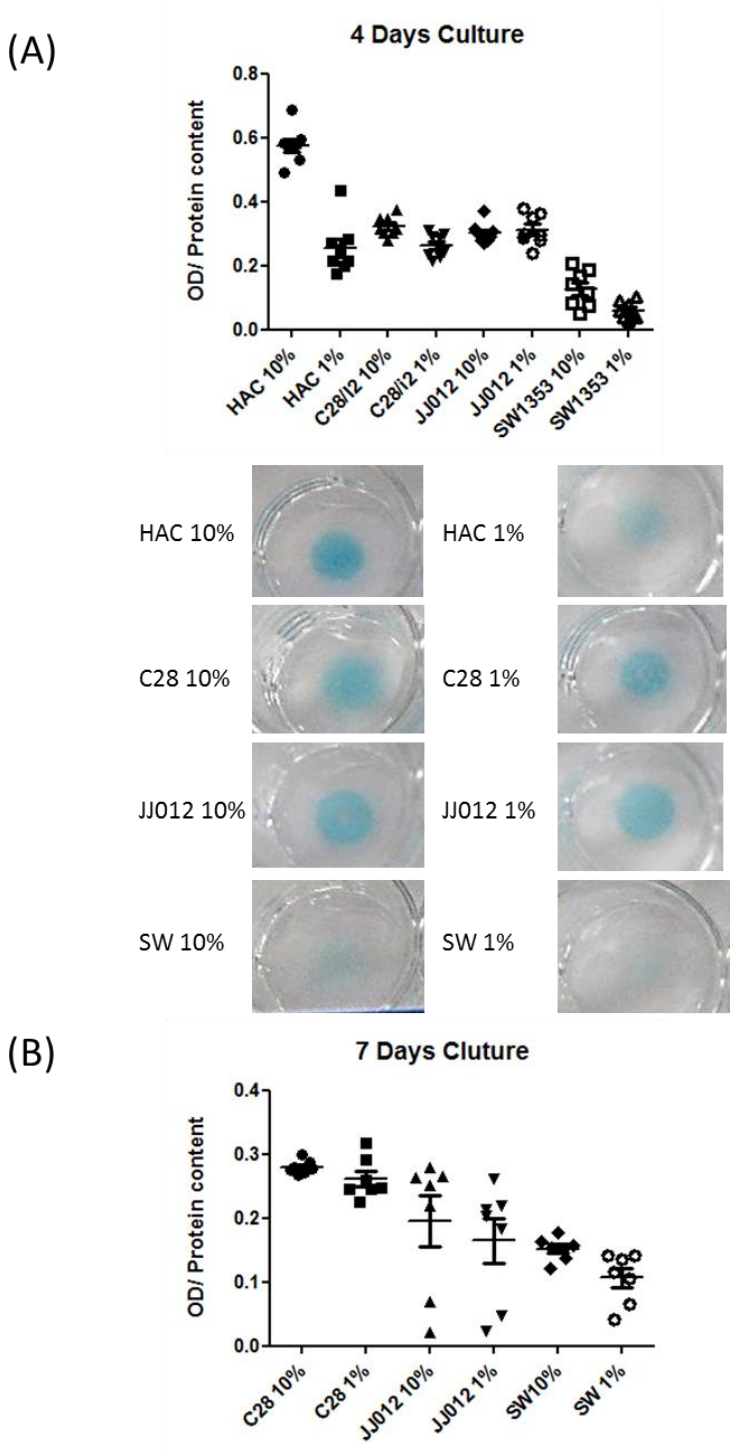

Figure 43: C28/I2 cells had the greatest capacity to form GAG rich ECM *in vitro*.

Chondrocytic cell lines (C28/JJ012/SW) and HAC were plated in micromass, allowed to adhere and cultured in complete medium containing 10% (v/v) serum for 24 hours, then switched to complete medium containing either 10% (v/v) or 1% (v/v) serum for 4 (A), or 7 (B), days before fixation and staining with alcian blue (pH0.2) to measure sulphated proteoglycan content. Values were normalised for protein content. Data represents 2 separate experiments (A and B) (N≥6).

The results from ***Figure 43*** (A) Show that HAC in the presence of 10%(v/v) FBS had the highest GAG content when compared to human chondrocytic cell lines. HAC in 1%(v/v) FBS had a lower GAG content, which was comparable to that of C28/I2 and JJ012. Finally, SW1353 had the lowest accumulation of sulphated GAGs. Both C28/I2 and SW1353 cells, like HAC, had a slightly higher GAG content in 10%(v/v) FBS. In ***Figure 43*** (B), which shows the GAG accumulation after 7 days in culture, C28/I2 had a higher GAG content than JJ012. As in (A), SW1353 had the lowest GAG content.

It was surprising that low serum conditions did not increase GAG content in C28/I2 cells which are well known undergo further chondrocytic differentiation in serum free conditions (Goldring, Birkhead et al. 1994). Possible explanations include short time point, to the presence of 1%(v/v) FBS in the low serum conditions or experimental error, given that this was one of the first experiments of my PhD. I did not consider completely serum-free conditions for my experiments because WNTs require serum for solubility and biological activity (Fuerer, Habib et al. 2010).

In primary HAC however, serum is a well-known inducer of GAG production, which is in keeping with my results (Luyten, Yu et al. 1992; Erickson, Harris et al. 1997).

These results indicate that, of the cell lines tested, C28/I2 cells have the greatest capacity to form a cartilage matrix when cultured in micromass in the presence of 10%(v/v) FBS.

C28/I2 have the highest expression of chondrocytic markers genes

To investigate whether C28/I2 were also the most chondrogenic in terms of differentiation markers, I assessed the expression of chondrocytic marker genes: Sox9, a chondrocyte transcription factor; Collagen type 2a1; and aggrecan, two matrix molecules. I achieved this by comparing mRNA expression levels by Q-PCR. I also included monolayer culture in my analysis (data shown in **Figure 44**).

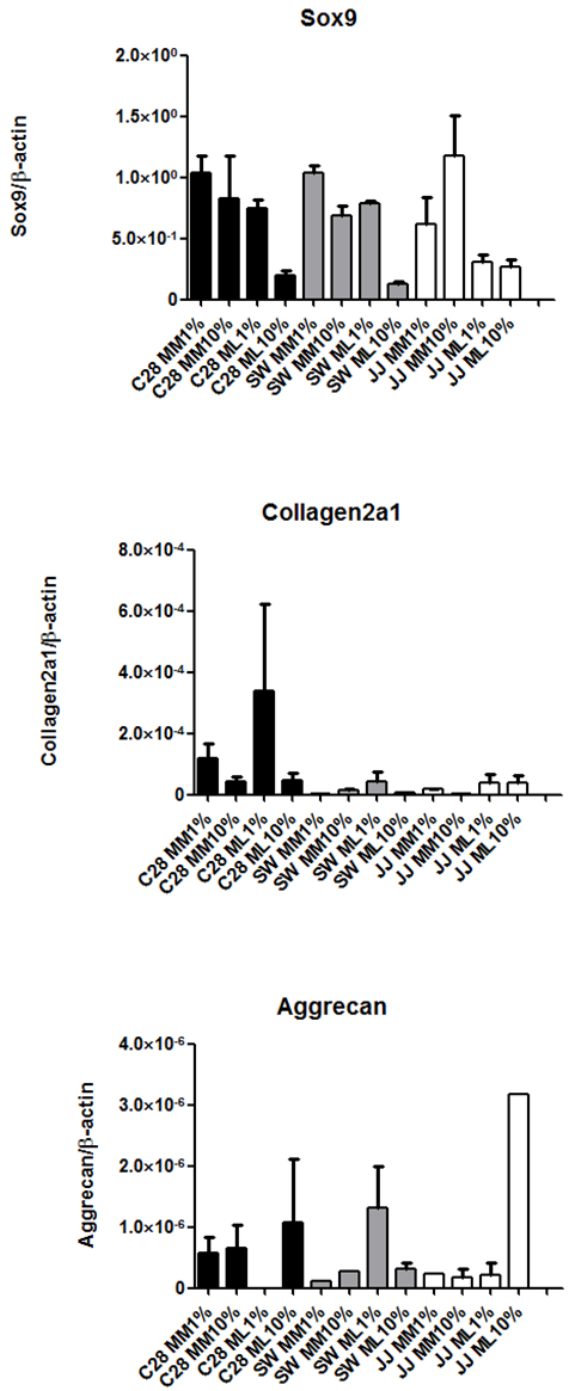

Figure 44: C28/I2 cells had the highest expression of Chondrocytic markers genes.

Cell lines were plated in micromass or monolayer and left to rest in complete medium containing 10% (v/v) serum, for 24 hours before stimulating with medium containing either 10% (v/v) or 1% (v/v) serum. The cells were harvested for gene expression analysis after a further 24 hours. Values were normalised for β-actin. N=3.

All three cell lines exhibited similar levels of sox9 expression, but C28/I2 had, on average, a higher expression of COL2A1 and aggrecan, particularly in micromass (**Figure 44**). This is in keeping with data from **Figure 43** showing that C28/I2 had a higher GAG content compared to JJ012 and SW1353. However, both in micromass and monolayer, C28/I2 had a higher expression of sox9 and COL2A1 in 1%(v/v) FBS. This is in contrast to the results seen in **Figure 43** where micromasses had a higher GAG content in 10%(v/v) FBS.
Overall, C28/I2 cells were the most chondrogenic of the three cell lines and therefore appeared best suited as a chondrocyte model in mechanistic experiments.

The aim of this study is to investigate the effects of WNT16 in chondrocytes. Therefore, it was important to know the basal levels of WNT16 in these cells. This was achieved by gene expression analysis (**Figure 45**).

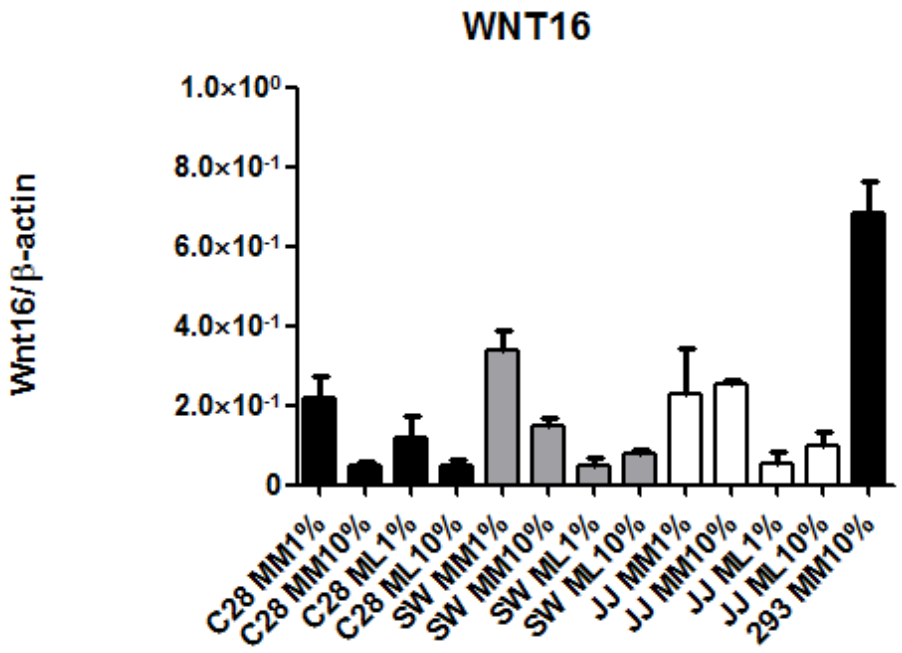

Figure 45: C28/I2 cells had a low basal expression of WNT16.

All cell lines show a relatively low basal expression of WNT16 when compared to HEK293 cells chosen as positive controls. Cell lines were plated in micromass or monolayer and left to rest in complete medium containing 10% (v/v) serum for 24 hours before exposure to medium containing either 10% (v/v) or 1% (v/v) serum. Cells were harvested for gene expression analysis after a further 24 hours. Values were normalised for β-actin. N=3. Data are from the same experiment as in **Figure 44**.

As shown in **Figure 45**, human embryonic kidney, HEK293 cells, were used as a positive control, as the kidney expresses high levels of WNT16 (Fear, Kelsell et al. 2000). Under all conditions C28/I2, JJ012 and SW1353 expressed less WNT16 than HEK293 cells. No significant differences were seen in WNT16 expression between the cell lines. C28/I2 cells expressed more WNT16 in low serum conditions making 10%(v/v) FBS more suited to overexpression experiments.

Jet Prime reagent is most efficient for transfecting C28/I2 cells.

At the beginning of my studies, no recombinant WNT16 was available. Therefore to achieve overexpression, I used expression plasmids encoding WNT16 (which were either kindly donated by Professor Teh, Queen Mary University, or generated by myself and my colleague Jessica Bertrand). In order to achieve overexpression using plasmids, relatively high transfection efficiency must be reached.

To optimise transfection efficiency, three transfection reagents were compared (**Figure 46**): Jet Prime (Polyplus-Transfection); FugeneHD (Roche)(two non liposomal reagent); and Lipofectamine2000 (invitrogen)(a liposomal reagent). Cells were transfected with enhanced green fluorescent protein (eGFP) expression plasmid which was used to measure transfection efficiency. HEK293 cells were used as a positive control as they are known to transfect well. Transfection was optimised for C28/I2 cells.

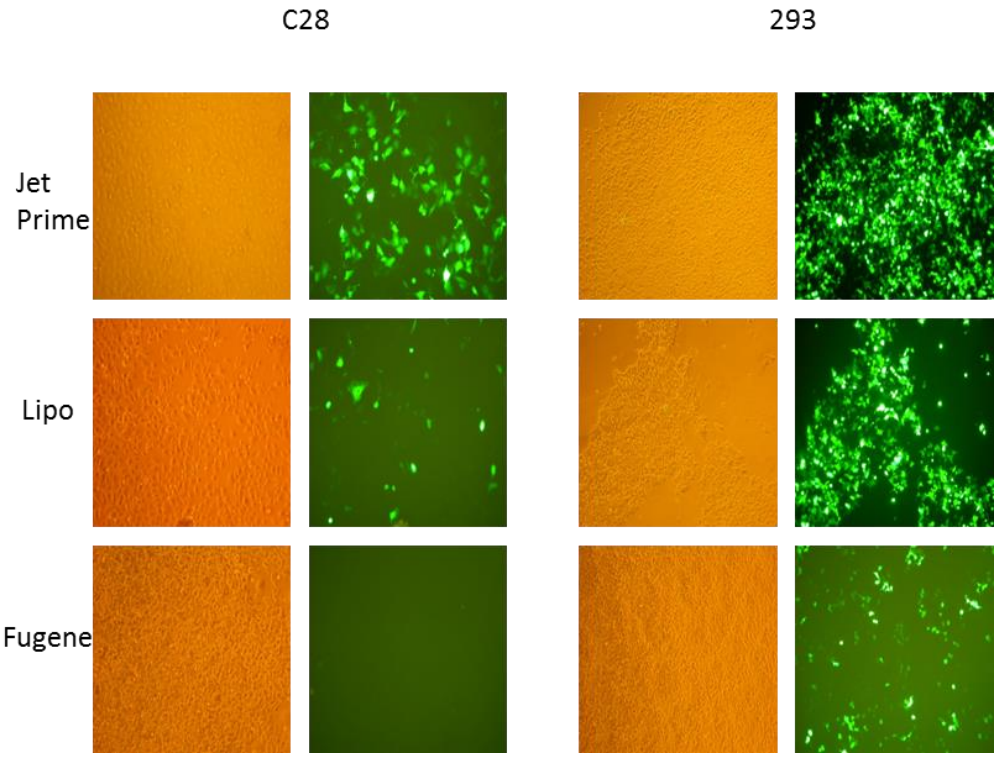

Figure 46: Jet prime reagent was the most efficient reagent for transfecting C28/I2 cells.

C28/I2 and HEK293 cells were transfected with eGFP plasmid using jet prime, lipofectamine, or fugene reagent. Transfection with each reagent was conducted in parallel with cells plated 24 hours previously in complete medium containing serum. 1µg of DNA was transfected for both cell types with all reagents. The efficiency of transfection was evaluated 48 hours later under an inverted microscope. Images are representative.

In HEK293 cells, a high level of transfection was achieved (>80%) using both Jet Prime and Lipofectamine2000. Transfection was also achieved using FugeneHD, but only at low levels. In C28/I2 cells, Jet Prime was the most effective reagent and therefore was used in all subsequent experiments (**Figure 46**).

***WNT16 was not detectable at protein level in C28/I12 cells*.**

Having established that C28/I2 cells have low mRNA expression for WNT16, I wanted to investigate whether this was true at protein level. Cells were transfected with either empty plasmid (pCDNA3.1), or WNT16 expression plasmid (pCDNA3.1wnt16), to confirm first that WNT16 protein levels under resting conditions reflected mRNA expression, and second, that the WNT16 expression plasmid led to the production of WNT16 whereas the empty plasmid did not. WNT16 protein detection was achieved by western blot and immunofluorescence histochemistry. This experiment was conducted in collaboration with Dr. Giovanna Nalesso (QMUL) and the data shown in **Figure 47**.

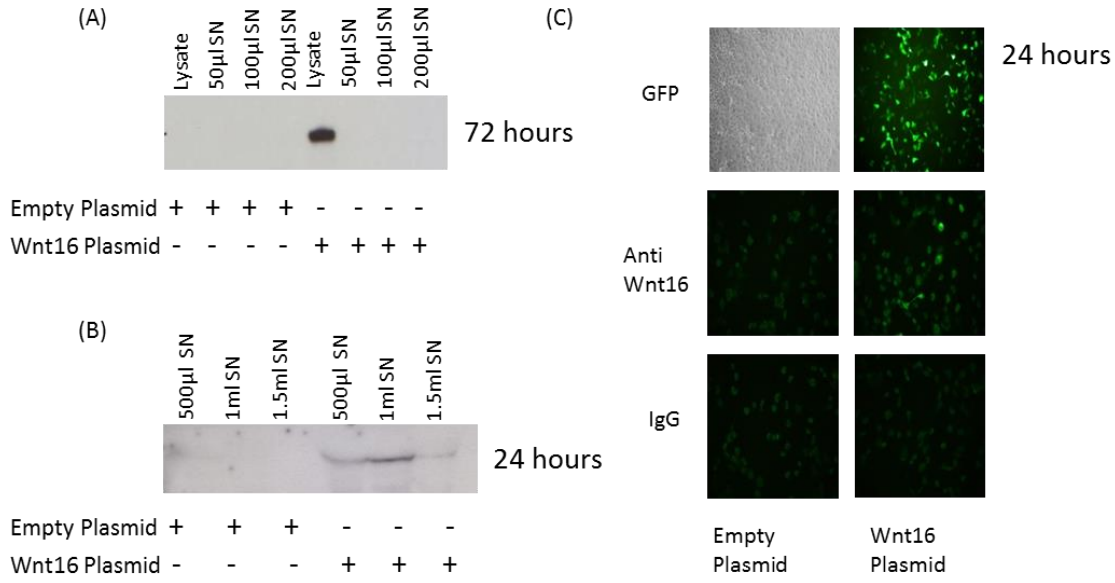

Figure 47: WNT16 was not expressed at protein level in C28/I2 cells.

C28/I2 cells did not show any detectable WNT16 protein at basal level, however transfection with WNT16 expressing plasmids induced protein expression detectable in cell lysates and supernatants. C28/I2 cells were transfected with either Empty plasmid or WNT16 expression plasmid. Lysate and Supernatants (TCA precipitated) where harvested 72 hours (A) or 24 hours (B) after transfection for western blotting, Or 24 hours after transfection for immunofluorescence (C) for WNT16 (Giovanna Nalesso). Experiments were conducted in complete medium containing serum. Each panel represents a separate experiment (n=1).

Western blot of whole cell lysates and supernatants (following TCA precipitation to concentrate proteins in the medium/supernatant), showed that C28/I2 cells have no detectable levels of WNT16 under basal conditions (**Figure 47**). However, upon transfection with WNT16 expression plasmid, WNT16 became detectable in the lysate and in the supernatant when 500µl or more is precipitated (A+B). This was confirmed by IHC on the cells (C).

Interestingly the amount of WNT16 decreased between 1ml and 1.5ml of supernatant following precipitation. This is likely due to difficulty in re-suspending the protein pellet, which worsens with increasing volume.

These experiments confirm that C28/I2 cells have little or no expression of WNT16 under resting conditions, making them an excellent model for gain of function experiments and that the WNT16 expressing plasmids produce a detectable protein.

Additional canonical pathway investigations using the WNT16 expression plasmid and the Super8TOPFlash reporter assay.

The Super8TOPFlash reporter assay is a well validated method for investigating the activity of the canonical WNT pathway. The plasmid expresses firefly luciferase under the transcriptional control of a promoter containing a tandem of TCF/Lef response elements. Upon activation of the canonical WNT pathway the gene is expressed and upon addition of the luciferase substrate, luminescence is released. The level of activation is measured by the intensity of luminescence. To normalise for transfection efficiency a second plasmid encoding Renilla luciferase under the transcriptional control of the CMV promoter is co transfected with the TCF/Lef plasmid. It targets a different substrate to the firefly luciferase and therefore can be used to normalise for the efficiency of expression.

Validation of controls

LiCl is used as a positive control for the Super8TOPFlash reporter assay as it inhibits GSK3β, therefore allowing nuclear translocation of β-catenin and transcriptional activation of target genes. In order to optimise the concentration of LiCl for my experiments, I transfected HEK293 cells with both TOPFlash and Renilla reporter plasmids, then stimulated with different concentrations of LiCl (**Figure 48**).

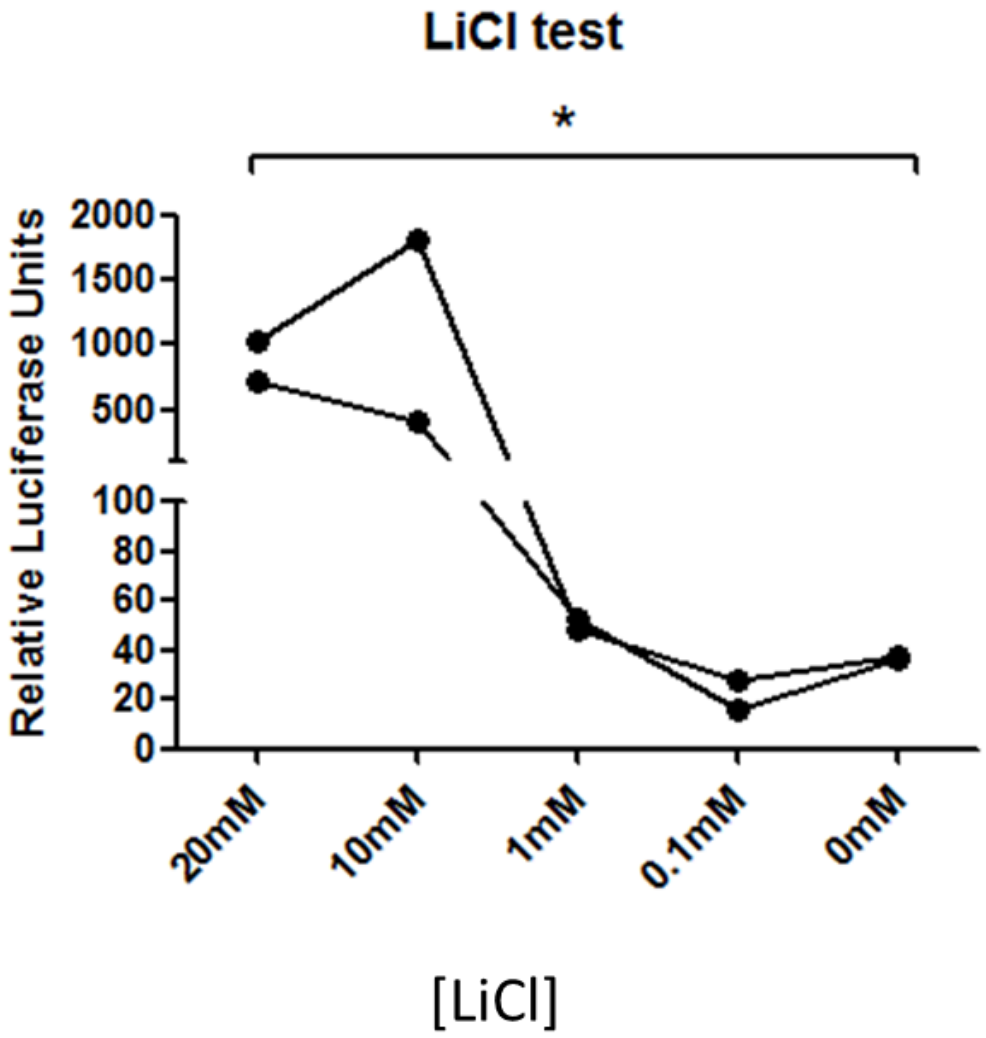

Figure 48: Validation of the TOPFlash reporter assay.

HEK293 cells were transfected with the Super8TOPFLASH plasmid and stimulated with different concentrations of LiCl (mM) 24 hours later. Cell lysates were harvested for the luciferase assay following a further 24 hours and analysed for the level of pathway activation by quantification of luciferase levels. Experiment was conducted in complete medium containing serum. Experiment represents a single experiment (n=2). An ANOVA with a post-test for linear trend was used for statistical analysis. Stats on the graph represent the result of the post-test.

The results from **Figure 48**, showed that the lowest concentration of LiCl that showed activation of the Super8TOPFlash reporter assay was 10mM. Therefore, I used this concentration in all future experiments.

Although the above experiment validated the activity of the TOPFlash plasmid it was also necessary to test the FOPflash plasmid (a negative control for the TOPflash plasmid that contains mutated TCF/lef elements). This plasmid should not transcribe luciferase. Negative control for LiCl, NaCl, was also included. The experiment was performed in C28/I2 to validate controls in the chondrocytic cell line with the data shown below in **Figure 49**.

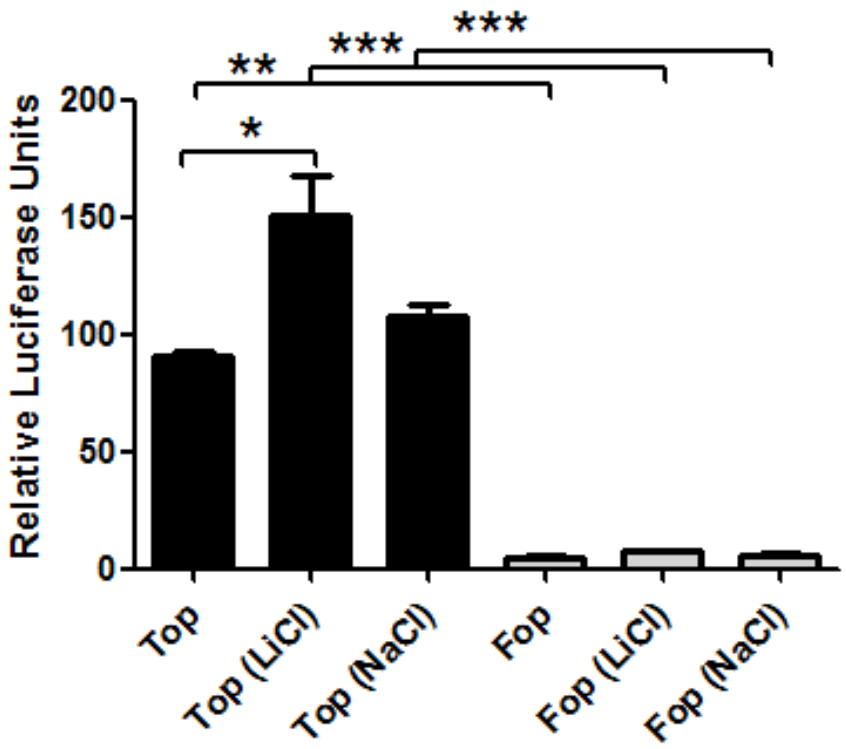

Figure 49: Both the TOP- and FOP- Flash reporter plasmids functioned correctly with positive and negative controls.

C28/I2 cells were transfected with either the TOP/ FOPFlash reporter plasmids as well as the CMV-renilla for normalising transfection efficiency. Twenty four hours later, 10mM LiCl or NaCl was added and, after additional 24 hours, the cells were harvested for the quantitation of the amount of luciferase as a measure of pathway activity. Values were normalised for the activity of renilla luciferase. Experiment was conducted in complete medium. Data are representative of a single experiment (n=2). An ANOVA with the Tukey post-test was used to test for significance.

As expected the FOPflash plasmid did not show any luciferase activity while the TOPFlash plasmid confirmed activation of the canonical WNT pathway upon addition to LiCl (**Figure 49**). Cells transfected with TOPFlash plasmid had significantly more pathway activity than those transfected with FOPflashs plasmid, indicating some basel WNT activity within the cells.

The WNT16 expression plasmid inhibits luciferase activity in the Super8TOPFlash reporter assay.

The previous experiments confirmed that the assay and all the relevant controls are working correctly. Next I investigated the effect of WNT16 on the TOP Flash reporter assay. I began my investigation using HEK293 cells as they are easily transfectable (**Figure 50**).

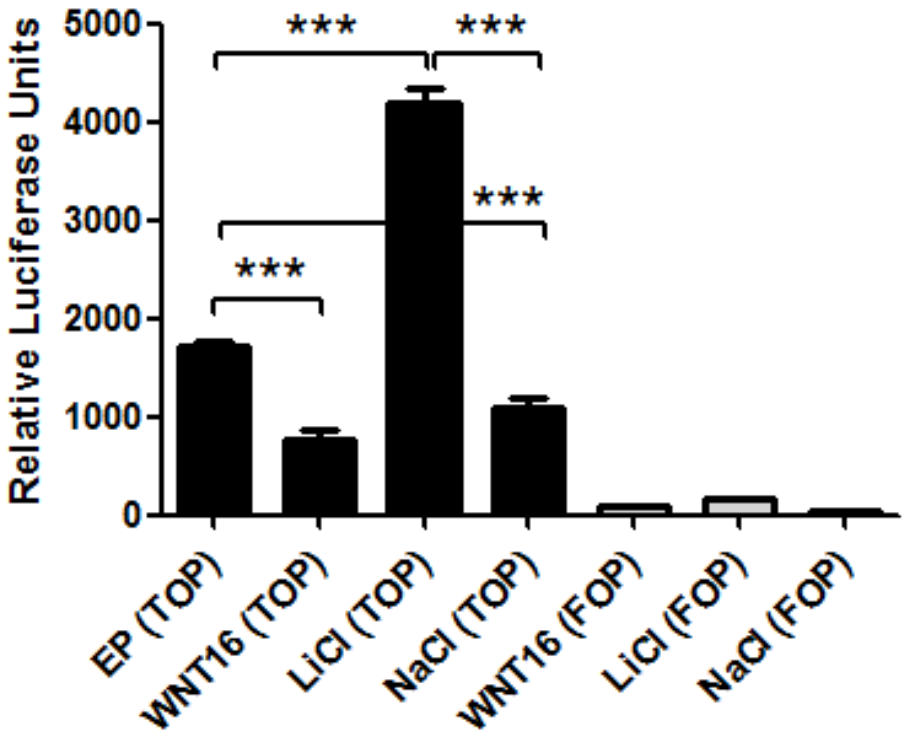

Figure 50: WNT16 inhibited the canonical WNT pathway in HEK293 cells.

Transfection of WNT16 plasmid showed less luciferase activity than that following transfection with empty plasmid, indicating that WNT16 inhibits the canonical WNT pathway. HEK293 cells were transfected with combinations of WNT16 plasmid or empty plasmid and TOP or FOP flash reporter plasmids, then stimulated with LiCL and NaCl (10mM), 24 hours later. Following a further 24 hours, cells were harvested for the reporter assay. Values normalised for renilla luciferase activity. Experiments were conducted in complete medium containing serum. Data are representative of a single experiment (n=3). An ANOVA with the tukey post-test to compare all columns was used to analyse statistical significance. All cells transfected with FOPflash plasmid were significantly lower than those transfected with TOPflash plasmid (stats not shown on graph).

The increase in signalling in cells transfected with the TOPflash reporter compared to the FOP flash reporter indicate basal WNT signalling within these cells. In this experiment (**Figure 50**), and at the WNT16 concentrations achieved by plasmid transfection, WNT16 downregulated the activity of the TOPFlash reporter assay. This was not completely surprising as from the experiments described in **Figure 28**, we already know that low concentrations of WNT16 inhibit the canonical WNT pathway. In addition, plasmid transfection does not provide a very high concentration of WNT16 since, in the dose responses reported in **Figure 25**, axin2 expression was inhibited compared to control at all concentrations of WNT16.

In order to validate this result in a chondrocytic cell I repeated the experiment in C28/I2 cells (**Figure 51**).

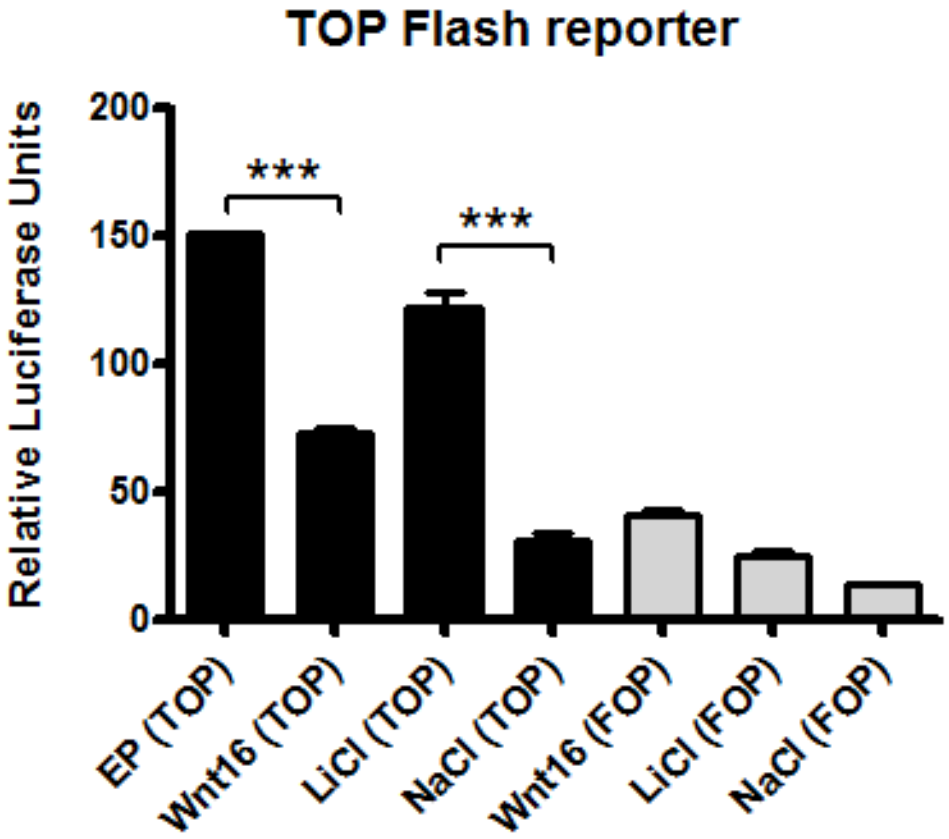

Figure 51: Transfection with a WNT16 plasmid inhibited the canonical WNT pathway in C28/I2 cells.

C28/I2 cells were transfected with either the WNT16 plasmid or the empty plasmid and either TOP of FOP flash reporter plasmid for 24 hours before stimulation with LiCl or NaCl (10mM) then harvested a after a further 24 hours. Values were normalised for renilla. Experiment were conducted in complete medium with serum. Data are representative of a single experiment (n=3). An ANOVA with the Tukey post-test was used to analyse significance of the data. Those cells transfected with FOPplasmid rather than the TOP plasmid showed a significant decrease in pathway activity as expected (stats not shown on graph).

As with HEK293 cells, transfection of a WNT16 plasmid also inhibited the canonical WNT pathway in C28/I2 cells when compared to empty plasmid (**Figure 51**). LiCl activated the reporter compared to NaCl, however the readout was not as high as the previous experiment in 293 cells. This is likely due to transfection efficiency, rather than cell type, as the potency of LiCl varied a lot even between 293 experiments. It is also possible that basal signalling in these cells was already reaching saturation level and so we do not observe an increase upon a stimulus with LiCl.

Finally, I investigated whether WNT16 activated or suppressed the canonical WNT pathway in SFZ and DZ cells (**Figure 52**).

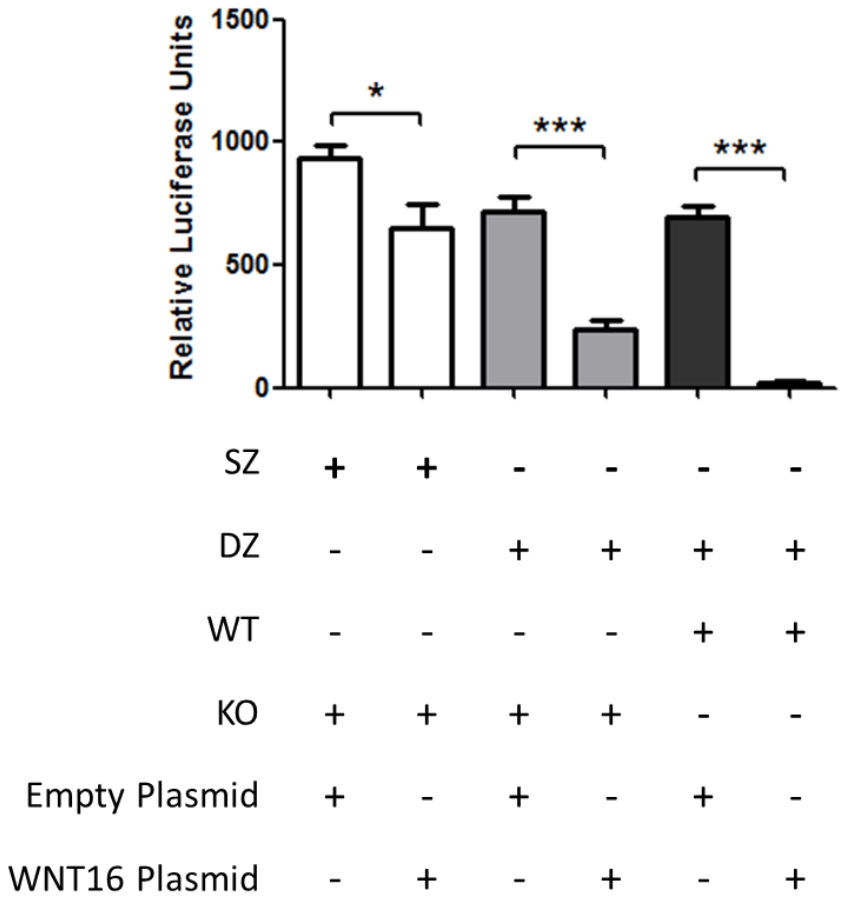

Figure 52: WNT16 inhibited the canonical WNT pathway in mouse articular chondrocytes from wild type and knockout mice.

SZC or DZC were transfected with the WNT16 plasmid or empty plasmid and TOPFlash and Renilla reporter plasmids, then harvested for the reporter assay 48 hours later. Values were normalised for renilla luciferase activity. Experiment was conducted in complete medium containing serum. Data are representative of a single experiment (n=3). An ANOVA with the Tukey post-test to compare all columns was used to test for significance.

WNT16 inhibited activation of the TOPflash reporter assay in SZC and DZC from wild type mice and DZC from wnt16-/- mice (**Figure 52**). This is in keeping with all previous reporter experiments. The basal WNT signalling in cells from different compartments or between DZC from wild type and WNT16-/- mice was not significantly different. Unfortunately no SFZ wild type cells were available at the time of the experiment.

To conclude this section, reporter assays experiments (all conducted using the WNT16 plasmid for overexpression) show that, at the expression levels achieved by plasmid transfection and under these experimental conditions, WNT16 inhibits the canonical WNT pathway when compared to empty plasmid in multiple, chondrocytic and non-chondrocytic cell types. These data also confirm that the concentration of WNT16 achieved by plasmid transfection is low, as results are in keeping with the lower end of a dose response conducted using recombinant WNT16 (**Figure 28**).

Optimisation of experimental conditions for WNT16 gain of function in C28/I2 cells

Upon availability of the recombinant protein which enabled identification of a coherent set of outcomes resulting from WNT16 stimulation in chondrocytes, I decided to test whether these results were still consistent in C28/I2 human cell line. The rationale behind this decision was that I sought confirmation of such results in human cells (as mentioned previously, human primary chondrocytes from OA joints suffered from a high degree of variability which impeded their use) and because a stable cell line is useful for mechanistic studies. Unfortunately C28/I2 cells differentiate in the absence of serum (Goldring, Birkhead et al. 1994), conditions in which WNTs are insoluble and lose their activity (Fuerer, Habib et al. 2010). It was necessary, therefore to optimise the experimental conditions for gain of function experiments to study biological effects of WNT16.

In order to achieve this, I analysed the response of C28/I2 cells to WNT16 in different serum conditions (**Figure 53**).

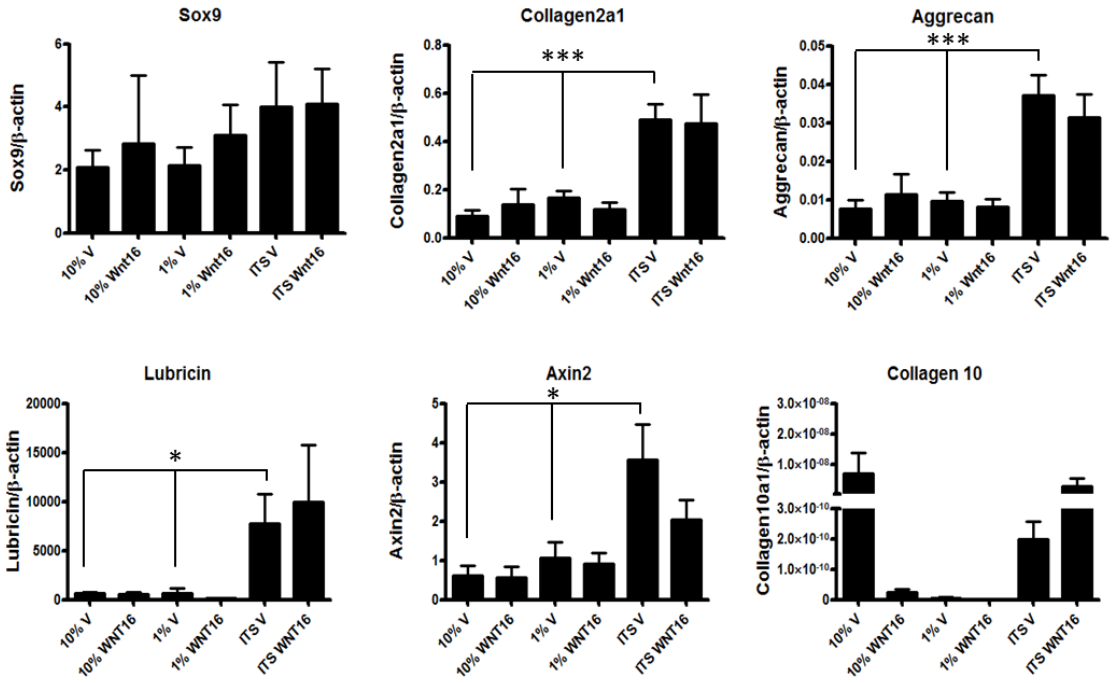

Figure 53: Recombinant WNT16 had no effect on chondrocyte marker genes in C28/I2 cells in the presence of FBS or serum free conditions.

C28/I2 cells were cultured in monolayer for 3 days in either 10% (v/v) or 1% (v/v) FBS or serum-free medium supplemented with ITS, then stimulated for 24hours with vehicle or 200ng/ml WNT16 under the same conditions. Gene expression was analysed by real time PCR. Values were normalised for β-actin. Response to serum was conditions were tested using an ANOVA. Data are representative of a single experiment (n=4).

The results from **Figure 53**, confirmed that C28/I2 cells are more chondrogenic in serum free conditions, shown by an increase in col2a1 and aggrecan. Lubricin and axin2 expression were also increased in these conditions. However, the result of WNT16 stimulation was not in keeping with previous experiments in SZC and bovine articular chondrocytes as no significant differences were seen. Although this may be a factor of cell specificity, further optimisation was required.

Interestingly, col10a1 (a marker of hypertrophy in chondrocytes) was downregulated by WNT16 in serum-containing conditions but upregulated in serum free conditions. Data from Maurizio Pacifici's laboratory (University of Pennsylvania), (Tamamura, Otani et al. 2005) showed that WNTs block the early transition from chondro-progenitors to chondrocytes but accelerate hypertrophy in mature chondrocytes (Tamamura, Otani et al. 2005). This may explain why in my experiment, WNT16 inhibited COL10A1 in the presence of serum (conditions that prevent differentiation of C28/I2 cells), and upregulated it in serum-free conditions, when C28/I2 cells differentiate. Alternatively, if like other WNTs, WNT16 is less active in serum free conditions, inconsistencies may be attributed to this.

To investigate this further, I performed a dose response experiment on previously differentiated C28/I2 cells (**Figure 54**).

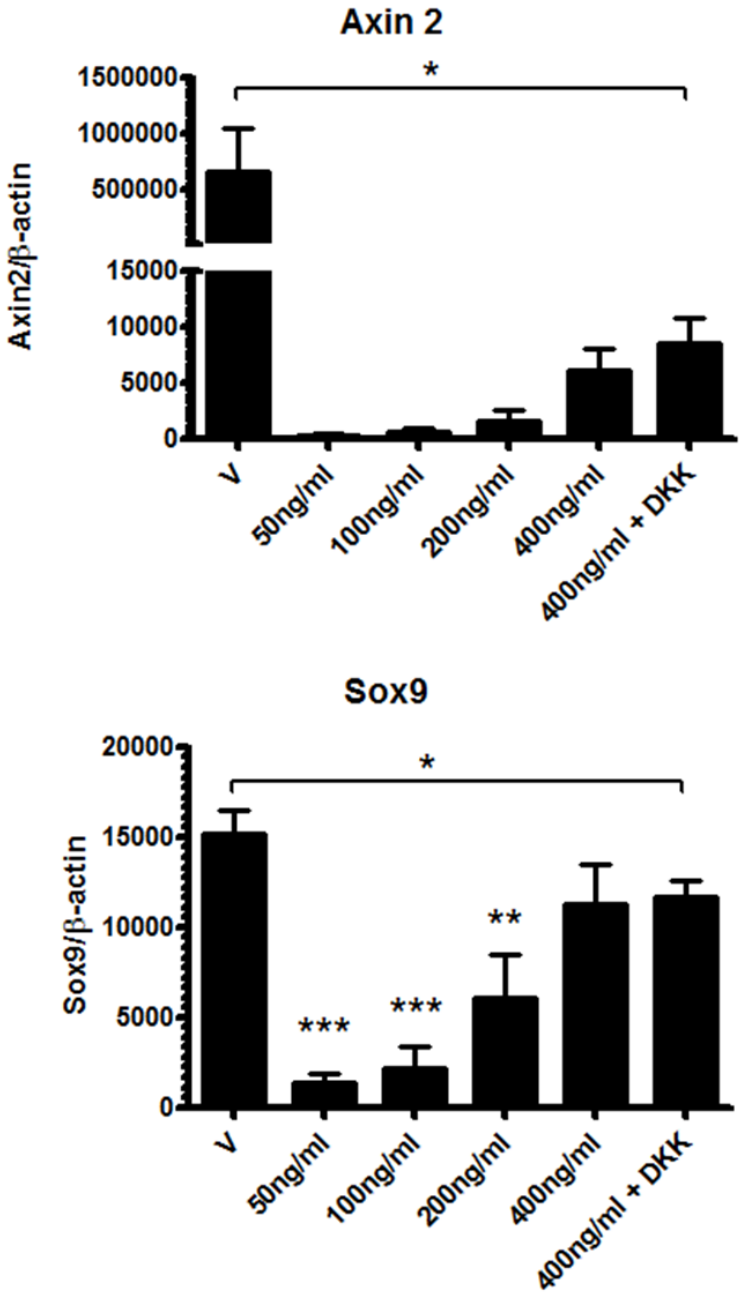

Figure 54: Recombinant WNT16 induced downregulation of axin2 and sox9 in serum free condition.

Cells were cultured in monolayer for 3 days in serum free medium supplemented with ITS, then stimulated with control or increasing concentrations of WNT16 recombinant (ng/ml), for 24 hours under the same conditions. Gene expression was analysed by real time PCR. Values were normalised for β-actin. Data represent a single experiment (n=4). ANOVA with the tukey post-test was used for statistical comparison. The result of the ANOVA is seen above all groups with the individual * representing the outcome of the tukey test comparing all columns to control.

The data from **Figure 54**, showed that WNT16 inhibited axin2 expression in C28/I2 cells cultured in serum free conditions. This is not in keeping with previous results where concentrations ≥200ng/ml dose dependently increased axin2 expression (**Figure 28**). If we also consider that low concentrations of WNT16 inhibit axin2 expression (**Figure 28**), then we can hypothesise that WNT16 activity is greatly reduced in the absence of serum. This is in keeping with data from Dr. Giovanna Nalesso, a member of our group, who saw a similar trend with WNT3A (a potent activator of canonical WNT signalling) as well as with previous literature (Fuerer, Habib et al. 2010).

Sox9 expression was also downregulated upon WNT16 stimulation, which is in keeping with previous data (**Figure 26** and **Figure 27**). Interestingly, downregulation is greatest at low concentrations of WNT16 and is reduced as the concentration increases. The loss of WNT16 activity in serum free conditions is likely caused by aggregation of the ligand, which will worsen as ligand concentration increases. We can therefore hypothesis that loss of activity will be greater at higher concentrations of WNT16.

In order to combine the differentiating conditions required for C28/I2 cells and the serum conditions for optimal WNT16 activity, I compared a number of conditions where cells were cultured in serum free medium for 3 days, then transferred to either 1% or 10% serum for 24 hours before stimulation with WNT16 for a further 24 hours (**Figure 55**).

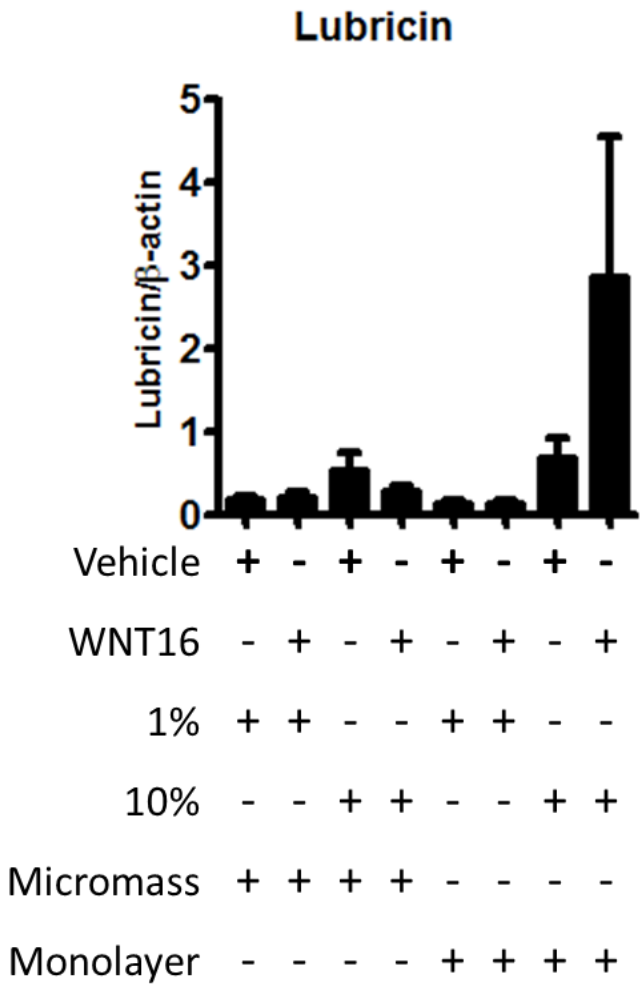

Figure 55: WNT16-induced lubricin upregulation was most striking when C28/I2 cells are first differentiated in serum free conditions, then exposed to WNT16 in 10% FBS, in monolayer.

Cells were cultured in monolayer or micromass for 3 days in serum free conditions then transferred to either 1% or 10% serum for 24 hours before stimulation for a further 24hours with vehicle or 200ng/ml WNT16. Gene expression was analysed by real time PCR. Values were normalised for β- actin. Data represent a single experiment (n=4). An ANOVA with the tukey post test was used to test for significance. No statistical significance was reached.

Optimal conditions for WNT16 stimulation in these cells included culturing in monolayer, and following differentiation, transfer to 10%(v/v) serum before WNT16 stimulation (**Figure 55**). This was deduced by the upregulation of lubricin under these conditions. It would also be useful to investigate the expression of axin2 and sox9 to confirm this, however I decided to focus my efforts on other cell types.

To conclude this section, the use of C28/I2 cells for WNT16 analysis requires pre-treatment of the cells for 3 days in serum free conditions, causing chondrocytic differentiation of the cells, before transfer to 10%(v/v) FBS for stimulation. Following this treatment the results of WNT16 stimulation were variable. Bovine articular chondrocytes are easy to manipulate in vitro and are a primary cell, therefore I will complete my mechanistic studies using these cells. C28/I2 cells will only be used when a human cell type is required for an experiment, for example, due to reagent specificity.

References

Aizawa, T., T. Kon, et al. (2001). "Induction of apoptosis in chondrocytes by tumor necrosis factor-alpha." J Orthop Res **19**(5): 785-796.

Alcaraz, M. J., J. Megías, et al. (2010). "New molecular targets for the treatment of osteoarthritis." Biochem Pharmacol **80**(1): 13-21.

Amour, A., C. G. Knight, et al. (2000). "The in vitro activity of ADAM-10 is inhibited by TIMP-1 and TIMP-3." FEBS Lett **473**(3): 275-279.

Amour, A., P. M. Slocombe, et al. (1998). "TNF-alpha converting enzyme (TACE) is inhibited by TIMP-3." FEBS Lett **435**(1): 39-44.

Arsenault, A. L. and M. D. Grynpas (1988). "Crystals in calcified epiphyseal cartilage and cortical bone of the rat." Calcif Tissue Int **43**(4): 219-225.

Bachner, D., M. Ahrens, et al. (1999). "Developmental expression analysis of murine autotaxin (ATX)." Mech Dev **84**(1-2): 121-125.

Baker, A. H., D. R. Edwards, et al. (2002). "Metalloproteinase inhibitors: biological actions and therapeutic opportunities." J Cell Sci **115**(Pt 19): 3719-3727.

Bau, B., P. M. Gebhard, et al. (2002). "Relative messenger RNA expression profiling of collagenases and aggrecanases in human articular chondrocytes in vivo and in vitro." Arthritis Rheum **46**(10): 2648-2657.

Baur, S. T., J. J. Mai, et al. (2000). "Combinatorial signaling through BMP receptor IB and GDF5: shaping of the distal mouse limb and the genetics of distal limb diversity." Development **127**(3): 605-619.

Benowitz, L. I. and P. G. Popovich (2011). "Inflammation and axon regeneration." Curr Opin Neurol **24**(6): 577-583.

Benya, P. D. and J. D. Shaffer (1982). "Dedifferentiated chondrocytes reexpress the differentiated collagen phenotype when cultured in agarose gels." Cell **30**(1): 215-224.

Bi, W., J. M. Deng, et al. (1999). "Sox9 is required for cartilage formation." Nat Genet **22**(1): 85-89.

Bi, Y., J. Huang, et al. (2009). "Wnt antagonist SFRP3 inhibits the differentiation of mouse hepatic progenitor cells." J Cell Biochem **108**(1): 295-303.

Binet, R., D. Ythier, et al. (2009). "WNT16B is a new marker of cellular senescence that regulates p53 activity and the phosphoinositide 3-kinase/AKT pathway." Cancer Res **69**(24): 9183-9191.

Blaney Davidson, E. N., E. L. Vitters, et al. (2007). "Elevated extracellular matrix production and degradation upon bone morphogenetic protein-2 (BMP-2) stimulation point toward a role for BMP-2 in cartilage repair and remodeling." Arthritis Res Ther **9**(5): R102.

Bondeson, J., S. D. Wainwright, et al. (2006). "The role of synovial macrophages and macrophage-produced cytokines in driving aggrecanases, matrix metalloproteinases, and other destructive and inflammatory responses in osteoarthritis." Arthritis Res Ther **8**(6): R187.

Borovina, A., S. Superina, et al. (2010). "Vangl2 directs the posterior tilting and asymmetric localization of motile primary cilia." Nat Cell Biol **12**(4): 407-412.

Bradley, E. W. and M. H. Drissi (2010). "WNT5A regulates chondrocyte differentiation through differential use of the CaN/NFAT and IKK/NF-kappaB pathways." Mol Endocrinol **24**(8): 1581-1593.

Brew, K., D. Dinakarpandian, et al. (2000). "Tissue inhibitors of metalloproteinases: evolution, structure and function." Biochim Biophys Acta **1477**(1-2): 267-283.

Burleigh, A., A. Chanalaris, et al. (2012). "Joint immobilization prevents murine osteoarthritis and reveals the highly mechanosensitive nature of protease expression in vivo." Arthritis Rheum **64**(7): 2278-2288.

Buschmann, M. D., Y. A. Gluzband, et al. (1995). "Mechanical compression modulates matrix biosynthesis in chondrocyte/agarose culture." J Cell Sci **108 (Pt 4)**: 1497-1508.

Candela, M. E., L. Cantley, et al. (2014). "Distribution of slow-cycling cells in epiphyseal cartilage and requirement of beta-catenin signaling for their maintenance in growth plate." J Orthop Res **32**(5): 661-668.

Caron, J. P., J. C. Fernandes, et al. (1996). "Chondroprotective effect of intraarticular injections of interleukin-1 receptor antagonist in experimental osteoarthritis. Suppression of collagenase-1 expression." Arthritis Rheum **39**(9): 1535-1544.

Chang, S. C., B. Hoang, et al. (1994). "Cartilage-derived morphogenetic proteins. New members of the transforming growth factor-beta superfamily predominantly expressed in long bones during human embryonic development." J Biol Chem **269**(45): 28227-28234.

Chia, S. L., Y. Sawaji, et al. (2009). "Fibroblast growth factor 2 is an intrinsic chondroprotective agent that suppresses ADAMTS-5 and delays cartilage degradation in murine osteoarthritis." Arthritis Rheum **60**(7): 2019-2027.

Chockalingam, P. S., W. Sun, et al. (2011). "Elevated aggrecanase activity in a rat model of joint injury is attenuated by an aggrecanase specific inhibitor." Osteoarthritis Cartilage **19**(3): 315-323.

Chung, U. I., E. Schipani, et al. (2001). "Indian hedgehog couples chondrogenesis to osteogenesis in endochondral bone development." J Clin Invest **107**(3): 295-304.

Clancy, R., J. Rediske, et al. (2001). "Activation of stress-activated protein kinase in osteoarthritic cartilage: evidence for nitric oxide dependence." Osteoarthritis Cartilage **9**(4): 294-299.

Clements, K. M., J. S. Price, et al. (2003). "Gene deletion of either interleukin-1beta, interleukin-1beta-converting enzyme, inducible nitric oxide synthase, or stromelysin 1 accelerates the development of knee osteoarthritis in mice after surgical transection of the medial collateral ligament and partial medial meniscectomy." Arthritis Rheum **48**(12): 3452-3463.

Clements, W. K., A. D. Kim, et al. (2011). "A somitic Wnt16/Notch pathway specifies haematopoietic stem cells." Nature **474**(7350): 220-224.

Clevers, H. and R. Nusse (2012). "Wnt/beta-catenin signaling and disease." Cell **149**(6): 1192-1205.

Coles, J. M., L. Zhang, et al. (2010). "Loss of cartilage structure, stiffness, and frictional properties in mice lacking PRG4." Arthritis Rheum **62**(6): 1666-1674.

Colige, A., I. Vandenberghe, et al. (2002). "Cloning and characterization of ADAMTS-14, a novel ADAMTS displaying high homology with ADAMTS-2 and ADAMTS-3." J Biol Chem **277**(8): 5756-5766.

Colnot, C., C. Lu, et al. (2004). "Distinguishing the contributions of the perichondrium, cartilage, and vascular endothelium to skeletal development." Dev Biol **269**(1): 55-69.

De Bari, C., F. Dell'Accio, et al. (2001). "Human periosteum-derived cells maintain phenotypic stability and chondrogenic potential throughout expansion regardless of donor age." Arthritis Rheum **44**(1): 85-95.

Dell'Accio, F., C. De Bari, et al. (2006). "Activation of WNT and BMP signaling in adult human articular cartilage following mechanical injury." Arthritis Res Ther **8**(5): R139.

Dell'accio, F., C. De Bari, et al. (2008). "Identification of the molecular response of articular cartilage to injury, by microarray screening: Wnt-16 expression and signaling after injury and in osteoarthritis." Arthritis Rheum **58**(5): 1410-1421.

Dell'Accio, F., J. Vanlauwe, et al. (2003). "Expanded phenotypically stable chondrocytes persist in the repair tissue and contribute to cartilage matrix formation and structural integration in a goat model of autologous chondrocyte implantation." J Orthop Res **21**(1): 123-131.

Dell'accio, F. and T. L. Vincent (2010). "Joint surface defects: clinical course and cellular response in spontaneous and experimental lesions." Eur Cell Mater **20**: 210-217.

Dercksen, M. W., I. S. Weimar, et al. (1995). "The value of flow cytometric analysis of platelet glycoprotein expression of CD34+ cells measured under conditions that prevent P-selectin-mediated binding of platelets." Blood **86**(10): 3771-3782.

Diarra, D., M. Stolina, et al. (2007). "Dickkopf-1 is a master regulator of joint remodeling." Nat Med **13**(2): 156-163.

Dieppe, P., K. Lim, et al. (2011). "Who should have knee joint replacement surgery for osteoarthritis?" Int J Rheum Dis **14**(2): 175-180.

Ding, C., F. Cicuttini, et al. (2007). "Tibial subchondral bone size and knee cartilage defects: relevance to knee osteoarthritis." Osteoarthritis Cartilage **15**(5): 479-486.

Ding, C., F. Cicuttini, et al. (2006). "Natural history of knee cartilage defects and factors affecting change." Arch Intern Med **166**(6): 651-658.

Ding, C., F. Cicuttini, et al. (2005). "The genetic contribution and relevance of knee cartilage defects: case-control and sib-pair studies." J Rheumatol **32**(10): 1937-1942.

Ding, C., P. Garnero, et al. (2005). "Knee cartilage defects: association with early radiographic osteoarthritis, decreased cartilage volume, increased joint surface area and type II collagen breakdown." Osteoarthritis Cartilage **13**(3): 198-205.

Dodd, A. W., C. Rodriguez-Fontenla, et al. (2011). "Deep sequencing of GDF5 reveals the absence of rare variants at this important osteoarthritis susceptibility locus." Osteoarthritis Cartilage **19**(4): 430-434.

Dowthwaite, G. P., J. C. Bishop, et al. (2004). "The surface of articular cartilage contains a progenitor cell population." J Cell Sci **117**(Pt 6): 889-897.

Dudhia, J. (2005). "Aggrecan, aging and assembly in articular cartilage." Cell Mol Life Sci **62**(19-20): 2241-2256.

Edwards, J. C., L. S. Wilkinson, et al. (1994). "The formation of human synovial joint cavities: a possible role for hyaluronan and CD44 in altered interzone cohesion." J Anat **185 (Pt 2)**: 355-367.

Eltawil, N. M., C. De Bari, et al. (2009). "A novel in vivo murine model of cartilage regeneration. Age and strain-dependent outcome after joint surface injury." Osteoarthritis Cartilage **17**(6): 695-704.

Erickson, D. M., S. E. Harris, et al. (1997). "Recombinant bone morphogenetic protein (BMP)-2 regulates costochondral growth plate chondrocytes and induces expression of BMP-2 and BMP-4 in a cell maturation-dependent manner." J Orthop Res **15**(3): 371-380.

Erickson, J. R., M. L. Joiner, et al. (2008). "A dynamic pathway for calcium-independent activation of CaMKII by methionine oxidation." Cell **133**(3): 462-474.

Erlacher, L., C. K. Ng, et al. (1998). "Presence of cartilage-derived morphogenetic proteins in articular cartilage and enhancement of matrix replacement in vitro." Arthritis Rheum **41**(2): 263-273.

Eyre, D. R. (2004). "Collagens and cartilage matrix homeostasis." Clin Orthop Relat Res(427 Suppl): S118-122.

Fear, M. W., D. P. Kelsell, et al. (2000). "Wnt-16a, a novel Wnt-16 isoform, which shows differential expression in adult human tissues." Biochem Biophys Res Commun **278**(3): 814-820.

Fitzgerald, J. B., M. Jin, et al. (2004). "Mechanical compression of cartilage explants induces multiple time-dependent gene expression patterns and involves intracellular calcium and cyclic AMP." J Biol Chem **279**(19): 19502-19511.

Flannery, C. R., R. Zollner, et al. (2009). "Prevention of cartilage degeneration in a rat model of osteoarthritis by intraarticular treatment with recombinant lubricin." Arthritis Rheum **60**(3): 840-847.

Francis-West, P. H., A. Abdelfattah, et al. (1999). "Mechanisms of GDF-5 action during skeletal development." Development **126**(6): 1305-1315.

Fredriksson, R., M. C. Lagerstrom, et al. (2003). "The G-protein-coupled receptors in the human genome form five main families. Phylogenetic analysis, paralogon groups, and fingerprints." Mol Pharmacol **63**(6): 1256-1272.

Fuerer, C., S. J. Habib, et al. (2010). "A study on the interactions between heparan sulfate proteoglycans and Wnt proteins." Dev Dyn **239**(1): 184-190.

Gao, B., H. Song, et al. (2011). "Wnt signaling gradients establish planar cell polarity by inducing Vangl2 phosphorylation through Ror2." Dev Cell **20**(2): 163-176.

Glasson, S. S. (2007). "In vivo osteoarthritis target validation utilizing genetically-modified mice." Curr Drug Targets **8**(2): 367-376.

Glasson, S. S., R. Askew, et al. (2005). "Deletion of active ADAMTS5 prevents cartilage degradation in a murine model of osteoarthritis." Nature **434**(7033): 644-648.

Goldring, M. B., J. R. Birkhead, et al. (1994). "Interleukin-1 beta-modulated gene expression in immortalized human chondrocytes." J Clin Invest **94**(6): 2307-2316.

Gosset, M., F. Berenbaum, et al. (2008). "Primary culture and phenotyping of murine chondrocytes." Nat Protoc **3**(8): 1253-1260.

Griffith, L. C., C. S. Lu, et al. (2003). "CaMKII, an enzyme on the move: regulation of temporospatial localization." Mol Interv **3**(7): 386-403.

Gruber, J., T. L. Vincent, et al. (2004). "Induction of interleukin-1 in articular cartilage by explantation and cutting." Arthritis Rheum **50**(8): 2539-2546.

Guerne, P. A., D. A. Carson, et al. (1990). "IL-6 production by human articular chondrocytes. Modulation of its synthesis by cytokines, growth factors, and hormones in vitro." J Immunol **144**(2): 499-505.

Guo, X., T. F. Day, et al. (2004). "Wnt/beta-catenin signaling is sufficient and necessary for synovial joint formation." Genes Dev **18**(19): 2404-2417.

Han, M. S., D. Y. Jung, et al. (2013). "JNK expression by macrophages promotes obesity-induced insulin resistance and inflammation." Science **339**(6116): 218-222.

Han, Y. and V. Lefebvre (2008). "L-Sox5 and Sox6 drive expression of the aggrecan gene in cartilage by securing binding of Sox9 to a far-upstream enhancer." Mol Cell Biol **28**(16): 4999-5013.

Hartmann, C. and C. J. Tabin (2000). "Dual roles of Wnt signaling during chondrogenesis in the chicken limb." Development **127**(14): 3141-3159.

Hartmann, C. and C. J. Tabin (2001). "Wnt-14 plays a pivotal role in inducing synovial joint formation in the developing appendicular skeleton." Cell **104**(3): 341-351.

Hatori, M., K. J. Klatte, et al. (1995). "End labeling studies of fragmented DNA in the avian growth plate: evidence of apoptosis in terminally differentiated chondrocytes." J Bone Miner Res **10**(12): 1960-1968.

Hayakawa, J., S. Mittal, et al. (2004). "Identification of promoters bound by c-Jun/ATF2 during rapid large-scale gene activation following genotoxic stress." Mol Cell **16**(4): 521-535.
Henry, S. P., S. Liang, et al. (2012). "The postnatal role of Sox9 in cartilage." J Bone Miner Res **27**(12): 2511-2525.
Hildebrand, A., M. Romaris, et al. (1994). "Interaction of the small interstitial proteoglycans biglycan, decorin and fibromodulin with transforming growth factor beta." Biochem J **302 (Pt 2)**: 527-534.
Hudmon, A. and H. Schulman (2002). "Structure-function of the multifunctional Ca2+/calmodulin-dependent protein kinase II." Biochem J **364**(Pt 3): 593-611.
Huelsken, J., R. Vogel, et al. (2001). "beta-Catenin controls hair follicle morphogenesis and stem cell differentiation in the skin." Cell **105**(4): 533-545.
Hyde, G., S. Dover, et al. (2007). "Lineage tracing using matrilin-1 gene expression reveals that articular chondrocytes exist as the joint interzone forms." Dev Biol **304**(2): 825-833.
Ito, M. M. and M. Y. Kida (2000). "Morphological and biochemical re-evaluation of the process of cavitation in the rat knee joint: cellular and cell strata alterations in the interzone." J Anat **197 Pt 4**: 659-679.
Jay, G. D., U. Tantravahi, et al. (2001). "Homology of lubricin and superficial zone protein (SZP): products of megakaryocyte stimulating factor (MSF) gene expression by human synovial fibroblasts and articular chondrocytes localized to chromosome 1q25." J Orthop Res **19**(4): 677-687.
Kan, A. and C. J. Tabin (2013). "c-Jun is required for the specification of joint cell fates." Genes Dev **27**(5): 514-524.
Karsenty, G. and E. F. Wagner (2002). "Reaching a genetic and molecular understanding of skeletal development." Dev Cell **2**(4): 389-406.
Kauskot, A., F. Adam, et al. (2007). "Involvement of the mitogen-activated protein kinase c-Jun NH2-terminal kinase 1 in thrombus formation." J Biol Chem **282**(44): 31990-31999.
Kavanagh, E., M. Abiri, et al. (2002). "Division and death of cells in developing synovial joints and long bones." Cell Biol Int **26**(8): 679-688.
Kawakami, Y., J. Capdevila, et al. (2001). "WNT signals control FGF-dependent limb initiation and AER induction in the chick embryo." Cell **104**(6): 891-900.
Kawakami, Y., C. Rodriguez Esteban, et al. (2006). "Wnt/beta-catenin signaling regulates vertebrate limb regeneration." Genes Dev **20**(23): 3232-3237.
Kevorkian, L., D. A. Young, et al. (2004). "Expression profiling of metalloproteinases and their inhibitors in cartilage." Arthritis Rheum **50**(1): 131-141.
Kiani, C., L. Chen, et al. (2002). "Structure and function of aggrecan." Cell Res **12**(1): 19-32.
Kikuchi, A. (2000). "Regulation of beta-catenin signaling in the Wnt pathway." Biochem Biophys Res Commun **268**(2): 243-248.
Kishida, S., H. Yamamoto, et al. (1999). "DIX domains of Dvl and axin are necessary for protein interactions and their ability to regulate beta-catenin stability." Mol Cell Biol **19**(6): 4414-4422.
Koyama, E., Y. Shibukawa, et al. (2008). "A distinct cohort of progenitor cells participates in synovial joint and articular cartilage formation during mouse limb skeletogenesis." Dev Biol **316**(1): 62-73.
Kühl, M., L. C. Sheldahl, et al. (2000). "Ca(2+)/calmodulin-dependent protein kinase II is stimulated by Wnt and Frizzled homologs and promotes ventral cell fates in Xenopus." J Biol Chem **275**(17): 12701-12711.
Kurz, B., A. K. Lemke, et al. (2005). "Pathomechanisms of cartilage destruction by mechanical injury." Ann Anat **187**(5-6): 473-485.

Lanske, B., M. Amling, et al. (1999). "Ablation of the PTHrP gene or the PTH/PTHrP receptor gene leads to distinct abnormalities in bone development." J Clin Invest **104**(4): 399-407.

Lanske, B., A. C. Karaplis, et al. (1996). "PTH/PTHrP receptor in early development and Indian hedgehog-regulated bone growth." Science **273**(5275): 663-666.

Lawrence, R. C., D. T. Felson, et al. (2008). "Estimates of the prevalence of arthritis and other rheumatic conditions in the United States. Part II." Arthritis Rheum **58**(1): 26-35.

Lawrence, R. C., C. G. Helmick, et al. (1998). "Estimates of the prevalence of arthritis and selected musculoskeletal disorders in the United States." Arthritis Rheum **41**(5): 778-799.

Lee, H. G. and J. H. Yang (2010). "PKC-δ mediates TCDD-induced apoptosis of chondrocyte in ROS-dependent manner." Chemosphere **81**(8): 1039-1044.

Lee, J. S., A. Ishimoto, et al. (1999). "Characterization of mouse dishevelled (Dvl) proteins in Wnt/Wingless signaling pathway." J Biol Chem **274**(30): 21464-21470.

Lefebvre, V., W. Huang, et al. (1997). "SOX9 is a potent activator of the chondrocyte-specific enhancer of the pro alpha1(II) collagen gene." Mol Cell Biol **17**(4): 2336-2346.

Li, X., M. Commane, et al. (2001). "IL-1-induced NFkappa B and c-Jun N-terminal kinase (JNK) activation diverge at IL-1 receptor-associated kinase (IRAK)." Proc Natl Acad Sci U S A **98**(8): 4461-4465.

Li, Y., M. J. Ahrens, et al. (2011). "Calcium/calmodulin-dependent protein kinase II activity regulates the proliferative potential of growth plate chondrocytes." Development **138**(2): 359-370.

Little, C. B., A. Barai, et al. (2009). "Matrix metalloproteinase 13-deficient mice are resistant to osteoarthritic cartilage erosion but not chondrocyte hypertrophy or osteophyte development." Arthritis Rheum **60**(12): 3723-3733.

Little, C. B., C. T. Meeker, et al. (2007). "Blocking aggrecanase cleavage in the aggrecan interglobular domain abrogates cartilage erosion and promotes cartilage repair." J Clin Invest **117**(6): 1627-1636.

Lodewyckx, L., F. P. Luyten, et al. (2012). "Genetic deletion of low-density lipoprotein receptor-related protein 5 increases cartilage degradation in instability-induced osteoarthritis." Rheumatology (Oxford) **51**(11): 1973-1978.

Logan, C. Y. and R. Nusse (2004). "The Wnt signaling pathway in development and disease." Annu Rev Cell Dev Biol **20**: 781-810.

Lories, R. J. and F. P. Luyten (2005). "Bone morphogenetic protein signaling in joint homeostasis and disease." Cytokine Growth Factor Rev **16**(3): 287-298.

Lories, R. J., J. Peeters, et al. (2007). "Articular cartilage and biomechanical properties of the long bones in Frzb-knockout mice." Arthritis Rheum **56**(12): 4095-4103.

Loughlin, J., B. Dowling, et al. (2004). "Functional variants within the secreted frizzled-related protein 3 gene are associated with hip osteoarthritis in females." Proc Natl Acad Sci U S A **101**(26): 9757-9762.

Luyten, F. P., V. C. Hascall, et al. (1988). "Insulin-like growth factors maintain steady-state metabolism of proteoglycans in bovine articular cartilage explants." Arch Biochem Biophys **267**(2): 416-425.

Luyten, F. P., Y. M. Yu, et al. (1992). "Natural bovine osteogenin and recombinant human bone morphogenetic protein-2B are equipotent in the maintenance of proteoglycans in bovine articular cartilage explant cultures." J Biol Chem **267**(6): 3691-3695.

Ma, H. L., T. J. Blanchet, et al. (2007). "Osteoarthritis severity is sex dependent in a surgical mouse model." Osteoarthritis Cartilage **15**(6): 695-700.

Macdonald, B. T., M. V. Semenov, et al. (2007). "SnapShot: Wnt/beta-catenin signaling." Cell **131**(6): 1204.

Macias, D., Y. Ganan, et al. (1997). "Role of BMP-2 and OP-1 (BMP-7) in programmed cell death and skeletogenesis during chick limb development." Development **124**(6): 1109-1117.

Maes, C., T. Kobayashi, et al. (2010). "Osteoblast precursors, but not mature osteoblasts, move into developing and fractured bones along with invading blood vessels." Dev Cell **19**(2): 329-344.

Mankin, H. J., H. Dorfman, et al. (1971). "Biochemical and metabolic abnormalities in articular cartilage from osteo-arthritic human hips. II. Correlation of morphology with biochemical and metabolic data." J Bone Joint Surg Am **53**(3): 523-537.

Mariani, F. V. and G. R. Martin (2003). "Deciphering skeletal patterning: clues from the limb." Nature **423**(6937): 319-325.

Mason, J. O., J. Kitajewski, et al. (1992). "Mutational analysis of mouse Wnt-1 identifies two temperature-sensitive alleles and attributes of Wnt-1 protein essential for transformation of a mammary cell line." Mol Biol Cell **3**(5): 521-533.

Messner, K. and W. Maletius (1996). "The long-term prognosis for severe damage to weight-bearing cartilage in the knee: a 14-year clinical and radiographic follow-up in 28 young athletes." Acta Orthop Scand **67**(2): 165-168.

Miller, J. R. (2002). "The Wnts." Genome Biol **3**(1): REVIEWS3001.

Minina, E., C. Kreschel, et al. (2002). "Interaction of FGF, Ihh/Pthlh, and BMP signaling integrates chondrocyte proliferation and hypertrophic differentiation." Dev Cell **3**(3): 439-449.

Minina, E., H. M. Wenzel, et al. (2001). "BMP and Ihh/PTHrP signaling interact to coordinate chondrocyte proliferation and differentiation." Development **128**(22): 4523-4534.

Mitchell, P. G., H. A. Magna, et al. (1996). "Cloning, expression, and type II collagenolytic activity of matrix metalloproteinase-13 from human osteoarthritic cartilage." J Clin Invest **97**(3): 761-768.

Mitrovic, D. (1982). "Development of the articular cavity in paralyzed chick embryos and in chick embryo limb buds cultured on chorioallantoic membranes." Acta Anat (Basel) **113**(4): 313-324.

Miyamoto, Y., A. Mabuchi, et al. (2007). "A functional polymorphism in the 5' UTR of GDF5 is associated with susceptibility to osteoarthritis." Nat Genet **39**(4): 529-533.

Moos, V., S. Fickert, et al. (1999). "Immunohistological analysis of cytokine expression in human osteoarthritic and healthy cartilage." J Rheumatol **26**(4): 870-879.

Moriguchi, T., K. Kawachi, et al. (1999). "Distinct domains of mouse dishevelled are responsible for the c-Jun N-terminal kinase/stress-activated protein kinase activation and the axis formation in vertebrates." J Biol Chem **274**(43): 30957-30962.

Nagase, H. and M. Kashiwagi (2003). "Aggrecanases and cartilage matrix degradation." Arthritis Res Ther **5**(2): 94-103.

Nakamura, N., S. Horibe, et al. (2008). "The location-specific healing response of damaged articular cartilage after ACL reconstruction: short-term follow-up." Knee Surg Sports Traumatol Arthrosc **16**(9): 843-848.

Nalesso, G., J. Sherwood, et al. (2011). "WNT-3A modulates articular chondrocyte phenotype by activating both canonical and noncanonical pathways." J Cell Biol **193**(3): 551-564.

Nalin, A. M., T. K. Greenlee, Jr., et al. (1995). "Collagen gene expression during development of avian synovial joints: transient expression of types II and XI collagen genes in the joint capsule." Dev Dyn **203**(3): 352-362.

Nateri, A. S., B. Spencer-Dene, et al. (2005). "Interaction of phosphorylated c-Jun with TCF4 regulates intestinal cancer development." Nature **437**(7056): 281-285.

Neuhold, L. A., L. Killar, et al. (2001). "Postnatal expression in hyaline cartilage of constitutively active human collagenase-3 (MMP-13) induces osteoarthritis in mice." J Clin Invest **107**(1): 35-44.

Noguchi, K., Y. Watanabe, et al. (2010). "A new chondrogenic differentiation initiator with the ability to up-regulate SOX trio expression." J Pharmacol Sci **112**(1): 89-97.

Nusse, R. and H. E. Varmus (1992). "Wnt genes." Cell **69**(7): 1073-1087.

Olsen, B. R., A. M. Reginato, et al. (2000). "Bone development." Annu Rev Cell Dev Biol **16**: 191-220.

Otsuki, S., S. R. Hanson, et al. (2010). "Extracellular sulfatases support cartilage homeostasis by regulating BMP and FGF signaling pathways." Proc Natl Acad Sci U S A **107**(22): 10202-10207.

Pacifici, M., M. Iwamoto, et al. (1993). "Tenascin is associated with articular cartilage development." Dev Dyn **198**(2): 123-134.

Pacifici, M., E. Koyama, et al. (2005). "Mechanisms of synovial joint and articular cartilage formation: recent advances, but many lingering mysteries." Birth Defects Res C Embryo Today **75**(3): 237-248.

Palumbo, R., M. Sampaolesi, et al. (2004). "Extracellular HMGB1, a signal of tissue damage, induces mesoangioblast migration and proliferation." J Cell Biol **164**(3): 441-449.

Paradowski, P. T., S. Bergman, et al. (2006). "Knee complaints vary with age and gender in the adult population. Population-based reference data for the Knee injury and Osteoarthritis Outcome Score (KOOS)." BMC Musculoskelet Disord **7**: 38.

Persson, M. (1983). "The role of movements in the development of sutural and diarthrodial joints tested by long-term paralysis of chick embryos." J Anat **137 (Pt 3)**: 591-599.

Pitsillides, A. A., C. W. Archer, et al. (1995). "Alterations in hyaluronan synthesis during developing joint cavitation." J Histochem Cytochem **43**(3): 263-273.

Polinkovsky, A., N. H. Robin, et al. (1997). "Mutations in CDMP1 cause autosomal dominant brachydactyly type C." Nat Genet **17**(1): 18-19.

Poole, A. R., T. Kojima, et al. (2001). "Composition and structure of articular cartilage: a template for tissue repair." Clin Orthop Relat Res(391 Suppl): S26-33.

Poole, A. R., L. C. Rosenberg, et al. (1996). "Contents and distributions of the proteoglycans decorin and biglycan in normal and osteoarthritic human articular cartilage." J Orthop Res **14**(5): 681-689.

Rannou, F., M. Francois, et al. (2006). "Cartilage breakdown in rheumatoid arthritis." Joint Bone Spine **73**(1): 29-36.

Rhee, D. K., J. Marcelino, et al. (2005). "The secreted glycoprotein lubricin protects cartilage surfaces and inhibits synovial cell overgrowth." J Clin Invest **115**(3): 622-631.

Rosenberg, L. (1971). "Chemical basis for the histological use of safranin O in the study of articular cartilage." J Bone Joint Surg Am **53**(1): 69-82.

Roughley, P. J. (2006). "The structure and function of cartilage proteoglycans." Eur Cell Mater **12**: 92-101.

Rountree, R. B., M. Schoor, et al. (2004). "BMP receptor signaling is required for postnatal maintenance of articular cartilage." PLoS Biol **2**(11): e355.

Ryu, J. H., S. J. Kim, et al. (2002). "Regulation of the chondrocyte phenotype by beta-catenin." Development **129**(23): 5541-5550.

Saadeddin, A., R. Babaei-Jadidi, et al. (2009). "The links between transcription, beta-catenin/JNK signaling, and carcinogenesis." Mol Cancer Res **7**(8): 1189-1196.

Sagara, N., G. Toda, et al. (1998). "Molecular cloning, differential expression, and chromosomal localization of human frizzled-1, frizzled-2, and frizzled-7." Biochem Biophys Res Commun **252**(1): 117-122.

Sahebjam, S., R. Khokha, et al. (2007). "Increased collagen and aggrecan degradation with age in the joints of Timp3(-/-) mice." Arthritis Rheum **56**(3): 905-909.

Saito, T., A. Fukai, et al. (2010). "Transcriptional regulation of endochondral ossification by HIF-2alpha during skeletal growth and osteoarthritis development." Nat Med **16**(6): 678-686.

Saris, D. B., J. Vanlauwe, et al. (2009). "Treatment of symptomatic cartilage defects of the knee: characterized chondrocyte implantation results in better clinical outcome at 36 months in a randomized trial compared to microfracture." Am J Sports Med **37 Suppl 1**: 10S-19S.

Schambony, A. and D. Wedlich (2007). "Wnt-5A/Ror2 regulate expression of XPAPC through an alternative noncanonical signaling pathway." Dev Cell **12**(5): 779-792.

Schumacher, B. L., C. E. Hughes, et al. (1999). "Immunodetection and partial cDNA sequence of the proteoglycan, superficial zone protein, synthesized by cells lining synovial joints." J Orthop Res **17**(1): 110-120.

Semenov, M. V., R. Habas, et al. (2007). "SnapShot: Noncanonical Wnt Signaling Pathways." Cell **131**(7): 1378.

Seol, D., D. J. McCabe, et al. (2012). "Chondrogenic progenitor cells respond to cartilage injury." Arthritis Rheum **64**(11): 3626-3637.

Serra, R., M. Johnson, et al. (1997). "Expression of a truncated, kinase-defective TGF-beta type II receptor in mouse skeletal tissue promotes terminal chondrocyte differentiation and osteoarthritis." J Cell Biol **139**(2): 541-552.

Settle, S. H., R. B. Rountree, et al. (2003). "Multiple joint and skeletal patterning defects caused by single and double mutations in the mouse Gdf6 and Gdf5 genes." Dev Biol **254**(1): 116-130.

Shelbourne, K. D., S. Jari, et al. (2003). "Outcome of untreated traumatic articular cartilage defects of the knee: a natural history study." J Bone Joint Surg Am **85-A Suppl 2**: 8-16.

Shimazaki, A., M. O. Wright, et al. (2006). "Calcium/calmodulin-dependent protein kinase II in human articular chondrocytes." Biorheology **43**(3-4): 223-233.

Slusarski, D. C., V. G. Corces, et al. (1997). "Interaction of Wnt and a Frizzled homologue triggers G-protein-linked phosphatidylinositol signalling." Nature **390**(6658): 410-413.

Später, D., T. P. Hill, et al. (2006). "Role of canonical Wnt-signalling in joint formation." Eur Cell Mater **12**: 71-80.

Spater, D., T. P. Hill, et al. (2006). "Wnt9a signaling is required for joint integrity and regulation of Ihh during chondrogenesis." Development **133**(15): 3039-3049.

Stanton, H., F. M. Rogerson, et al. (2005). "ADAMTS5 is the major aggrecanase in mouse cartilage in vivo and in vitro." Nature **434**(7033): 648-652.

Stenzel, K. H., T. Miyata, et al. (1974). "Collagen as a biomaterial." Annu Rev Biophys Bioeng **3**(0): 231-253.

Stone, A. V., R. F. Loeser, et al. (2014). "Pro-inflammatory stimulation of meniscus cells increases production of matrix metalloproteinases and additional catabolic factors involved in osteoarthritis pathogenesis." Osteoarthritis Cartilage **22**(2): 264-274.

Storm, E. E., T. V. Huynh, et al. (1994). "Limb alterations in brachypodism mice due to mutations in a new member of the TGF beta-superfamily." Nature **368**(6472): 639-643.

Swingler, T. E., J. G. Waters, et al. (2009). "Degradome expression profiling in human articular cartilage." Arthritis Res Ther **11**(3): R96.

Szczepankiewicz, B. G., C. Kosogof, et al. (2006). "Aminopyridine-based c-Jun N-terminal kinase inhibitors with cellular activity and minimal cross-kinase activity." J Med Chem **49**(12): 3563-3580.

Taelman, V. F., R. Dobrowolski, et al. (2010). "Wnt signaling requires sequestration of glycogen synthase kinase 3 inside multivesicular endosomes." Cell **143**(7): 1136-1148.

Tamai, K., M. Semenov, et al. (2000). "LDL-receptor-related proteins in Wnt signal transduction." Nature **407**(6803): 530-535.

Tamamura, Y., T. Otani, et al. (2005). "Developmental regulation of Wnt/beta-catenin signals is required for growth plate assembly, cartilage integrity, and endochondral ossification." J Biol Chem **280**(19): 19185-19195.

Teh, M. T., D. Blaydon, et al. (2007). "Role for WNT16B in human epidermal keratinocyte proliferation and differentiation." J Cell Sci **120**(Pt 2): 330-339.

Tetlow, L. C., D. J. Adlam, et al. (2001). "Matrix metalloproteinase and proinflammatory cytokine production by chondrocytes of human osteoarthritic cartilage: associations with degenerative changes." Arthritis Rheum **44**(3): 585-594.

Thomas, J. T., M. W. Kilpatrick, et al. (1997). "Disruption of human limb morphogenesis by a dominant negative mutation in CDMP1." Nat Genet **17**(1): 58-64.

Thomas, J. T., K. Lin, et al. (1996). "A human chondrodysplasia due to a mutation in a TGF-beta superfamily member." Nat Genet **12**(3): 315-317.

Torii, K., K. Nishizawa, et al. (2008). "Anti-apoptotic action of Wnt5a in dermal fibroblasts is mediated by the PKA signaling pathways." Cell Signal **20**(7): 1256-1266.

Upholt, W. B., C. M. Strom, et al. (1985). "Structure of the type II collagen gene." Ann N Y Acad Sci **460**: 130-140.

Urist, M. R. (1965). "Bone: formation by autoinduction." Science **150**(3698): 893-899.

Valhmu, W. B., E. J. Stazzone, et al. (1998). "Load-controlled compression of articular cartilage induces a transient stimulation of aggrecan gene expression." Arch Biochem Biophys **353**(1): 29-36.

van Beuningen, H. M., H. L. Glansbeek, et al. (1998). "Differential effects of local application of BMP-2 or TGF-beta 1 on both articular cartilage composition and osteophyte formation." Osteoarthritis Cartilage **6**(5): 306-317.

van der Sluijs, J. A., R. G. Geesink, et al. (1992). "The reliability of the Mankin score for osteoarthritis." J Orthop Res **10**(1): 58-61.

van Osch, G. J., W. B. van den Berg, et al. (1998). "Differential effects of IGF-1 and TGF beta-2 on the assembly of proteoglycans in pericellular and territorial matrix by cultured bovine articular chondrocytes." Osteoarthritis Cartilage **6**(3): 187-195.

Verzijl, N., J. DeGroot, et al. (2000). "Effect of collagen turnover on the accumulation of advanced glycation end products." J Biol Chem **275**(50): 39027-39031.

Vincent, T., M. Hermansson, et al. (2002). "Basic FGF mediates an immediate response of articular cartilage to mechanical injury." Proc Natl Acad Sci U S A **99**(12): 8259-8264.

Vincent, T. L., C. J. McLean, et al. (2007). "FGF-2 is bound to perlecan in the pericellular matrix of articular cartilage, where it acts as a chondrocyte mechanotransducer." Osteoarthritis Cartilage **15**(7): 752-763.

Vortkamp, A., K. Lee, et al. (1996). "Regulation of rate of cartilage differentiation by Indian hedgehog and PTH-related protein." Science **273**(5275): 613-622.

Vu, T. H., J. M. Shipley, et al. (1998). "MMP-9/gelatinase B is a key regulator of growth plate angiogenesis and apoptosis of hypertrophic chondrocytes." Cell **93**(3): 411-422.

Waller, K. A., L. X. Zhang, et al. (2013). "Role of lubricin and boundary lubrication in the prevention of chondrocyte apoptosis." Proc Natl Acad Sci U S A **110**(15): 5852-5857.

Wallingford, J. B. and R. Habas (2005). "The developmental biology of Dishevelled: an enigmatic protein governing cell fate and cell polarity." Development **132**(20): 4421-4436.
Wang, Y., C. Ding, et al. (2006). "Factors affecting progression of knee cartilage defects in normal subjects over 2 years." Rheumatology (Oxford) **45**(1): 79-84.
Warman, M. (2014). Supericial Zone Cartilage and OA Development. OARSI 2014 World congress on Osteoarthritis.
Watanabe, H., Y. Yamada, et al. (1998). "Roles of aggrecan, a large chondroitin sulfate proteoglycan, in cartilage structure and function." J Biochem **124**(4): 687-693.
Wieland, H. A., M. Michaelis, et al. (2005). "Osteoarthritis - an untreatable disease?" Nat Rev Drug Discov **4**(4): 331-344.
Williams, R., I. M. Khan, et al. (2010). "Identification and clonal characterisation of a progenitor cell sub-population in normal human articular cartilage." PLoS One **5**(10): e13246.
Wozney, J. M. (1995). "The potential role of bone morphogenetic proteins in periodontal reconstruction." J Periodontol **66**(6): 506-510.
Wu, X., X. Tu, et al. (2008). "Rac1 activation controls nuclear localization of beta-catenin during canonical Wnt signaling." Cell **133**(2): 340-353.
Wuelling, M. and A. Vortkamp (2010). "Transcriptional networks controlling chondrocyte proliferation and differentiation during endochondral ossification." Pediatr Nephrol **25**(4): 625-631.
Xu, Y. K. and R. Nusse (1998). "The Frizzled CRD domain is conserved in diverse proteins including several receptor tyrosine kinases." Curr Biol **8**(12): R405-406.
Yanagawa, S., F. van Leeuwen, et al. (1995). "The dishevelled protein is modified by wingless signaling in Drosophila." Genes Dev **9**(9): 1087-1097.
Yang-Snyder, J., J. R. Miller, et al. (1996). "A frizzled homolog functions in a vertebrate Wnt signaling pathway." Curr Biol **6**(10): 1302-1306.
Yang, S., J. Kim, et al. (2010). "Hypoxia-inducible factor-2alpha is a catabolic regulator of osteoarthritic cartilage destruction." Nat Med **16**(6): 687-693.
Yasuhara, R., Y. Ohta, et al. (2011). "Roles of β-catenin signaling in phenotypic expression and proliferation of articular cartilage superficial zone cells." Lab Invest **91**(12): 1739-1752.
Yoo, S. A., B. H. Park, et al. (2007). "Calcineurin modulates the catabolic and anabolic activity of chondrocytes and participates in the progression of experimental osteoarthritis." Arthritis Rheum **56**(7): 2299-2311.
Yu, H., X. Ye, et al. (2012). "Frizzled 2 and frizzled 7 function redundantly in convergent extension and closure of the ventricular septum and palate: evidence for a network of interacting genes." Development **139**(23): 4383-4394.
Yuasa, T., N. Kondo, et al. (2009). "Transient activation of Wnt/{beta}-catenin signaling induces abnormal growth plate closure and articular cartilage thickening in postnatal mice." Am J Pathol **175**(5): 1993-2003.
Zhang, Y., S. Y. Neo, et al. (1999). "Axin forms a complex with MEKK1 and activates c-Jun NH(2)-terminal kinase/stress-activated protein kinase through domains distinct from Wnt signaling." J Biol Chem **274**(49): 35247-35254.
Zhen, G., C. Wen, et al. (2013). "Inhibition of TGF-beta signaling in mesenchymal stem cells of subchondral bone attenuates osteoarthritis." Nat Med **19**(6): 704-712.
Zheng, H. F., J. H. Tobias, et al. (2012). "WNT16 influences bone mineral density, cortical bone thickness, bone strength, and osteoporotic fracture risk." PLoS Genet **8**(7): e1002745.
Zhu, M., M. Chen, et al. (2008). "Inhibition of beta-catenin signaling in articular chondrocytes results in articular cartilage destruction." Arthritis Rheum **58**(7): 2053-2064.

Zhu, M., D. Tang, et al. (2009). "Activation of beta-catenin signaling in articular chondrocytes leads to osteoarthritis-like phenotype in adult beta-catenin conditional activation mice." J Bone Miner Res **24**(1): 12-21.